WebSky2.0 LIM Forecasts:
What can LIM surveys tell us about the very early universe?

Nathan J. Carlson (PhD candidate, CITA / Toronto)
Dick Bond, Dongwoo Chung, Patrick Horlaville, Zack Li, Thomas Morrison, Doğa Tolgay

LIM25 - June 2025

I use the *WebSky2.0* simulations to study the effects of early-universe physics on cosmic structure.

$$|\mathrm{Web}\rangle \otimes \frac{|\mathrm{Ski}\rangle + |\mathrm{Sky}\rangle}{\sqrt{2}}$$

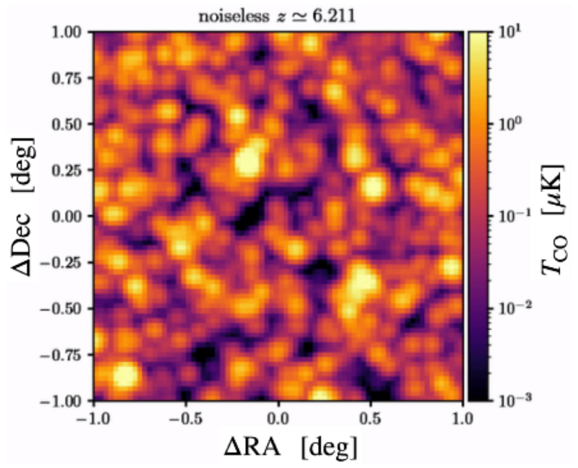

WebSky2.0 LIM Mocks

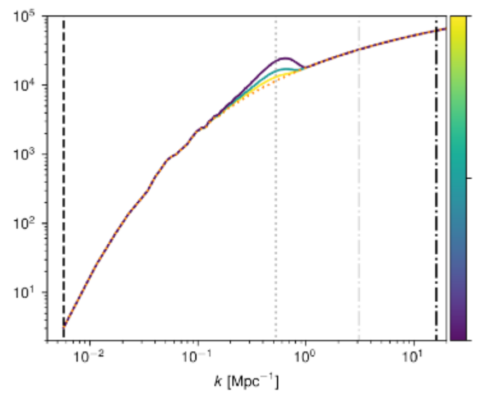

Primordial non-Gaussianity (PNG): a science case for LIM surveys

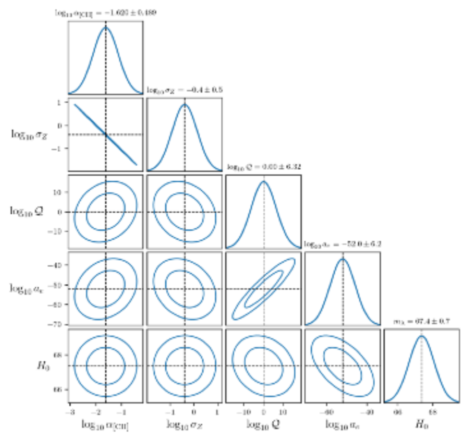

Using forecasts to refine our models and constrain PNG

Upcoming public release of *WebSky* catalogues feature new observables and an array of non-Gaussian initial conditions.

Line Intensity Mapping (LIM)

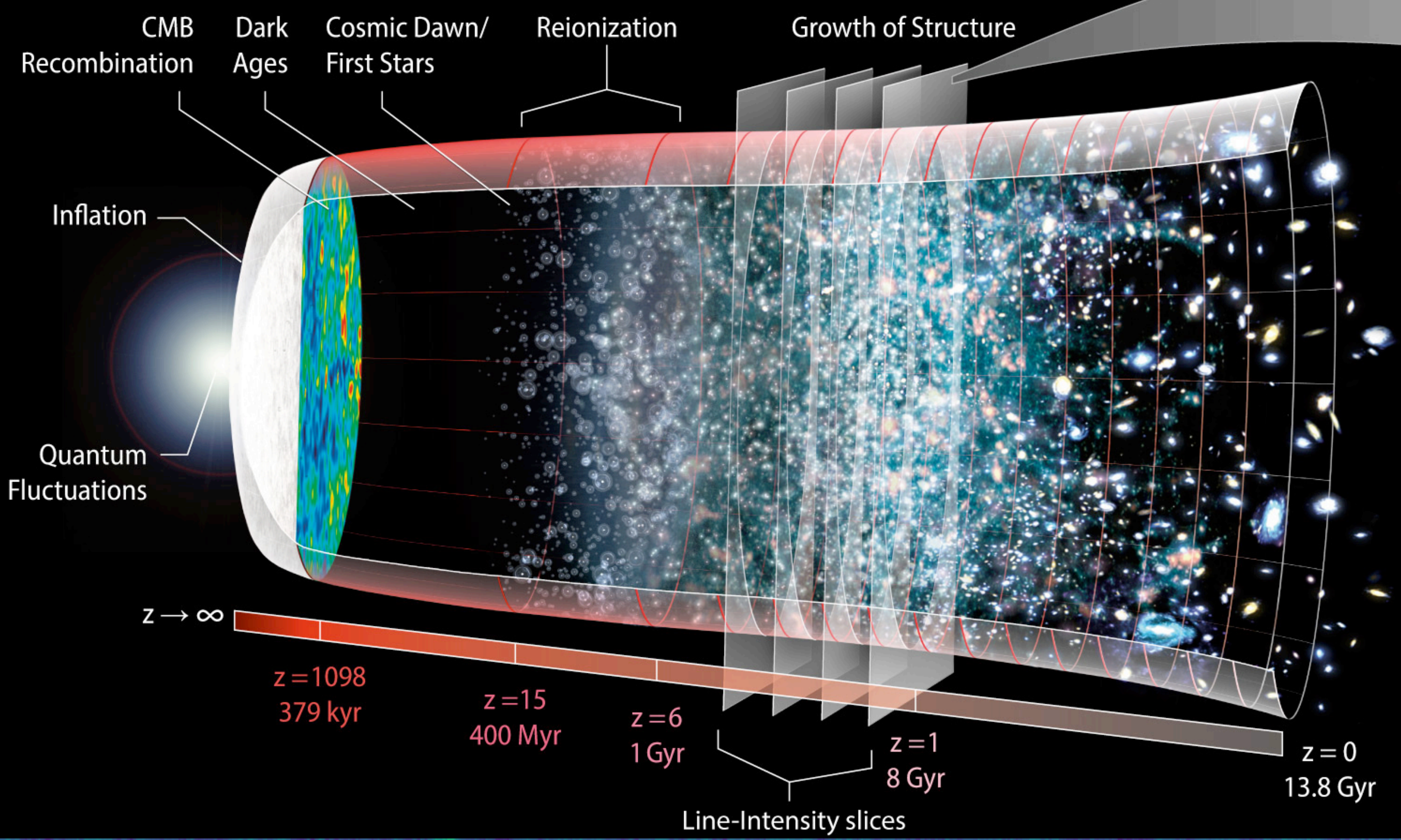

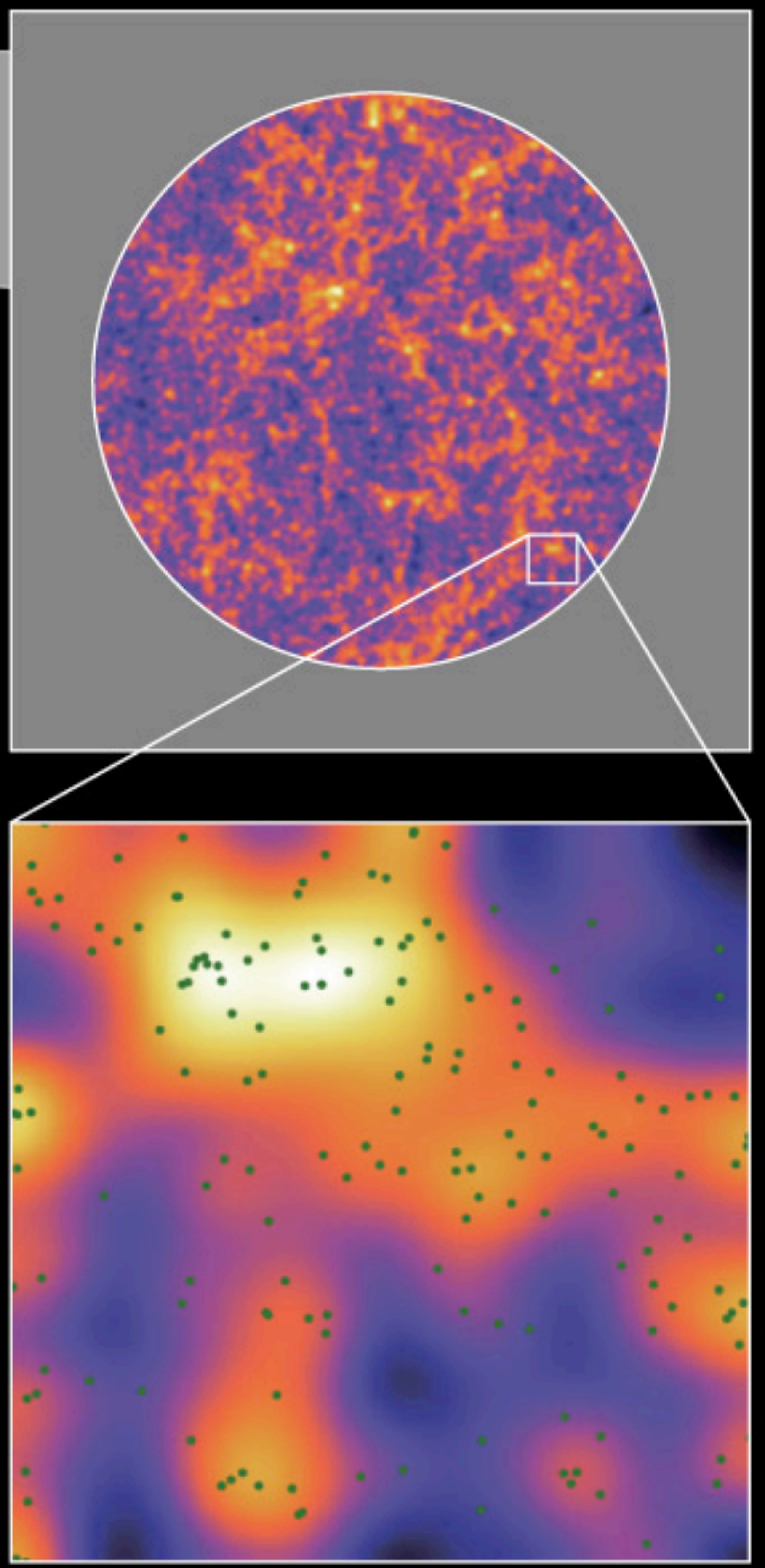

Line-Intensity Mapping simulation with galaxy distributions

Image credit: NASA/Lambda.

WebSky2.0 LIM Mocks

generating mock observables for next-generation cosmological surveys

Our code in context:

Peak Patch in the DM halo code landscape

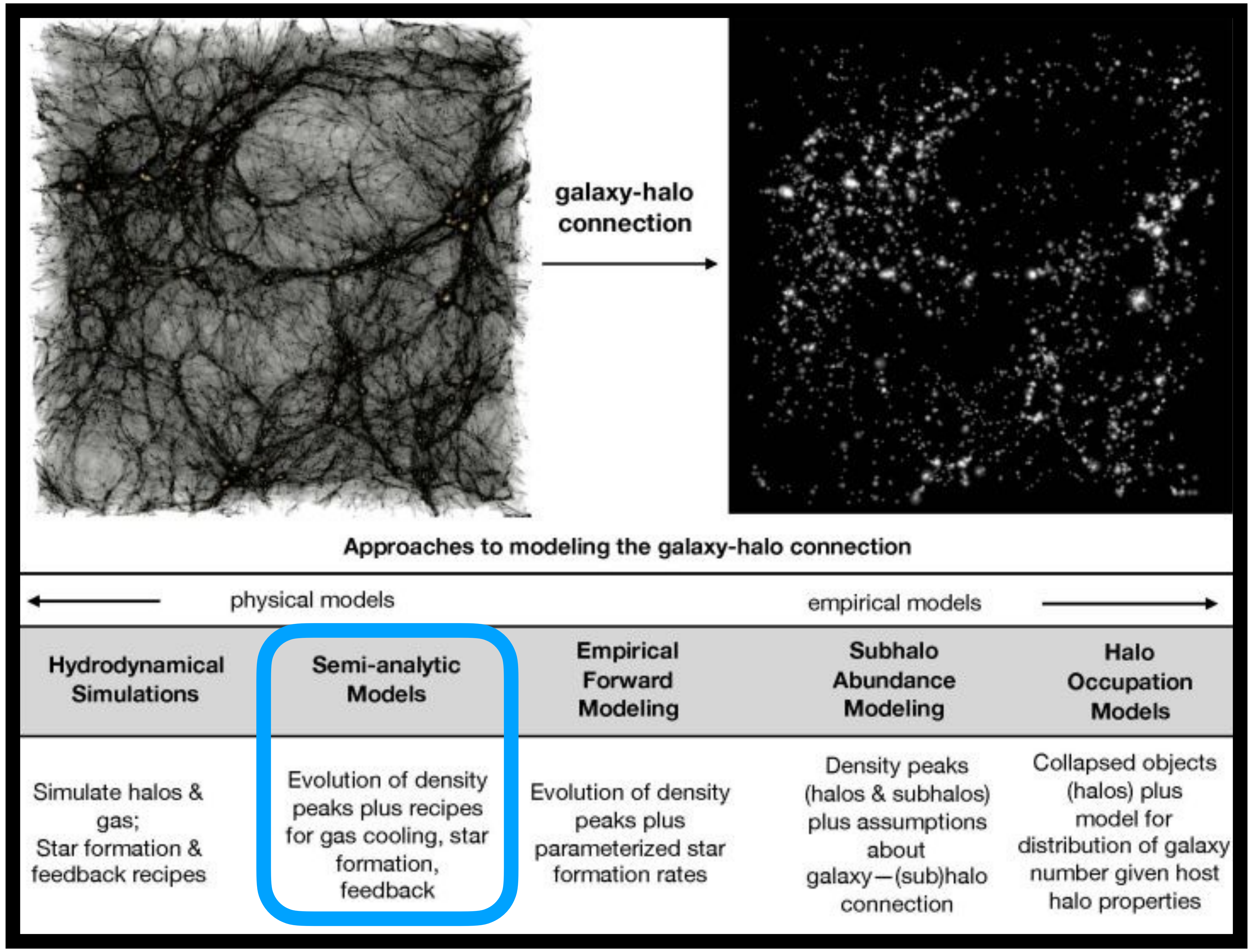

Wechsler+Tinker18 ARA&A

WebSky in the mock map landscape

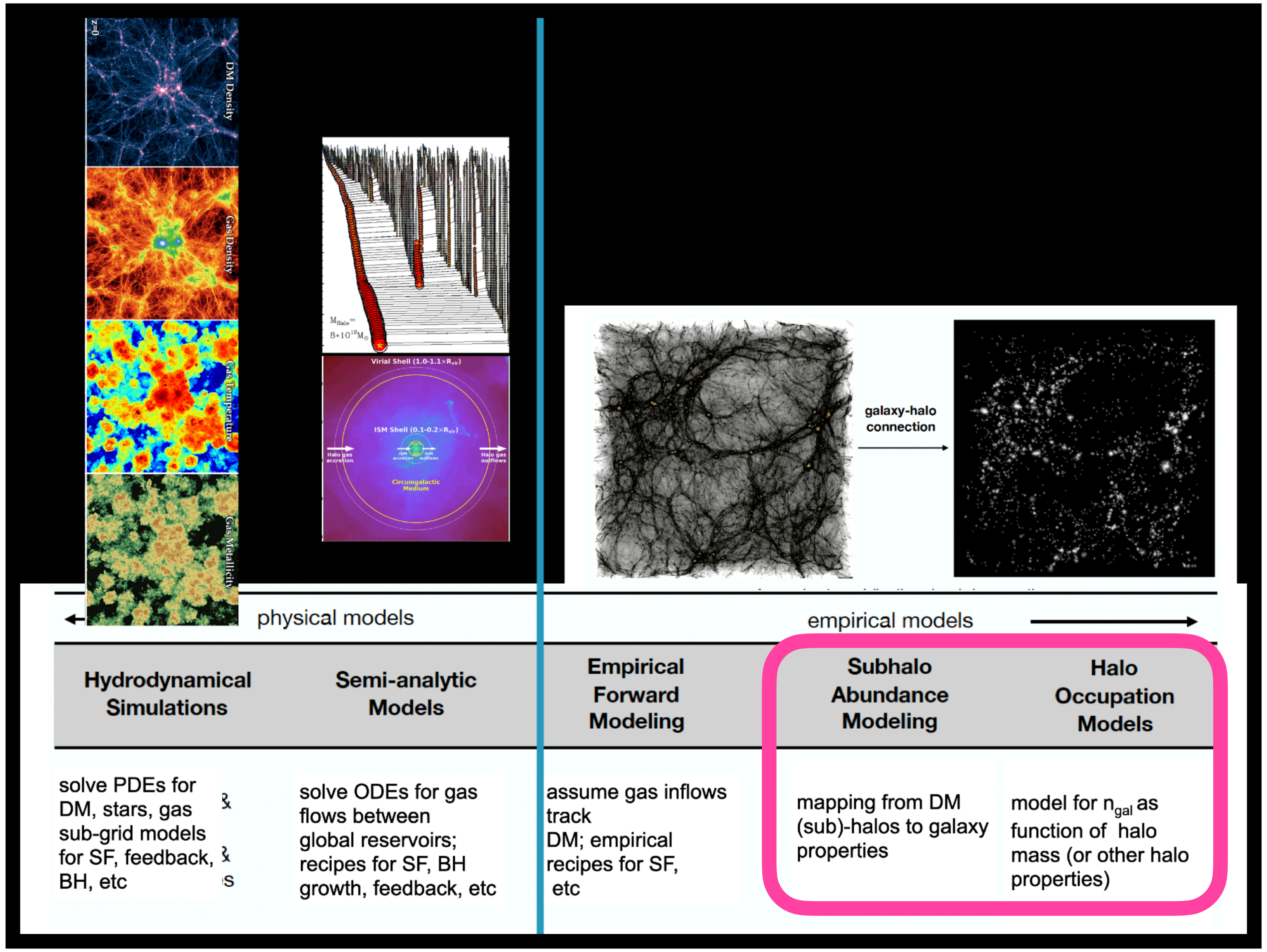

Somerville @ LIM25

Peak Patch simulates a lightcone DM halo distribution by identifying peaks in a linear density field. Ellipsoidal collapse and LPT are used to translate to a final distribution.

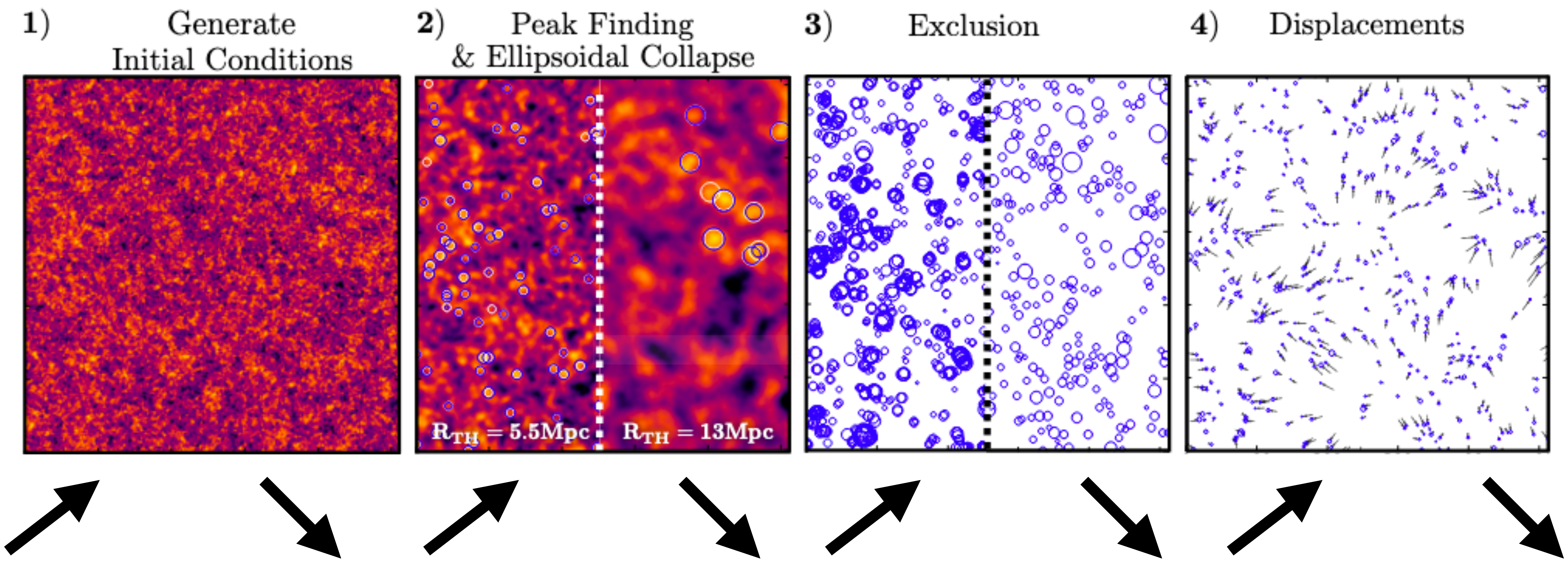

Figure from Stein *et al.*, 2018 [1810.07727].

Start with a power spectrum describing matter distribution, generate realization of a random field with that power.

Identify where structures will form using peak finding and gravitational collapse of homogeneous ellipsoids (HEC) at a series of real-space spherical top-hat filter scales.

Run **merging and exclusion** algorithm to avoid double counting mass in overlapping patches.

Displace halos based on laplacian of initial fields, using low order perturbation theory.

The result is a **catalogue of all DM halos** above a threshold size.

The *WebSky* simulations paint a suite of observables onto *Peak Patch* halos. Integrates over halos along lines of sight for observable response in each pixel.

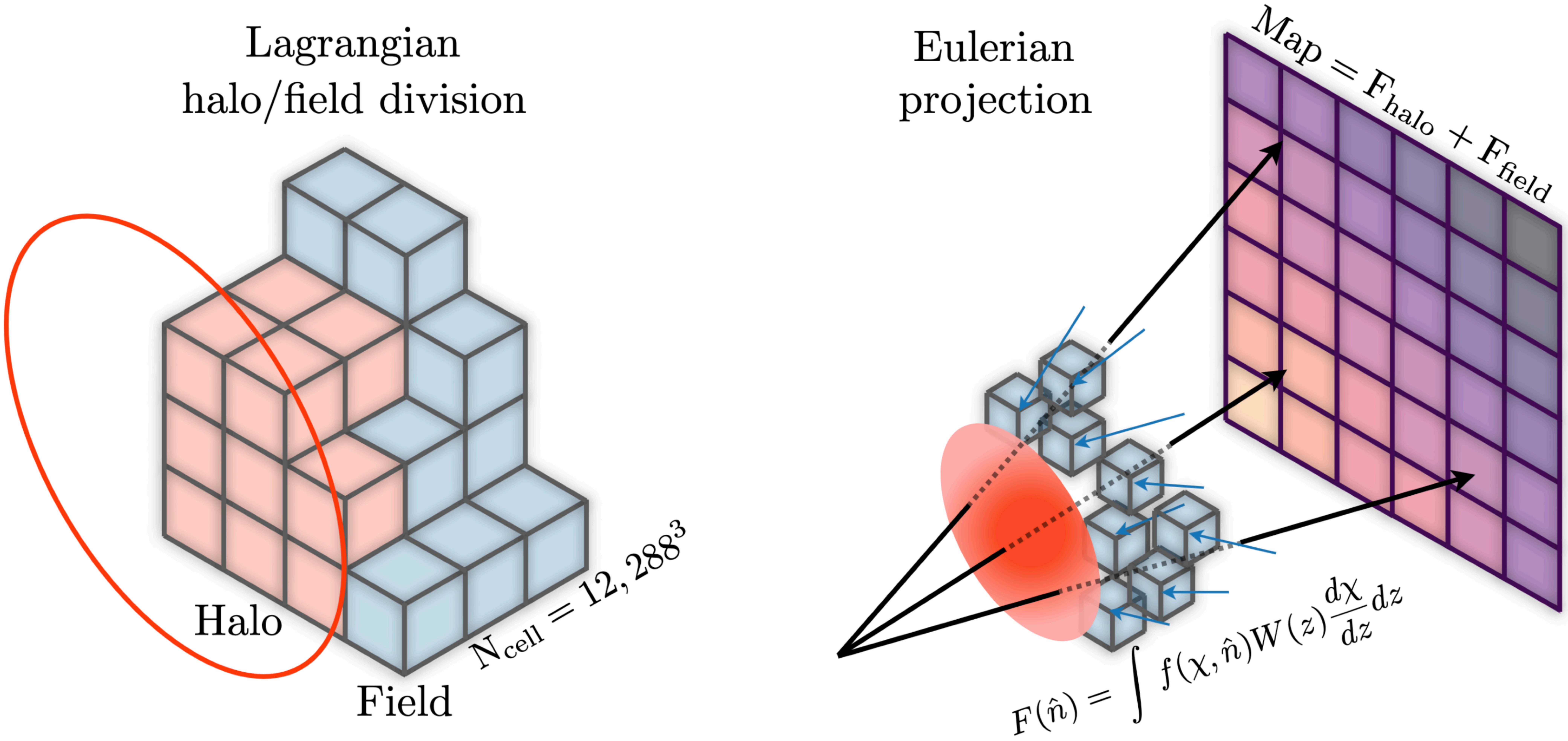

Figures from Stein *et al.*, 2020 [2001.08787].

WebSky2.0 reconstructs a host of varied mock maps for both CMB and LIM surveys.

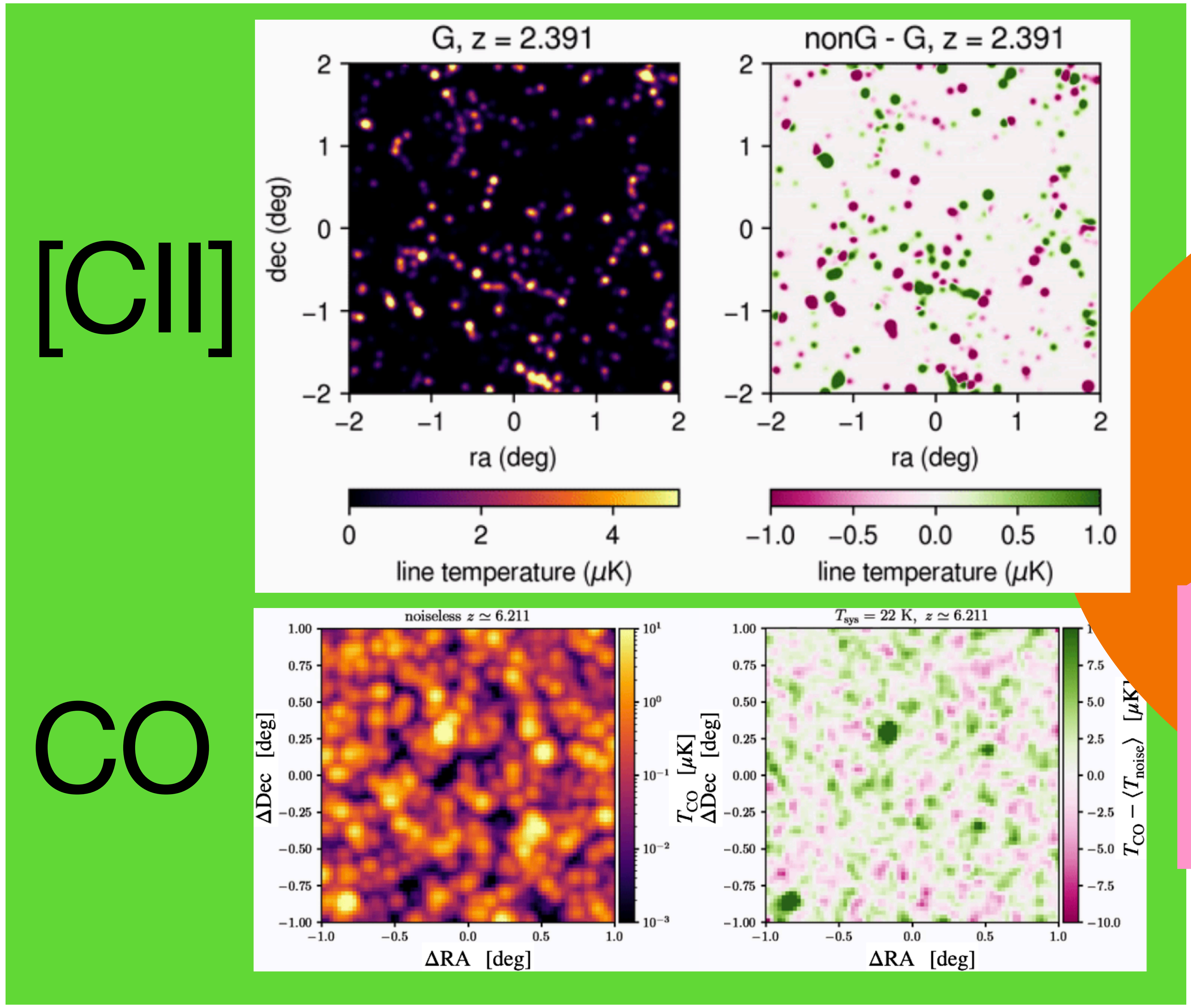

LIM Mocks

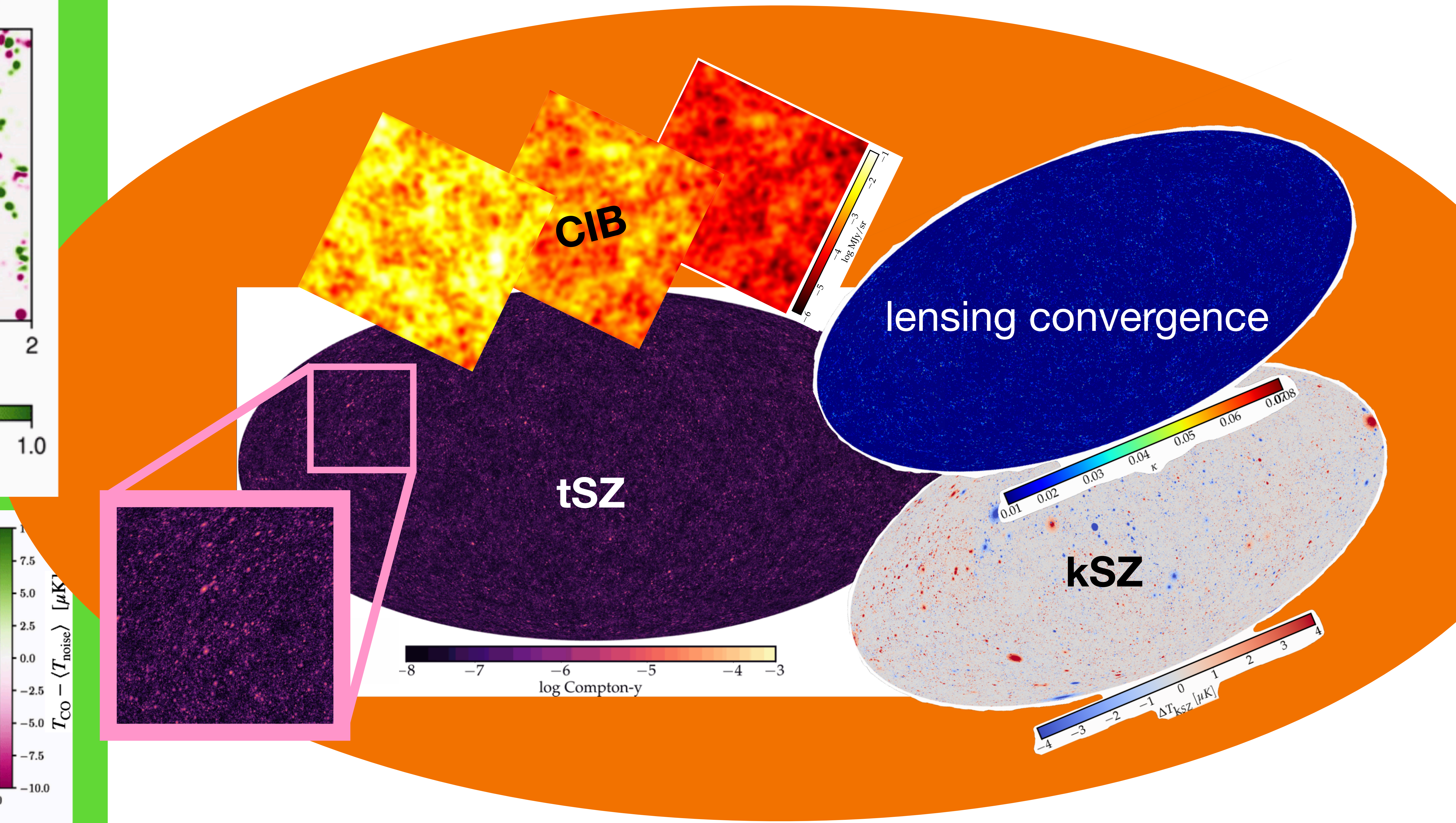

CMB foregrounds

To translate from DM halos to LIM mocks, we must formulate a line emission model

The [CII] model from Horlaville *et al*., [2309.15733], given a cluster of mass M_c and redshift z_c the [CII] luminosity is

$$\frac{L_{[\mathrm{CII}],c}(M_c, z_c)}{L_\odot} = \alpha_{[\mathrm{CII}]} \frac{M_{\mathrm{HI},c}(M_c)}{M_\odot} \frac{\zeta_Z Z_c(M_c, z_c)}{Z_\odot}$$

where $\alpha_{[\mathrm{CII}]} \sim 0.024$ and ζ_Z is drawn from a log-normal distribution with scatter $\sigma_Z \sim 0.4$. The intensity per voxel

To translate from DM halos to LIM mocks, we must formulate a line emission model

The [CII] model from Horlaville *et al*., [2309.15733], given a cluster of mass M_c and redshift z_c the [CII] luminosity is

$$\frac{L_{[\mathrm{CII}],c}(M_c, z_c)}{L_\odot} = \alpha_{[\mathrm{CII}]} \frac{M_{\mathrm{HI},c}(M_c)}{M_\odot} \frac{\zeta_Z Z_c(M_c, z_c)}{Z_\odot}$$

where $\alpha_{[\mathrm{CII}]} \sim 0.024$ and ζ_Z is drawn from a log-normal distribution with scatter $\sigma_Z \sim 0.4$. The intensity per voxel

$$I_{[\mathrm{CII}]}(z_{\mathrm{voxel}}, \hat{\theta}_{\mathrm{voxel}}) = \frac{1}{4\pi\nu_{\mathrm{CII},0} H(z_{\mathrm{voxel}})} \frac{\iiint_{\mathrm{voxel}} L_{[\mathrm{CII}]} dz d\Omega}{\iiint_{\mathrm{voxel}} dz d\Omega}$$

To translate from DM halos to LIM mocks, we must formulate a line emission model

The [CII] model from Horlaville *et al*., [2309.15733], given a cluster of mass M_c and redshift z_c the [CII] luminosity is

$$\frac{L_{[}\ \cdots}{\cdots} \quad \cdots \quad \frac{\cdots(M_c, z_c)}{Z_\odot}$$

Is this model cosmic truth?

where $\alpha_{[CII]} \sim 0.$ … distribution with scatter $\sigma_Z \sim 0.4$. The intensity per voxel

$$I_{[CII]}(z_{\text{voxel}}, \hat{\theta}_{\text{voxel}}) = \frac{1}{4\pi\nu_{\text{CII},0}H(z_{\text{voxel}})} \frac{\iiint_{\text{voxel}} L_{[CII]} dz d\Omega}{\iiint_{\text{voxel}} dz d\Omega}$$

No.

Learn response functions from sims (Doğa Tolgay)

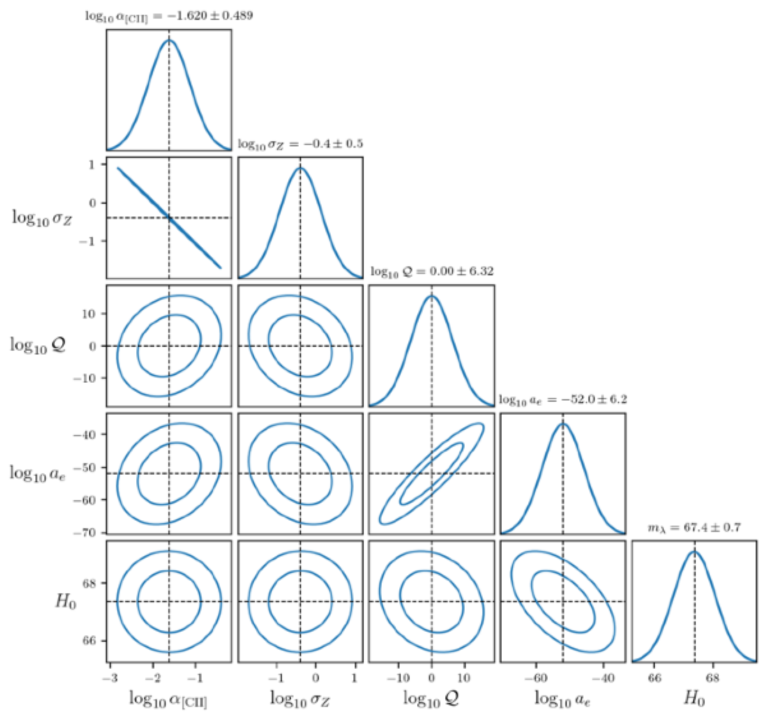

Make forecasts so data can eventually clear things up

Forecasting for a next-generation CCAT survey that could be achieved with extension of the CCAT-DSS survey with EoR-Spec instrument, or similar.

	CCAT-DSS	**Next-gen CCAT survey**
Beam FWHM	48”	48”
NEFD	72.5 mJy s^1/2	72.5 mJy s^1/2
No. of feeds	120	120
Redshift range	3.5 < z < 8	3.5 < z < 8
Minimum observable halo mass	~ 4e10 Msun	~ 4e10 Msun
No. of fields	2	2
FOV/field	4 deg^2	4 deg^2
Observing time/field	2,000 hours	40,000 hours

Same dish (FYST), similar instrument (EoR-Spec)

Similar survey area to CCAT-DSS

Longer duration survey

Using *WebSky*, we produce a 3D [CII] intensity field as we will see with future CCAT surveys.

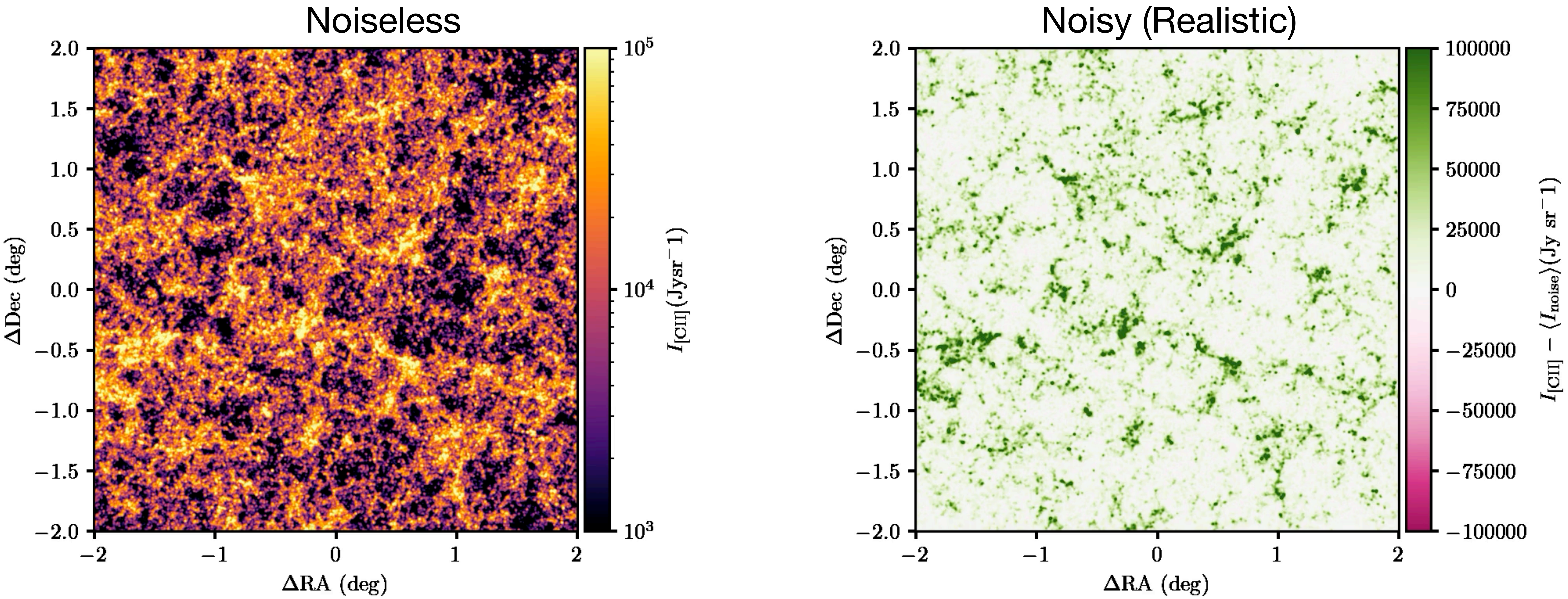

Because of low noise and high resolution, we get a sharp image even in noise added maps.

Primordial non-Gaussianity (PNG)

a science case for LIM surveys

CMB: the distribution of energy in the early universe was very nearly Gaussian. *Inflation:* all models predict some deviation from purely Gaussian statistics, or primordial non-Gaussianity (PNG).

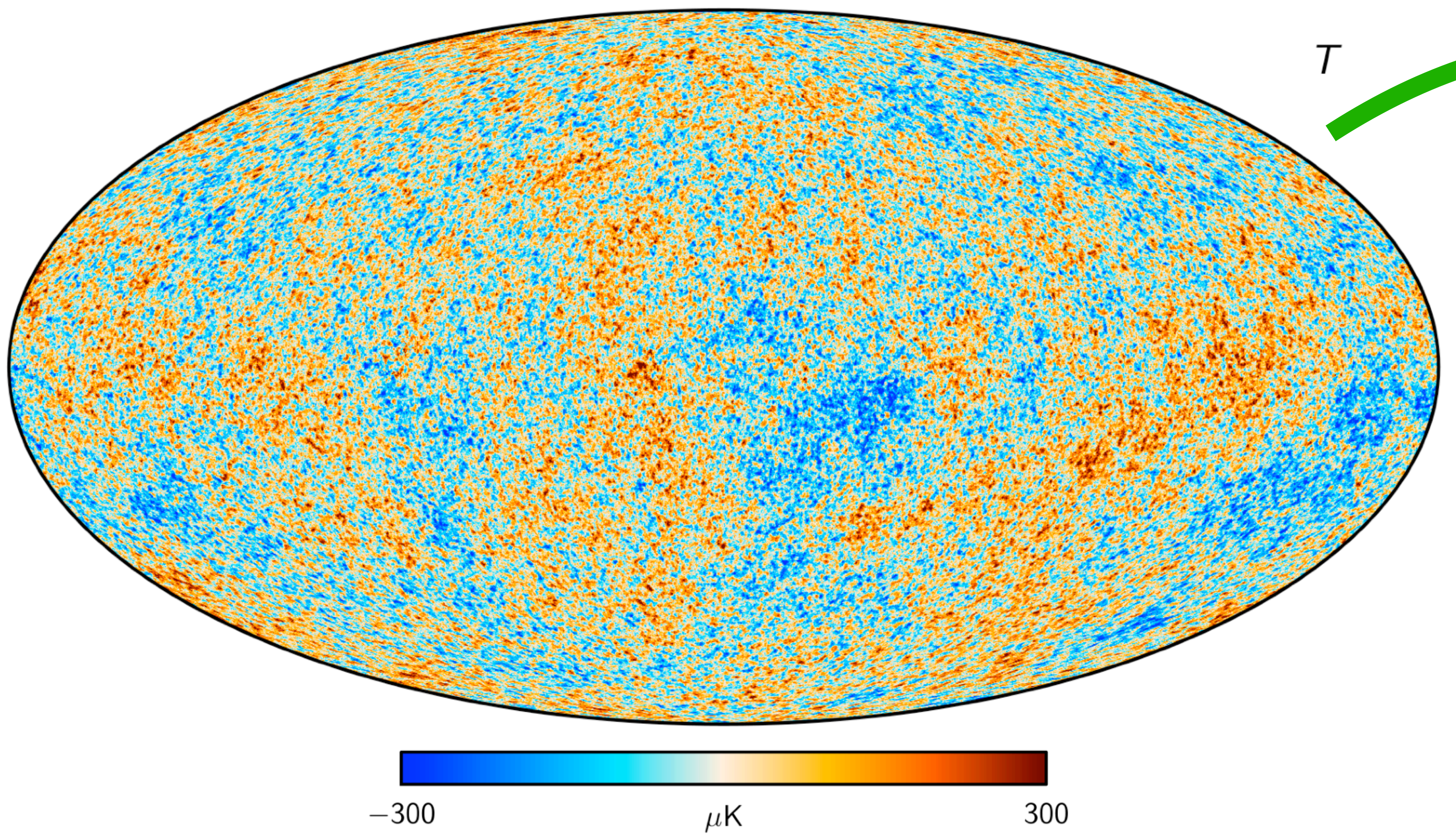

The CMB is (nearly) **Gaussian**!

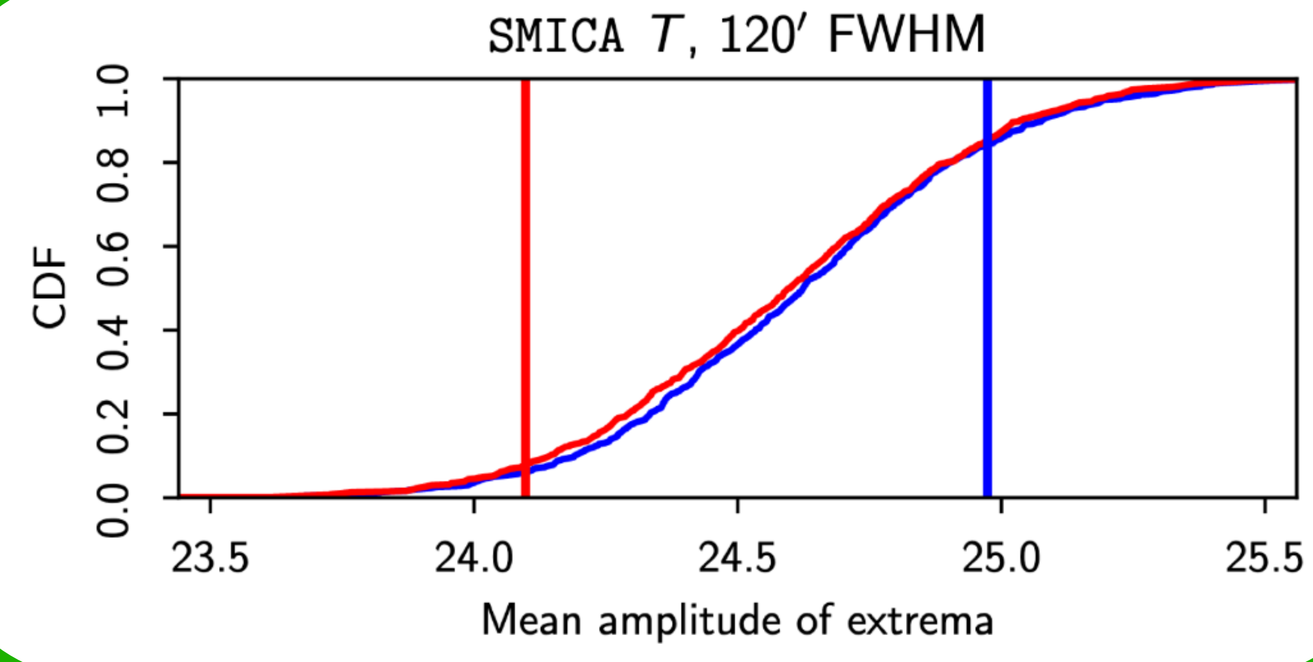

Inflation produces **PNG**, but non-linear physics after inflation also introduces non-Gaussianities. To learn about the early universe, we seek to understand PNG while isolating post-inflation foregrounds.

Figures from 1807.06208 and 1906.02552v2.

Perturbatively, PNG is a small correction to a Gaussian field.

$$\zeta(\mathbf{x}) = \zeta_G(\mathbf{x}) + \Delta\zeta(\mathbf{x})$$

Total post-inflation

Nearly Gaussian

NG deviation

Single-field inflation can only produce a PNG term from non-linear self-couplings of the sole Gaussian quantum field.

$$\zeta(\mathbf{x}) = \zeta_G(\mathbf{x}) + f_{\mathrm{NL}}\left(\zeta_G{}^2(\mathbf{x}) - \langle\zeta_G{}^2(\mathbf{x})\rangle\right)$$

Coupling constant

Quadratic Coupling

The CMB bispectrum constrains $f_{\mathrm{NL}} = 0.9 \pm 5.1$ with 1-σ C.L. [1905.05697].

ζ_G is of order 10^{-5}, so f_{NL}-type PNG is very small.

Multi-field inflation can give rise to PNG sourced by a functional relationship to uncorrelated fields.

$$\zeta(\mathbf{x}) = \zeta_G(\mathbf{x}) + F_{\mathrm{NL}}\left[\chi(\mathbf{x})\right]$$

Non-linear functional

Second early universe field

(independent of ζ_G)

This does not have the same tight CMB constraints!

Morrison *et al*. show that multi-field inflation produces primordial intermittent non-Gaussianity (PING) with spike power spectrum.

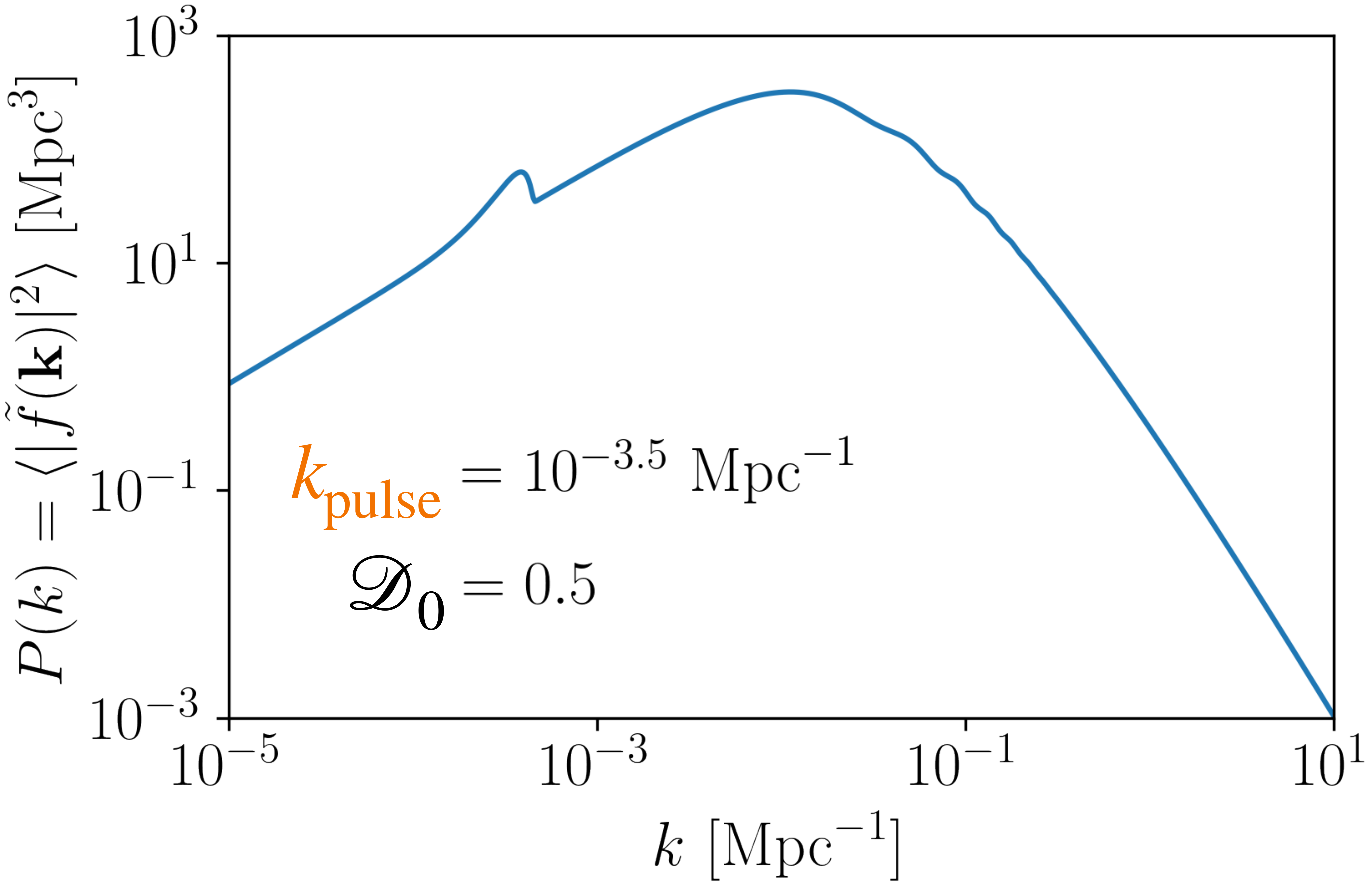

Power spectrum spike has **characteristic scale**

$$k_{\mathrm{pulse}}(\mathcal{Q}, a_e)$$

where $\mathcal{Q}$ and a_e are free parameters in inflation model.

Stay tuned for Morrison *et al* in prep

Morrison *et al*. show that multi-field inflation produces primordial intermittent non-Gaussianity (PING) with spike power spectrum.

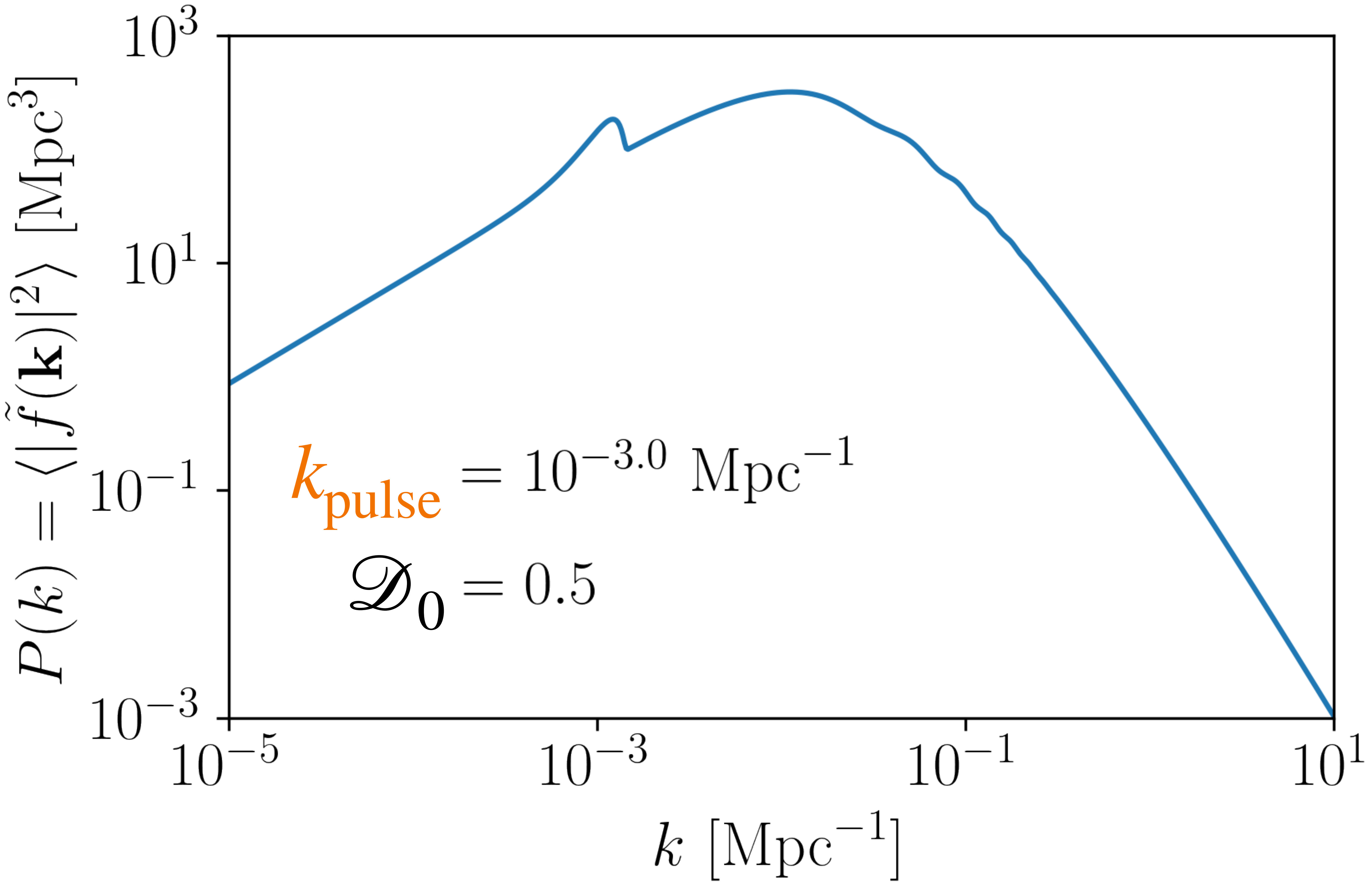

Power spectrum spike has **characteristic scale**

$$k_{\rm pulse}(\mathcal{Q}, a_e)$$

where $\mathcal{Q}$ and a_e are free parameters in inflation model.

Stay tuned for Morrison *et al* in prep

Morrison *et al*. show that multi-field inflation produces primordial intermittent non-Gaussianity (PING) with spike power spectrum.

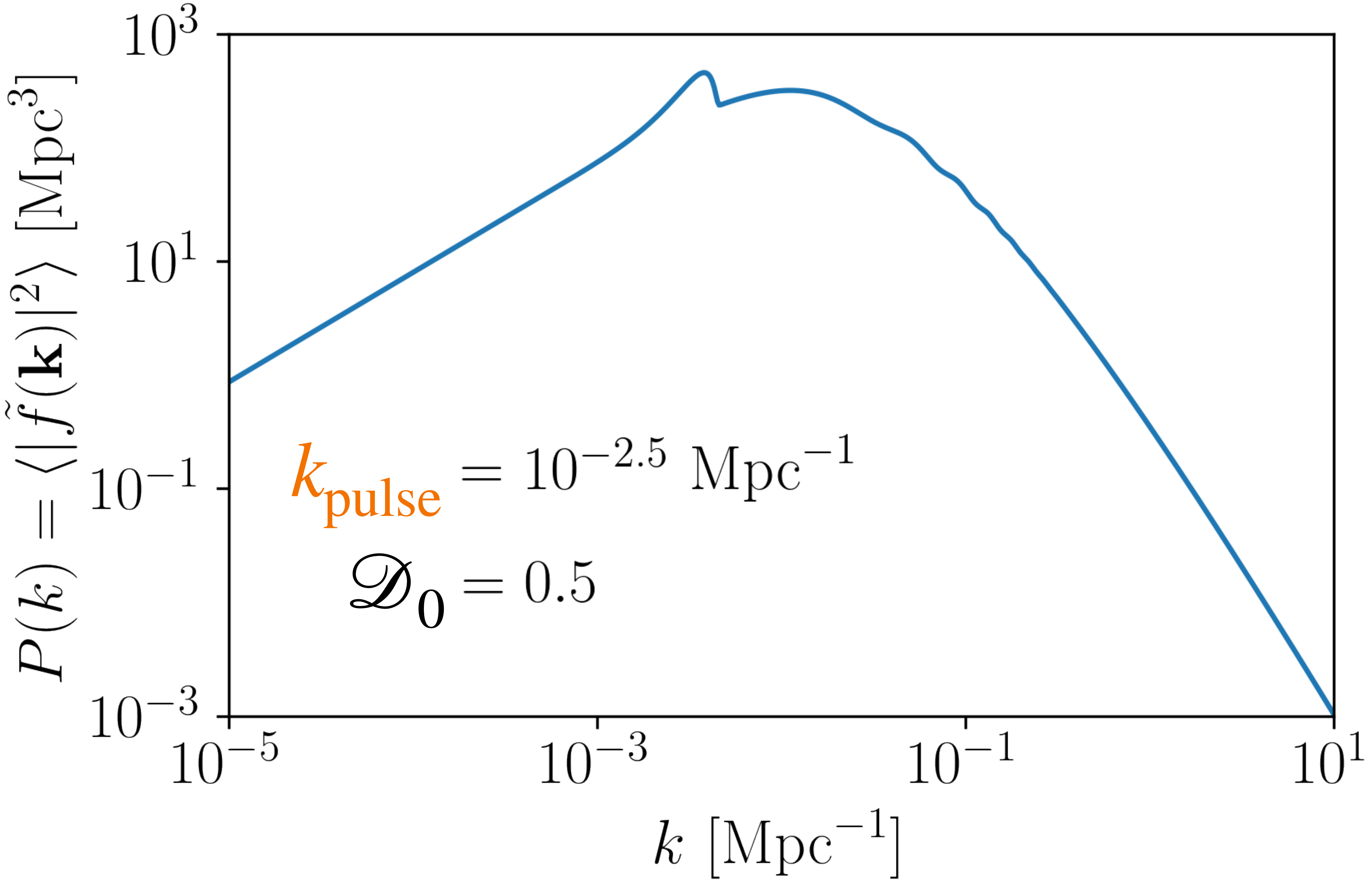

Power spectrum spike has **characteristic scale**

$$k_{\text{pulse}}(\mathcal{Q}, a_e)$$

where $\mathcal{Q}$ and a_e are free parameters in inflation model.

Stay tuned for Morrison *et al* in prep

Morrison *et al*. show that multi-field inflation produces primordial intermittent non-Gaussianity (PING) with spike power spectrum.

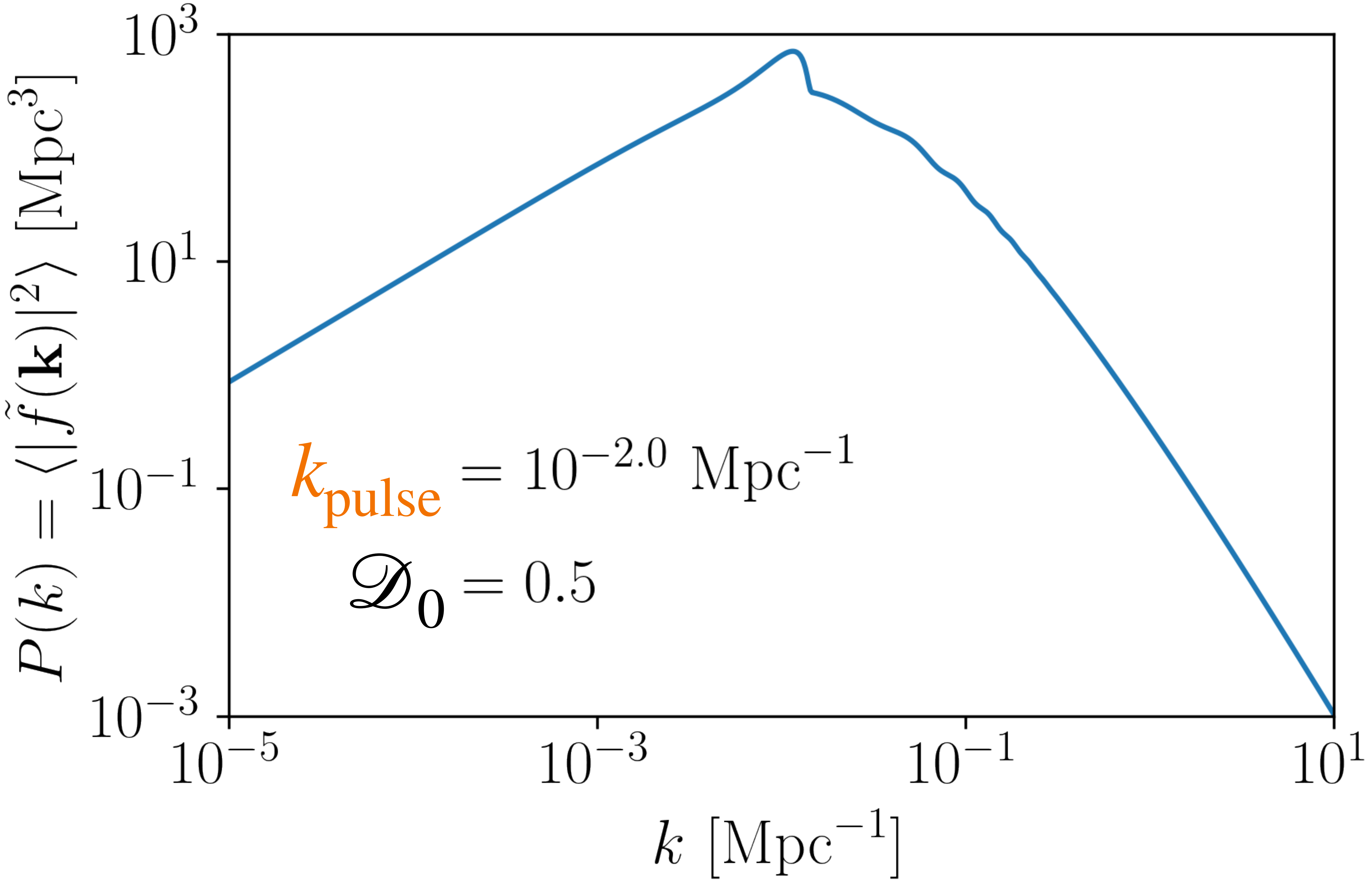

Power spectrum spike has **characteristic scale**

$$k_{\text{pulse}}(\mathcal{Q}, a_e)$$

where $\mathcal{Q}$ and a_e are free parameters in inflation model.

Stay tuned for Morrison *et al* in prep

Morrison *et al*. show that multi-field inflation produces primordial intermittent non-Gaussianity (PING) with spike power spectrum.

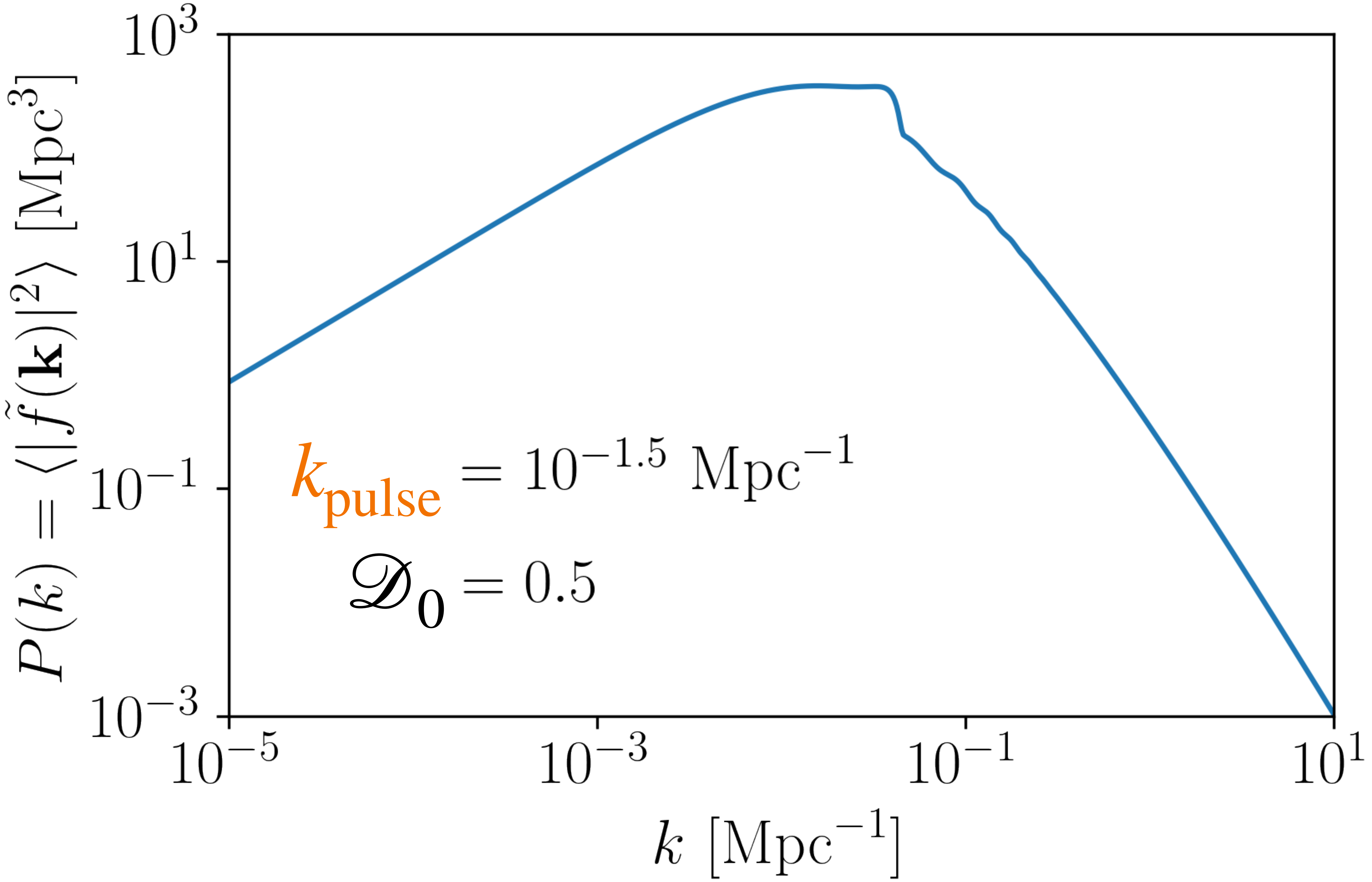

Power spectrum spike has **characteristic scale**

$$k_{\text{pulse}}(\mathcal{Q}, a_e)$$

where $\mathcal{Q}$ and a_e are free parameters in inflation model.

Stay tuned for Morrison *et al* in prep

Morrison *et al*. show that multi-field inflation produces primordial intermittent non-Gaussianity (PING) with spike power spectrum.

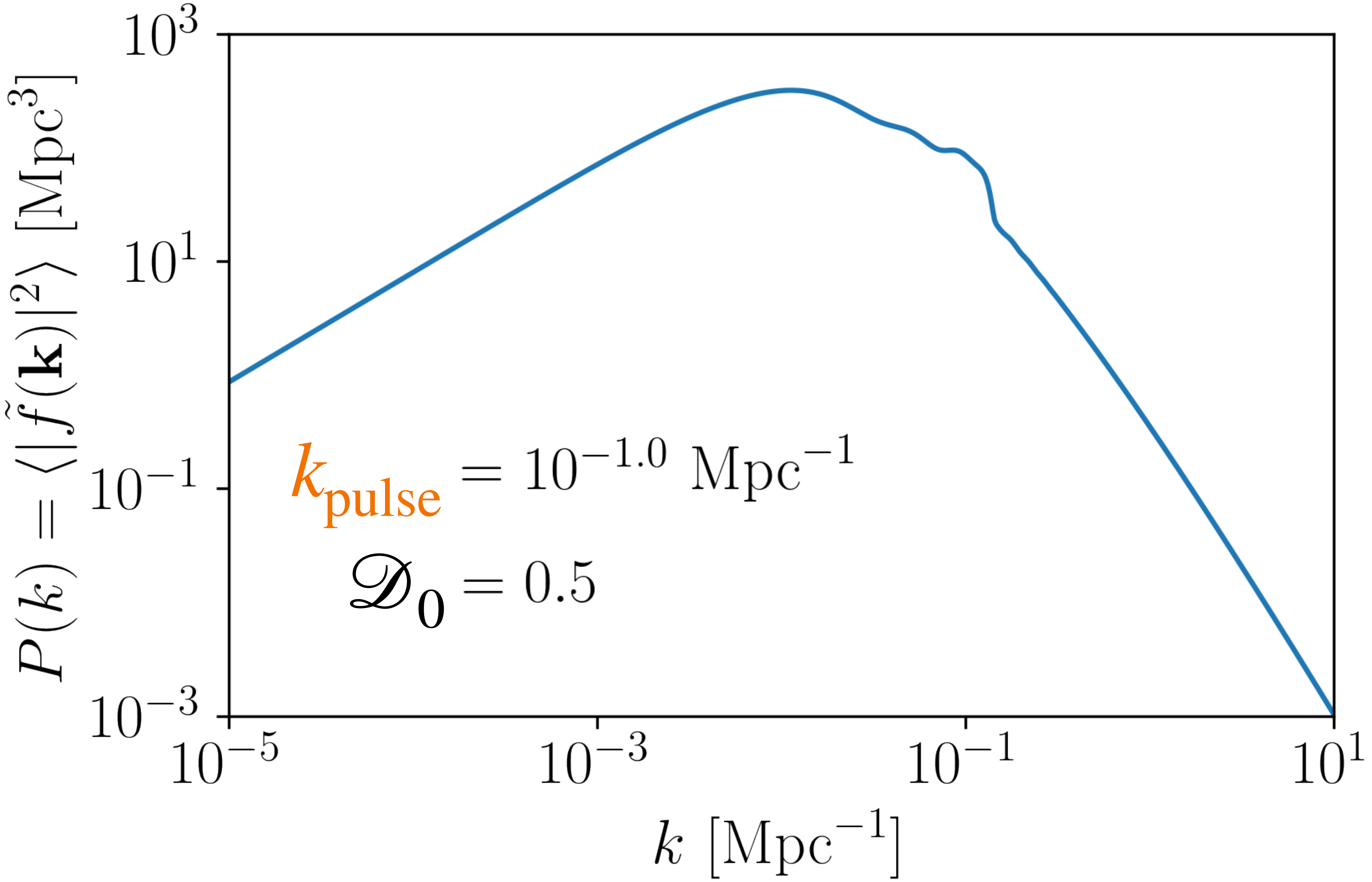

Power spectrum spike has **characteristic scale**

$$k_{\rm pulse}(\mathscr{Q}, a_e)$$

where $\mathscr{Q}$ and a_e are free parameters in inflation model.

Stay tuned for Morrison *et al* in prep

Morrison *et al*. show that multi-field inflation produces primordial intermittent non-Gaussianity (PING) with spike power spectrum.

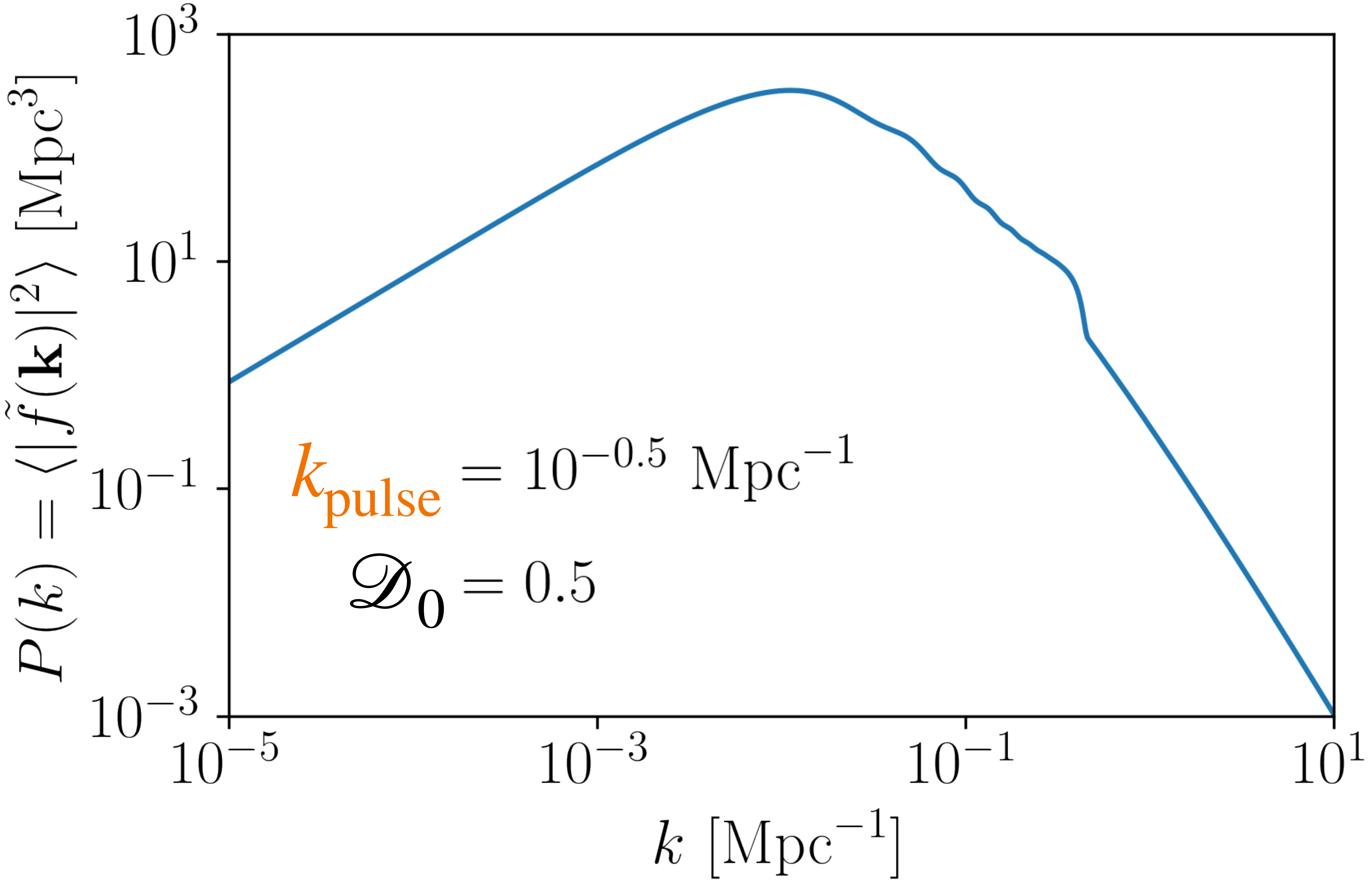

Power spectrum spike has **characteristic scale**

$$k_{\text{pulse}}(\mathcal{Q}, a_e)$$

where $\mathcal{Q}$ and a_e are free parameters in inflation model.

Stay tuned for Morrison *et al* in prep

Morrison *et al*. show that multi-field inflation produces primordial intermittent non-Gaussianity (PING) with spike power spectrum.

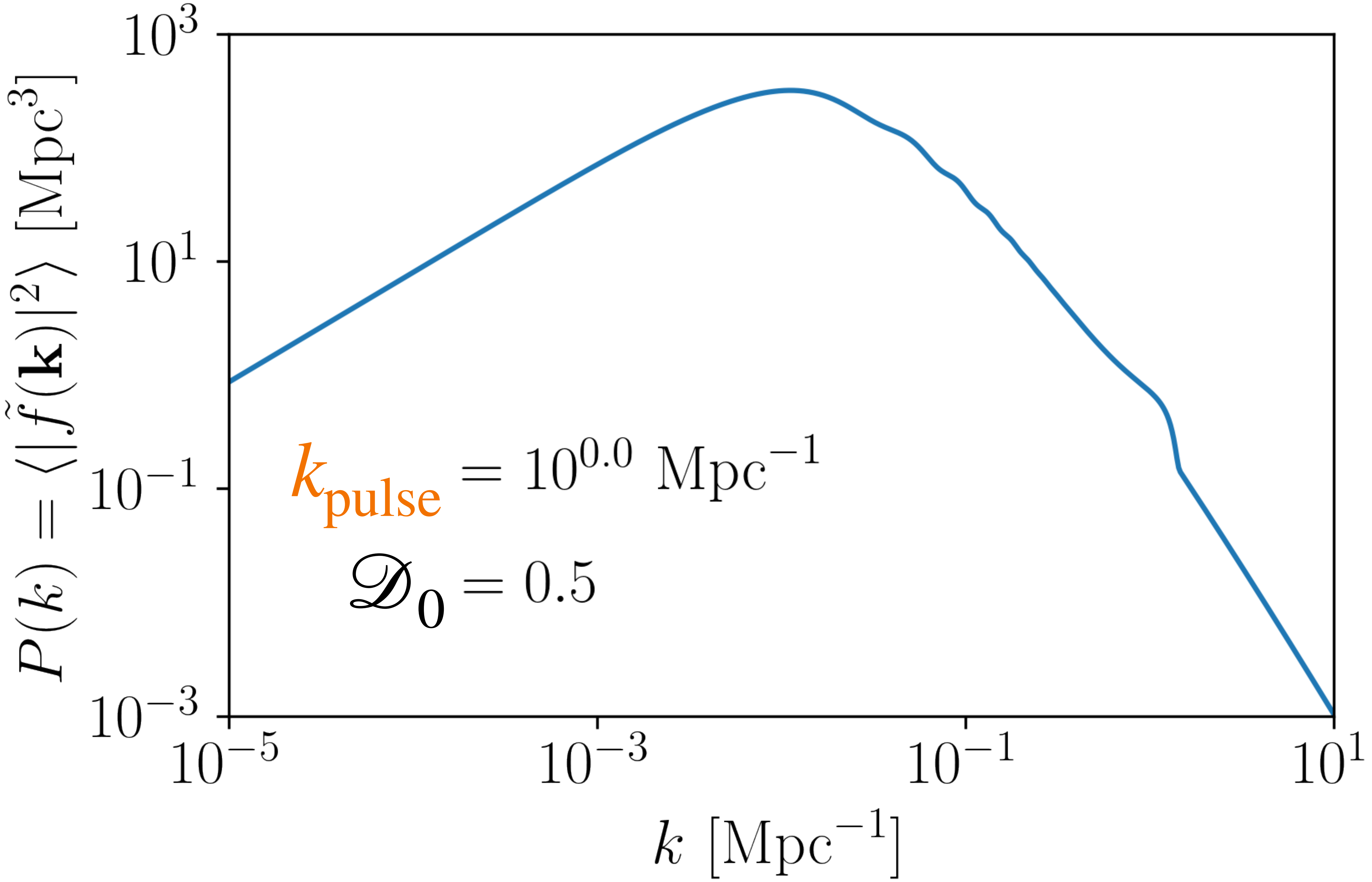

Power spectrum spike has **characteristic scale**

$$k_{\rm pulse}(\mathcal{Q}, a_e)$$

where $\mathcal{Q}$ and a_e are free parameters in inflation model.

Stay tuned for Morrison *et al* in prep

Morrison *et al*. show that multi-field inflation produces primordial intermittent non-Gaussianity (PING) with spike power spectrum.

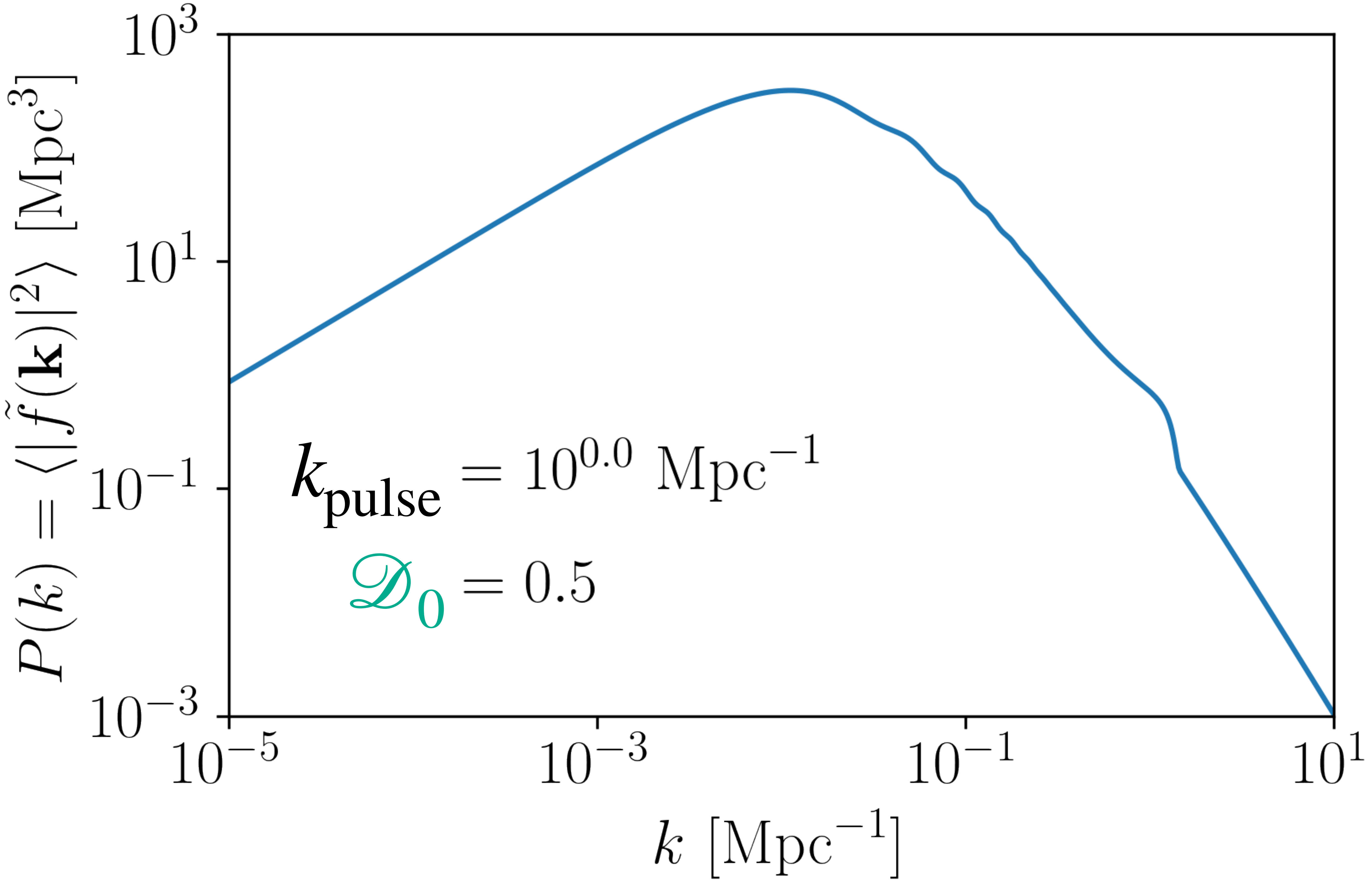

Power spectrum spike has **characteristic scale**

$$k_{\text{pulse}}(\mathcal{Q}, a_e)$$

and **relative amplitude**

$$\mathscr{D}_0(\mathcal{Q})$$

where $\mathcal{Q}$ and a_e are free parameters in inflation model.

Stay tuned for Morrison *et al* in prep

Morrison *et al*. show that multi-field inflation produces primordial intermittent non-Gaussianity (PING) with spike power spectrum.

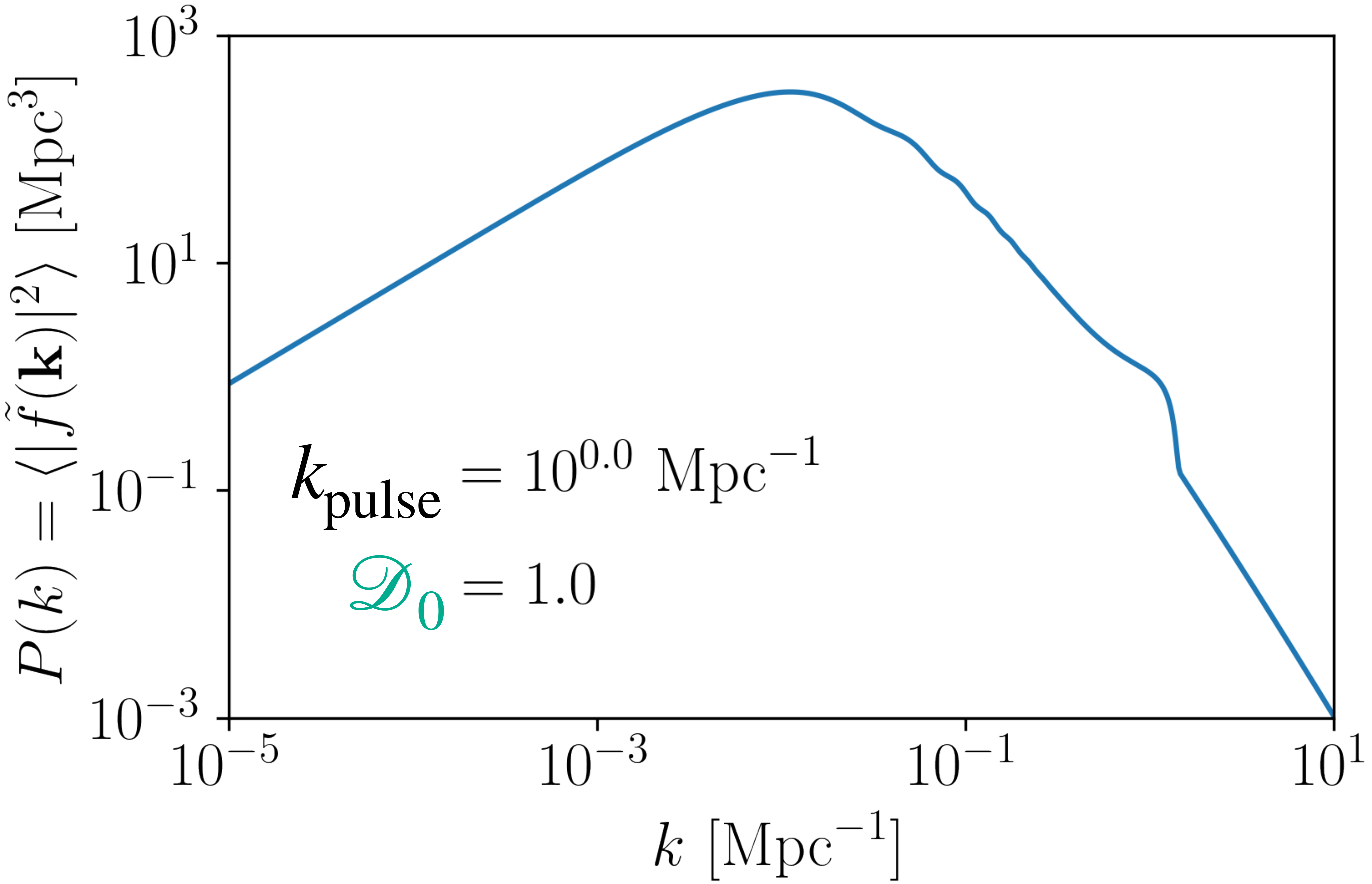

Power spectrum spike has **characteristic scale**

$$k_{\rm pulse}(\mathscr{Q}, a_e)$$

and **relative amplitude**

$$\mathscr{D}_0(\mathscr{Q})$$

where $\mathscr{Q}$ and a_e are free parameters in inflation model.

Stay tuned for Morrison *et al* in prep

Morrison *et al*. show that multi-field inflation produces primordial intermittent non-Gaussianity (PING) with spike power spectrum.

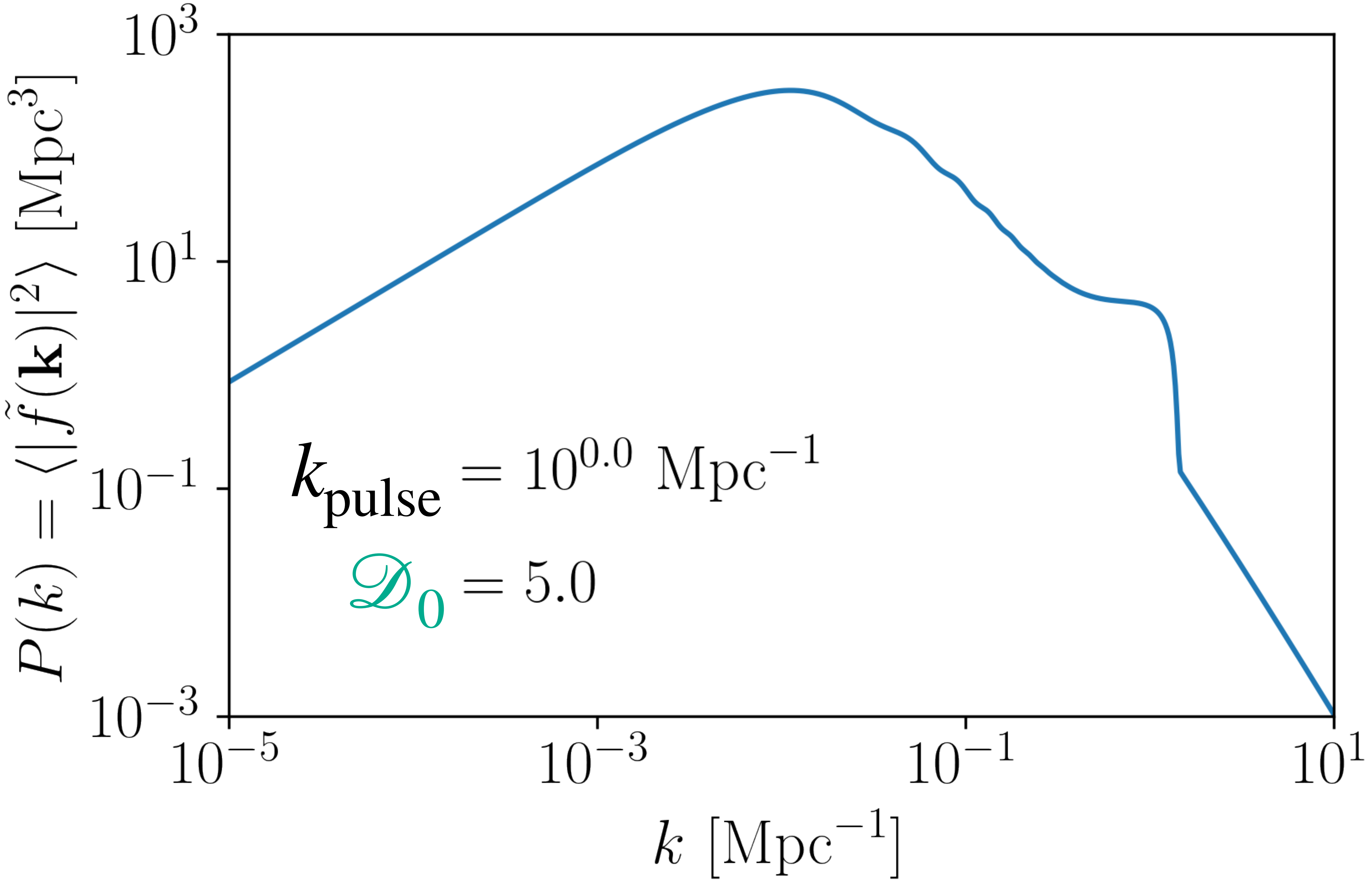

Power spectrum spike has **characteristic scale**

$$k_{\rm pulse}(\mathcal{Q}, a_e)$$

and **relative amplitude**

$$\mathscr{D}_0(\mathcal{Q})$$

where $\mathcal{Q}$ and a_e are free parameters in inflation model.

Stay tuned for Morrison *et al* in prep

Morrison *et al*. show that multi-field inflation produces primordial intermittent non-Gaussianity (PING) with spike power spectrum.

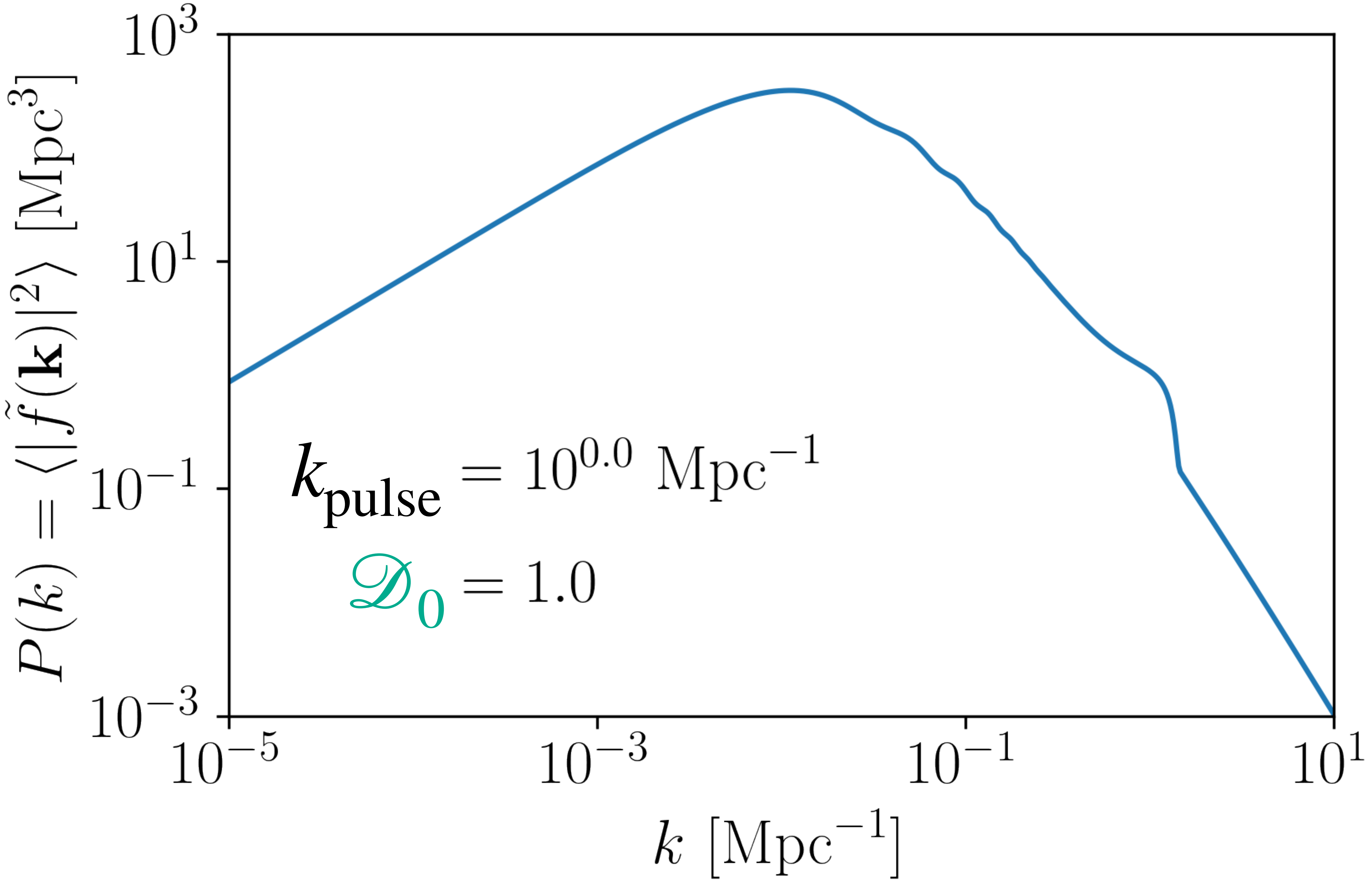

Power spectrum spike has **characteristic scale**

$$k_{\rm pulse}(\mathcal{Q}, a_e)$$

and **relative amplitude**

$$\mathscr{D}_0(\mathcal{Q})$$

where $\mathcal{Q}$ and a_e are free parameters in inflation model.

Stay tuned for Morrison *et al* in prep

Morrison *et al*. show that multi-field inflation produces primordial intermittent non-Gaussianity (PING) with spike power spectrum.

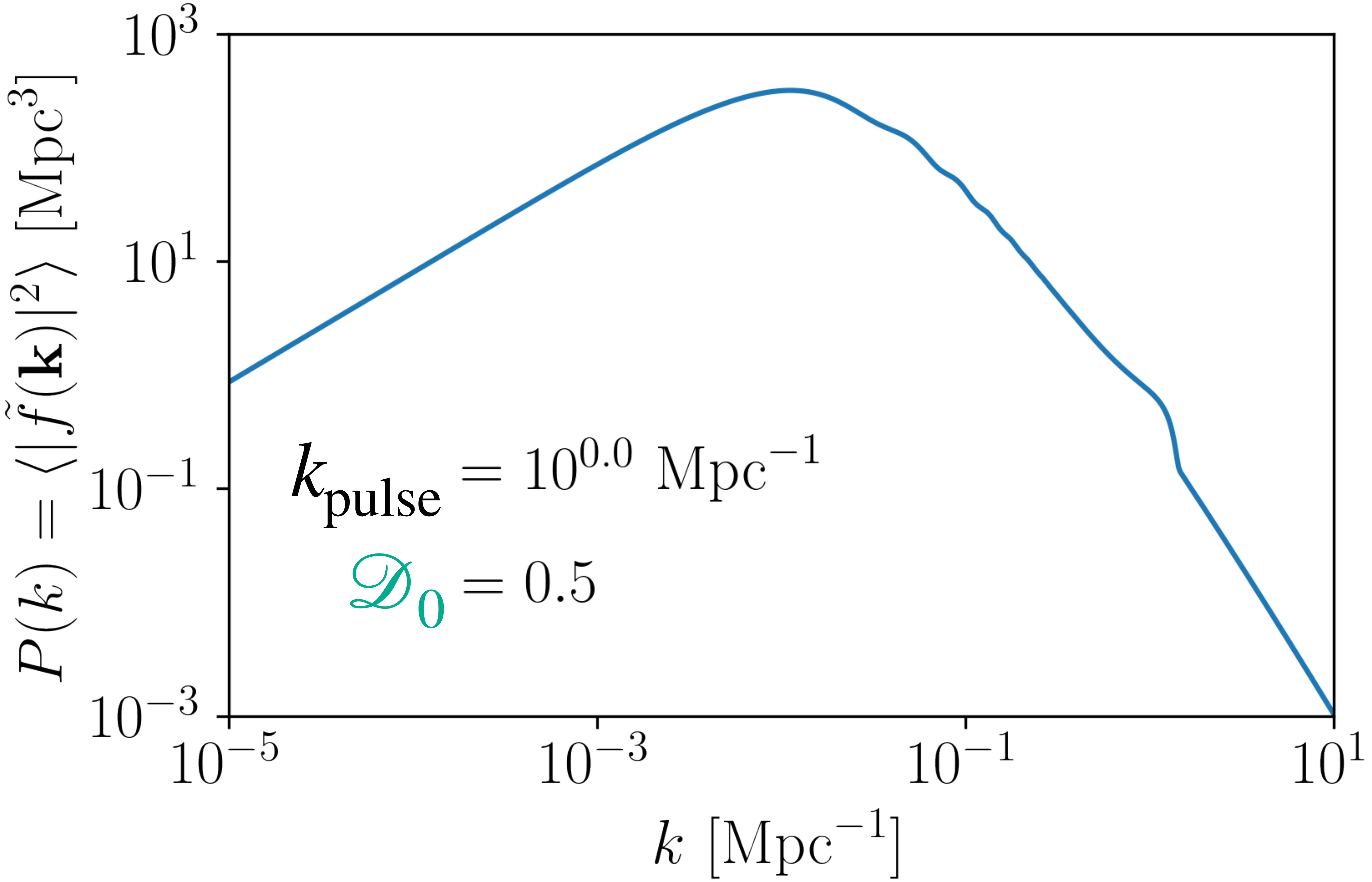

Power spectrum spike has **characteristic scale**

$$k_{\mathrm{pulse}}(\mathscr{Q}, a_e)$$

and **relative amplitude**

$$\mathscr{D}_0(\mathscr{Q})$$

where $\mathscr{Q}$ and a_e are free parameters in inflation model.

Stay tuned for Morrison *et al* in prep

Morrison *et al*. show that multi-field inflation produces primordial intermittent non-Gaussianity (PING) with spike power spectrum.

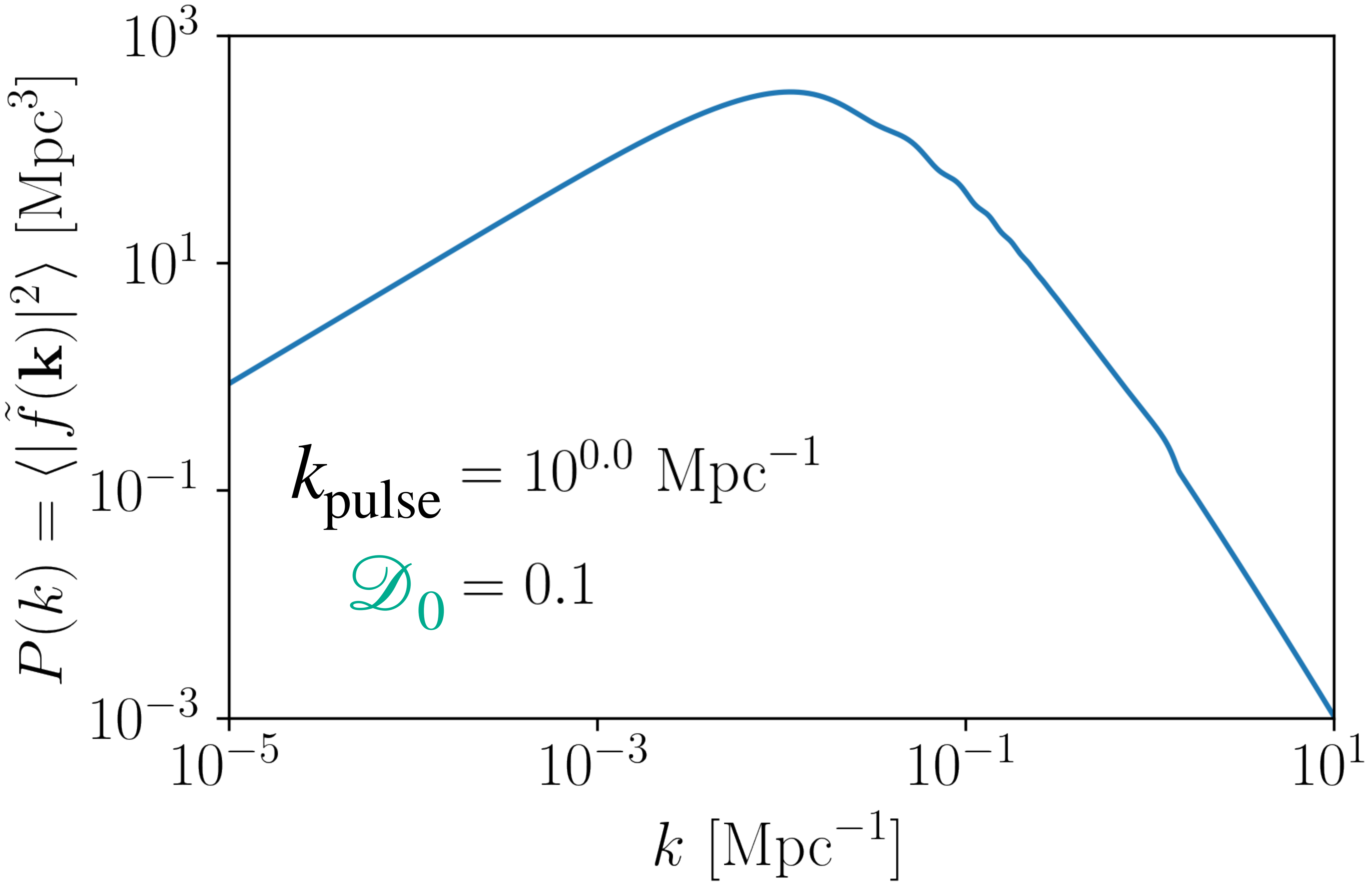

Power spectrum spike has **characteristic scale**

$$k_{\text{pulse}}(\mathcal{Q}, a_e)$$

and **relative amplitude**

$$\mathscr{D}_0(\mathcal{Q})$$

where $\mathcal{Q}$ and a_e are free parameters in inflation model.

Stay tuned for Morrison *et al* in prep

Morrison *et al*. show that multi-field inflation produces primordial intermittent non-Gaussianity (PING) with spike power spectrum.

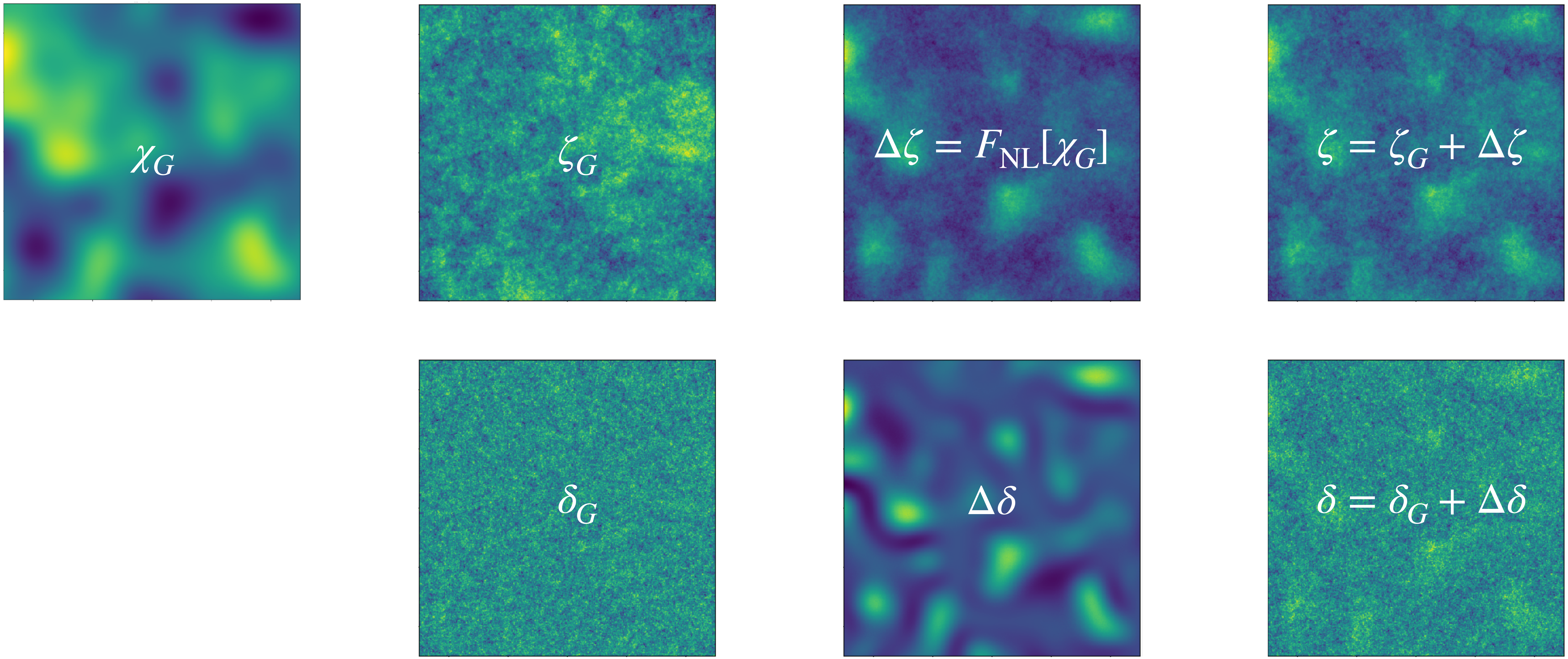

Stay tuned for Morrison *et al* in prep

WebSky2.0 non-Gaussian LIM Forecasting

using forecasts to refine our LIM models and constrain PING

The voxel intensity distribution (VID) as a statistic for forecasting.

Theoretical **noise-free** VID

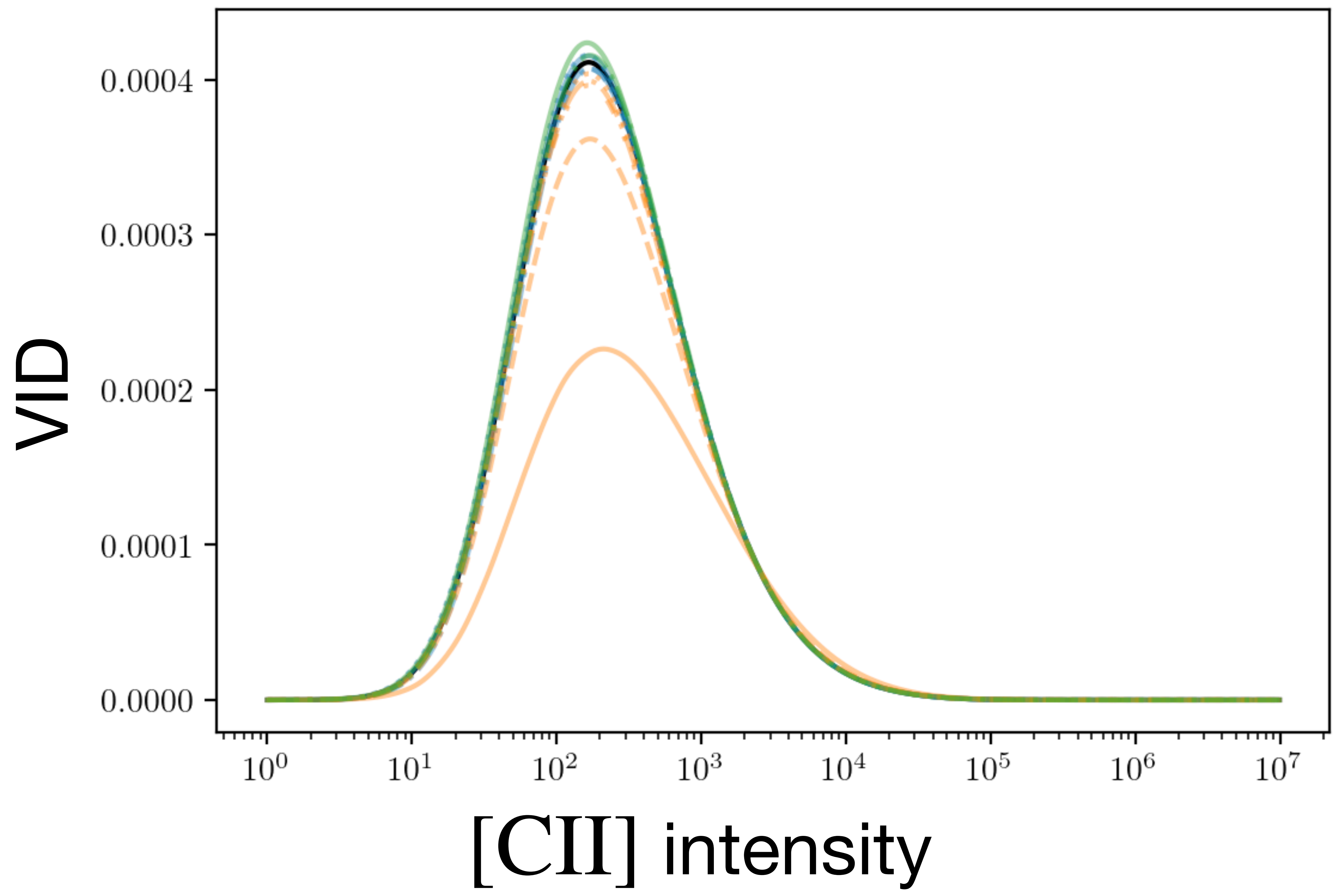

VID with **next-gen CCAT noise**

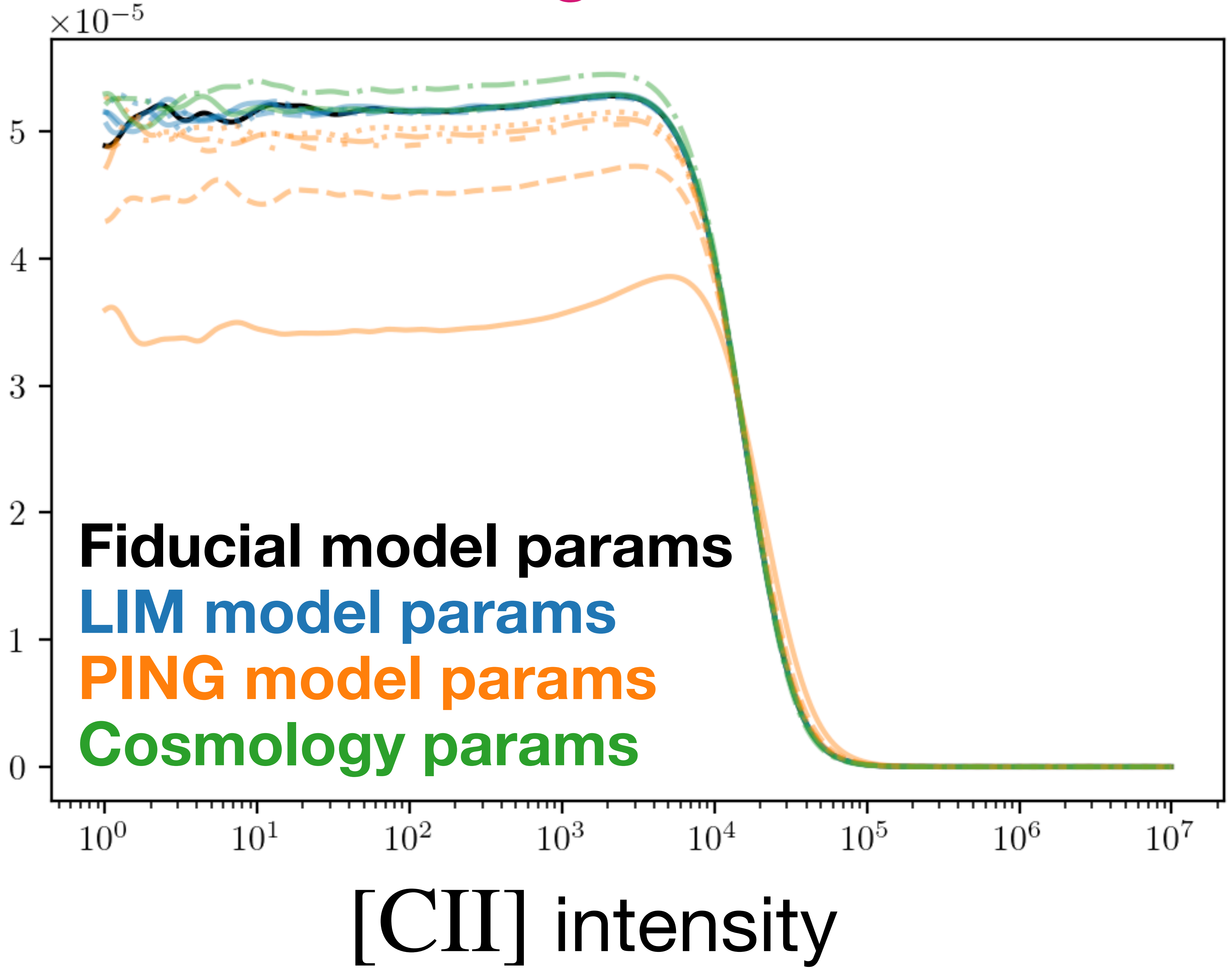

To quantify the degree of surprise between the fiducial and other models, we look at **relative entropy**.

Differential relative (negative) entropy tells us about information content in intensity space for each model parameter.

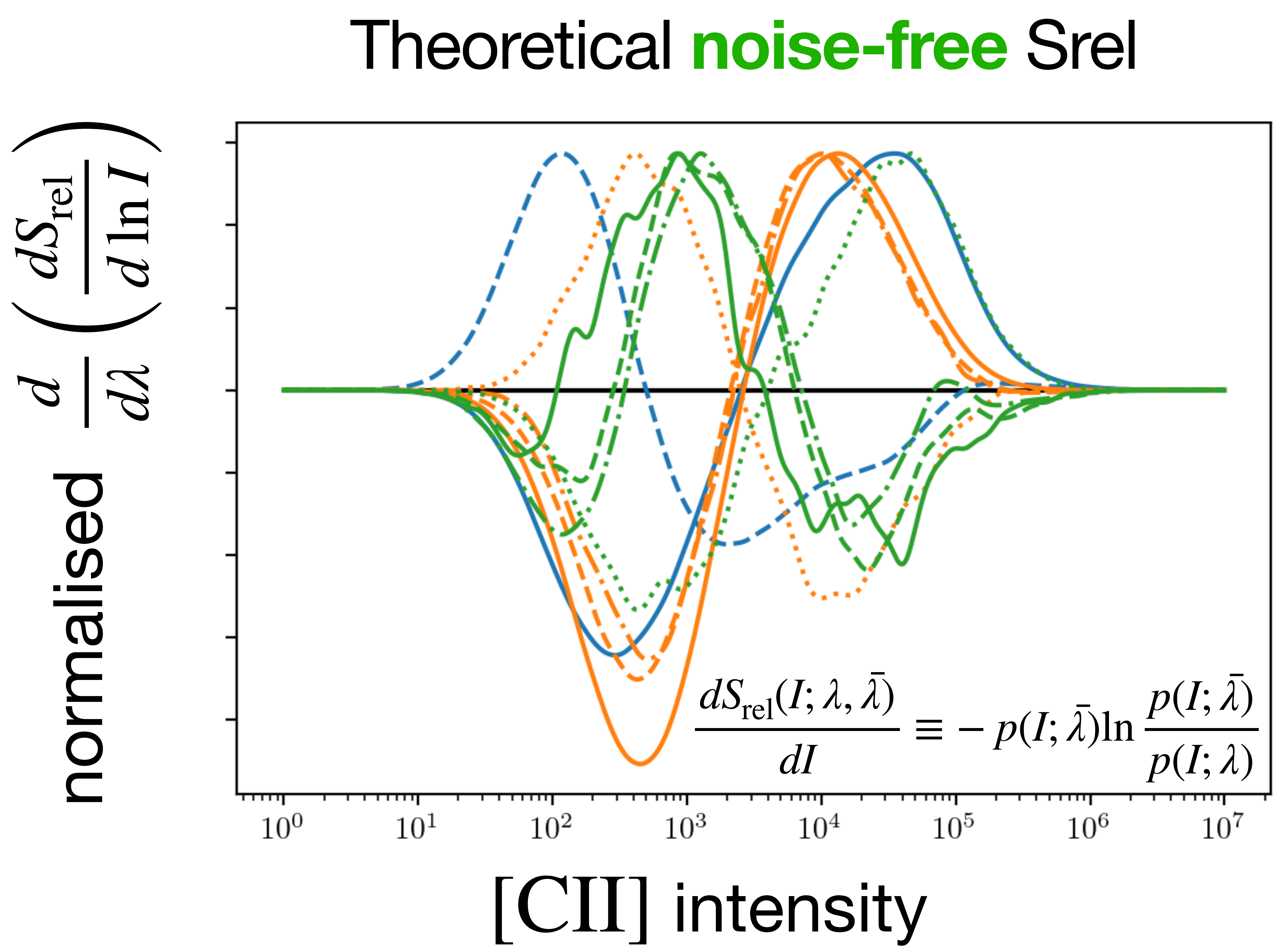

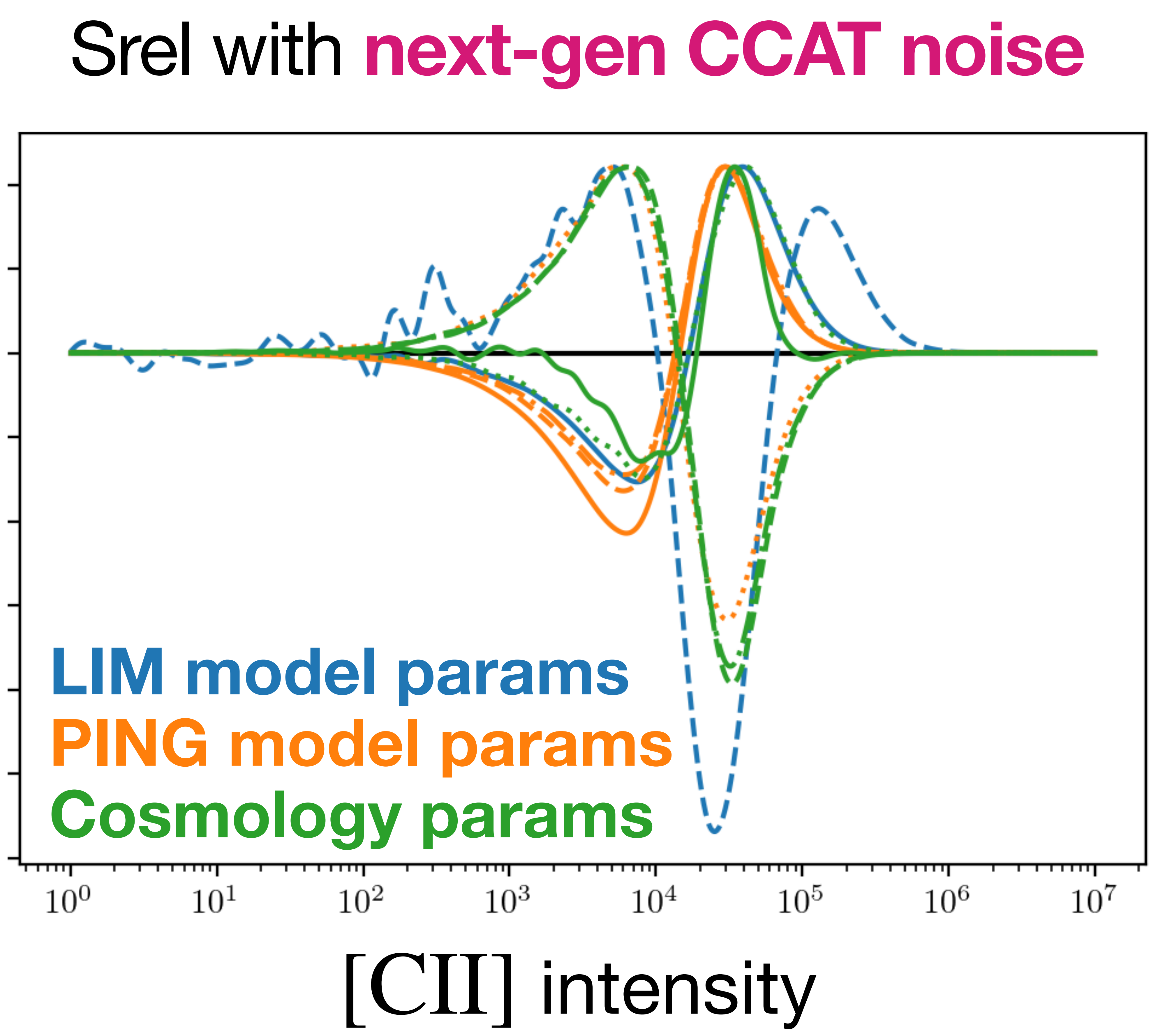

In both noise-free and noisy sims, we see hints that LIM model parameters have a different information content than PING model parameters and cosmology. We can feed this into a **Fisher Forecast**.

Marginalising over minimally cross-correlated variables, the correlations between parameters of distinct physics models are minimal.

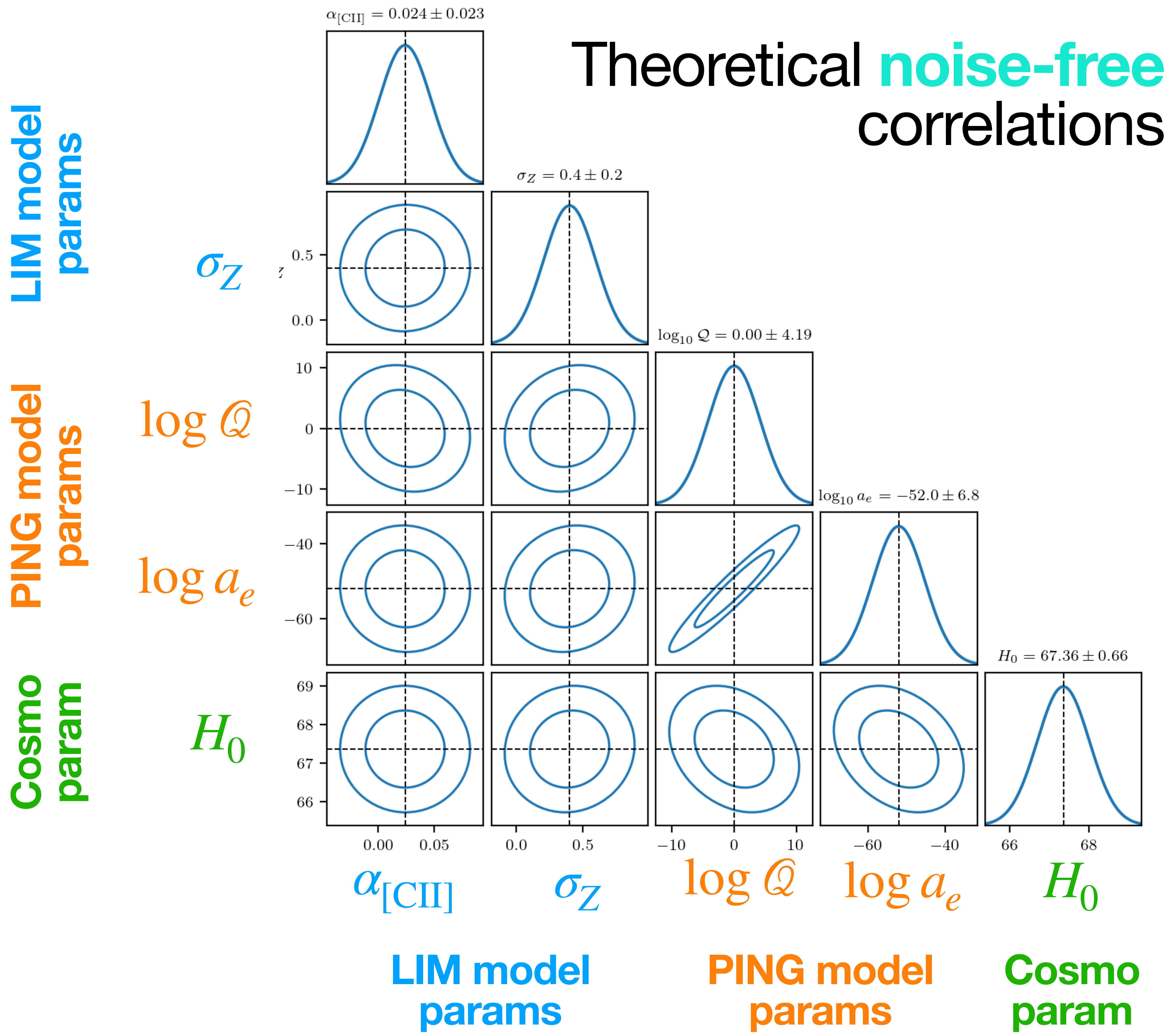

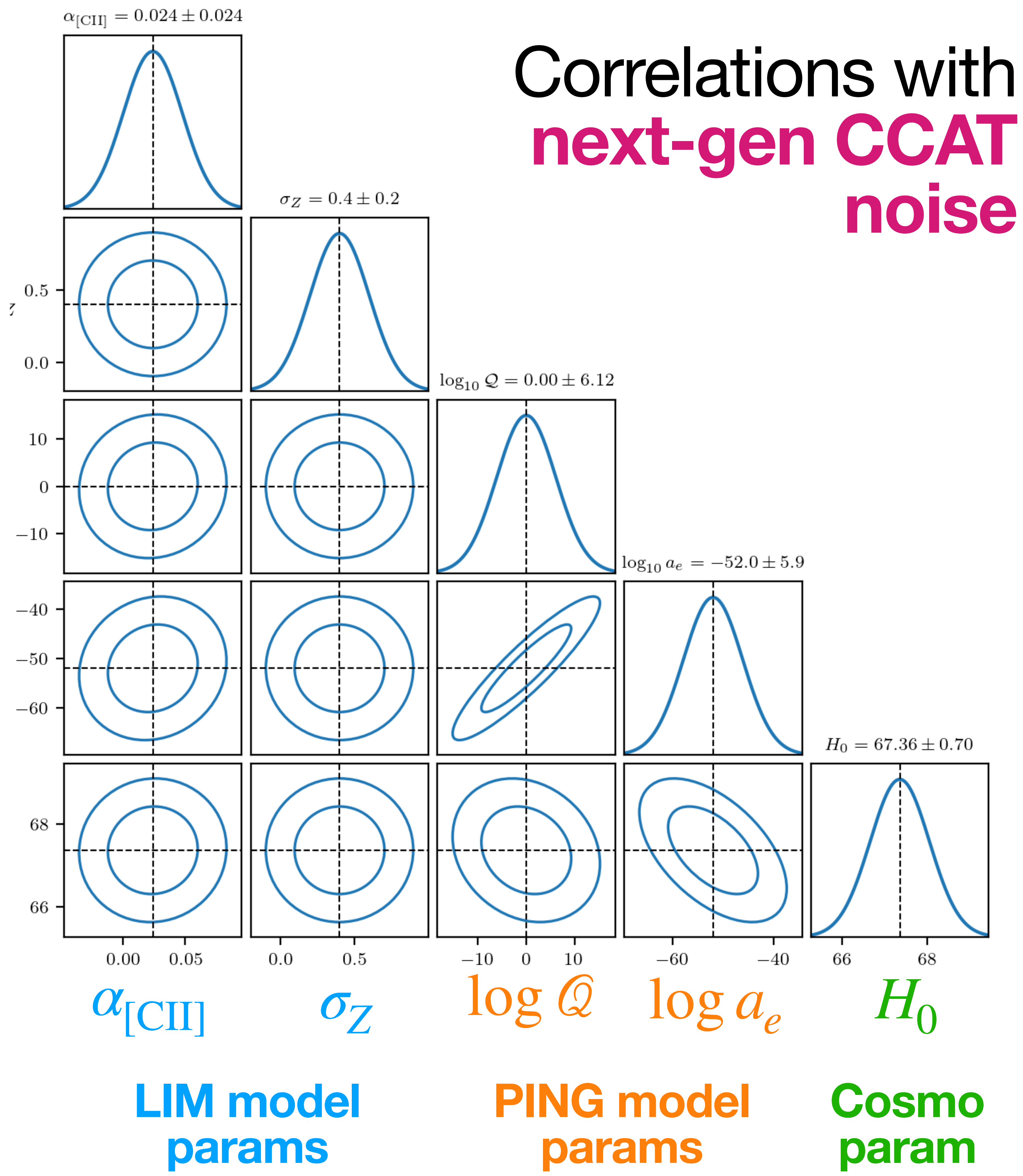

Marginalising over minimally cross-correlated variables, the correlations between parameters of distinct physics models are minimal.

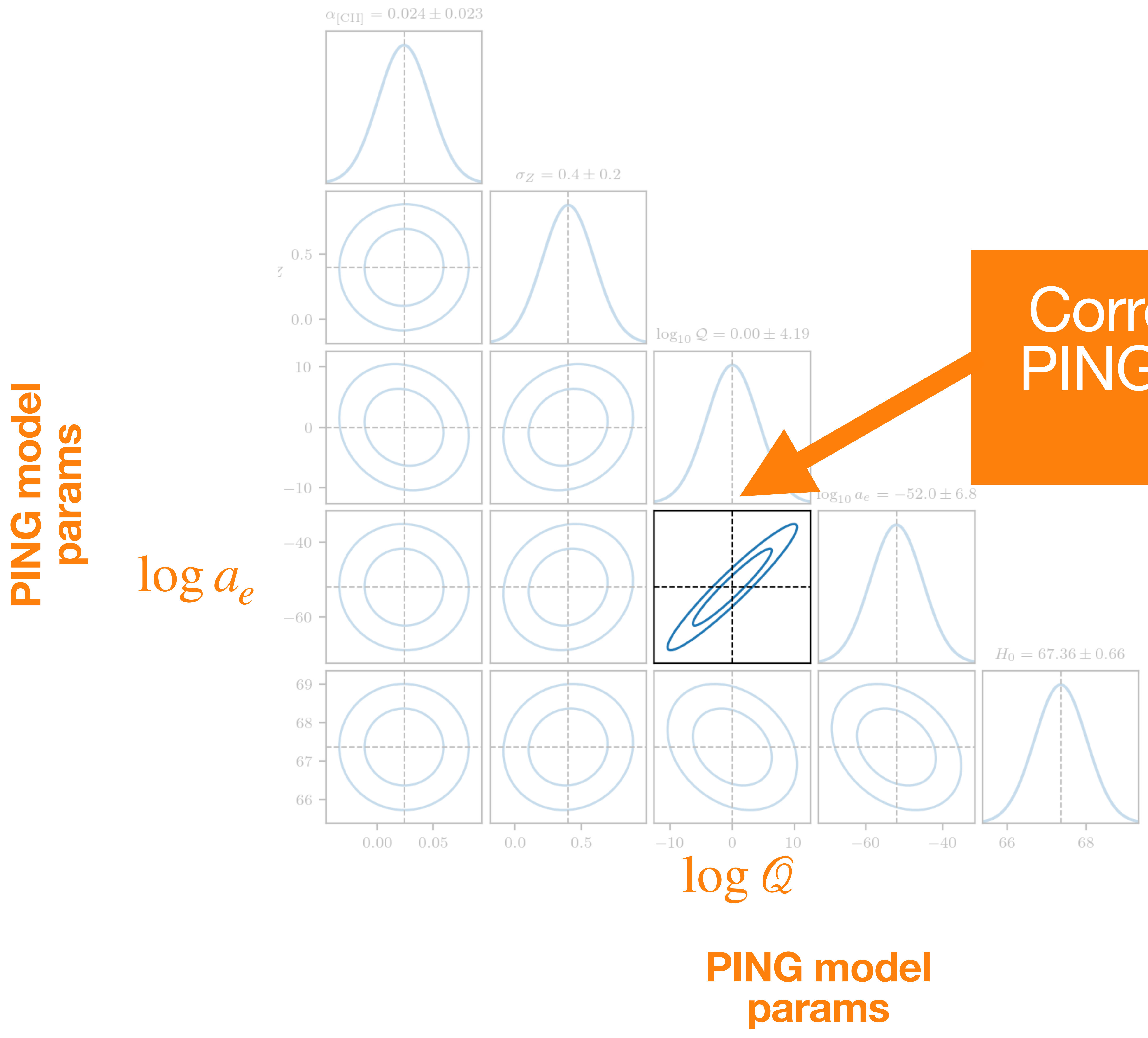

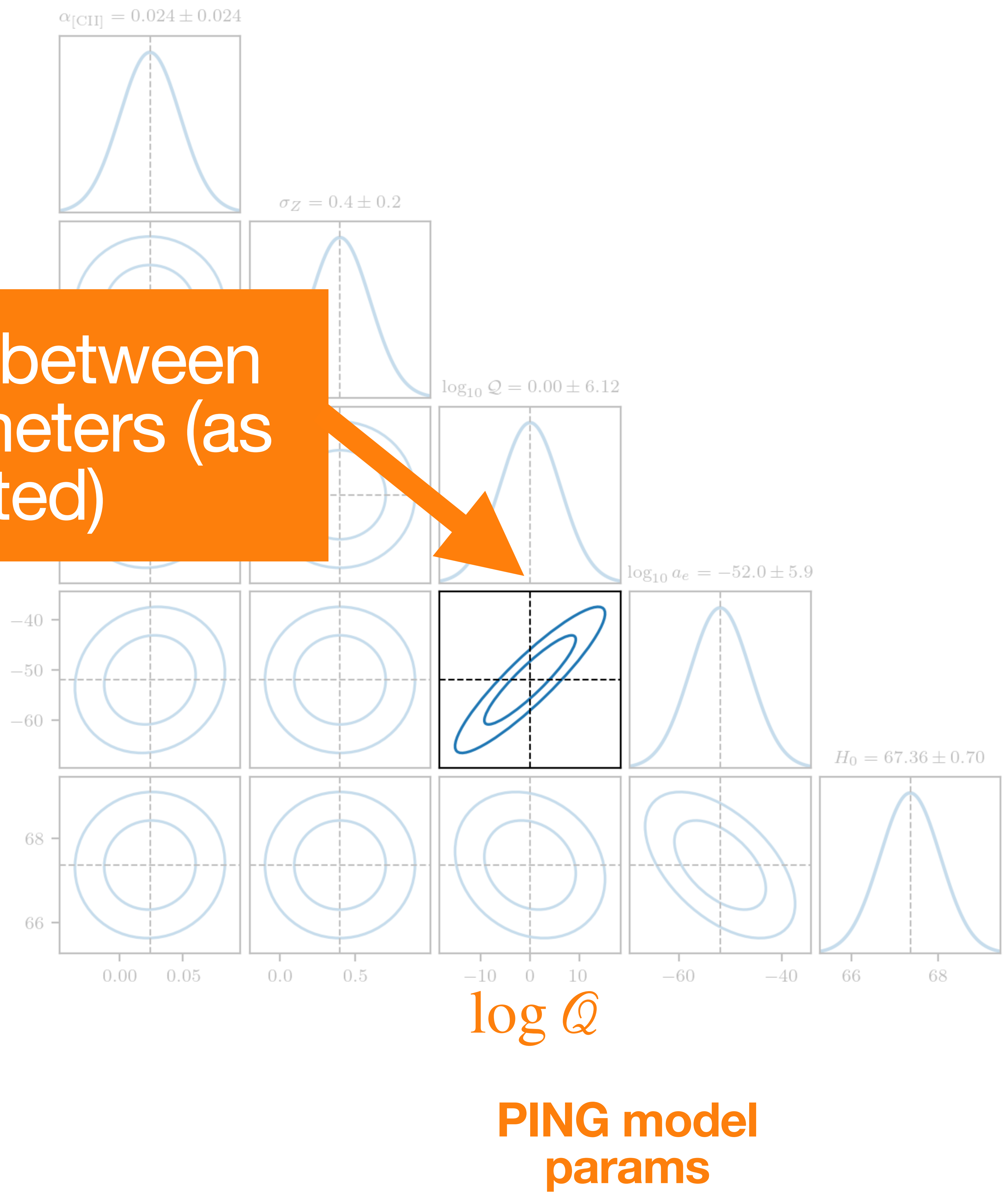

Correlation between PING parameters (as expected)

Marginalising over minimally cross-correlated variables, the correlations between parameters of distinct physics models are minimal.

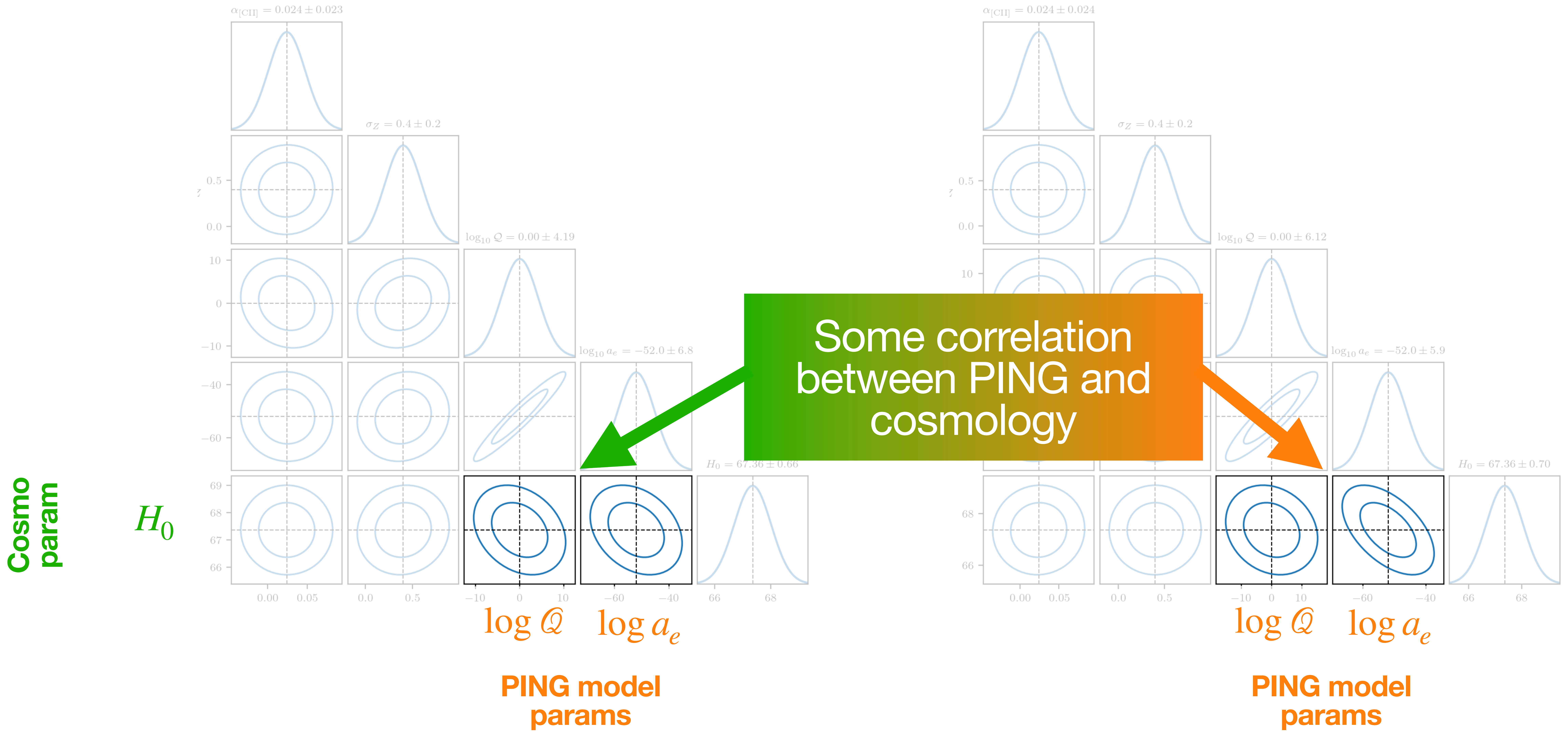

Marginalising over minimally cross-correlated variables, the correlations between parameters of distinct physics models are minimal.

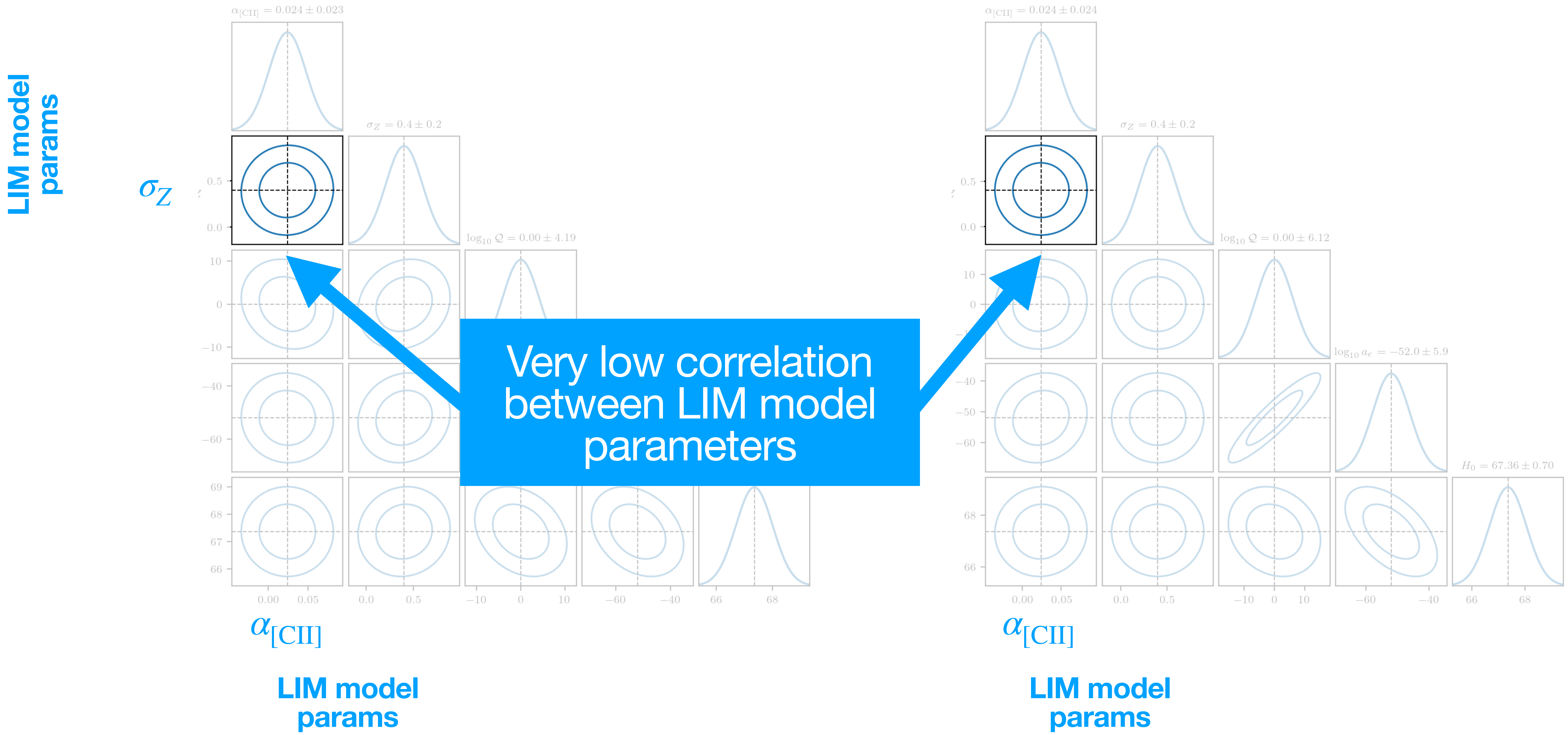

Marginalising over minimally cross-correlated variables, the correlations between parameters of distinct physics models are minimal.

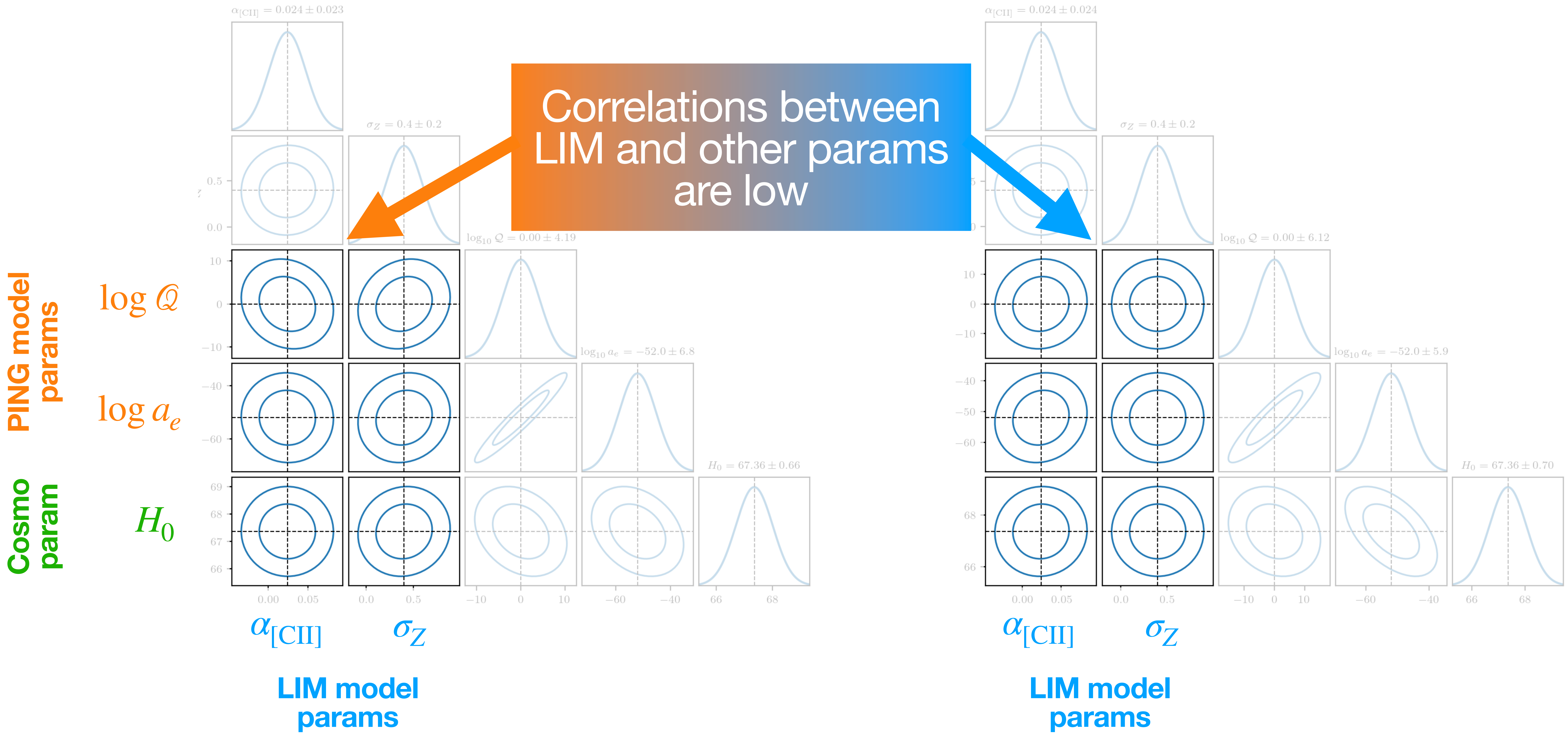

Conclusions

Conclusions

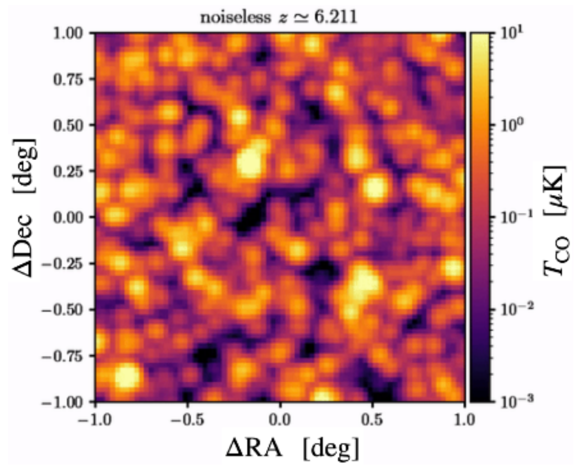

WebSky2.0 produces mock maps for upcoming LIM surveys that are much needed as new observatories come online.

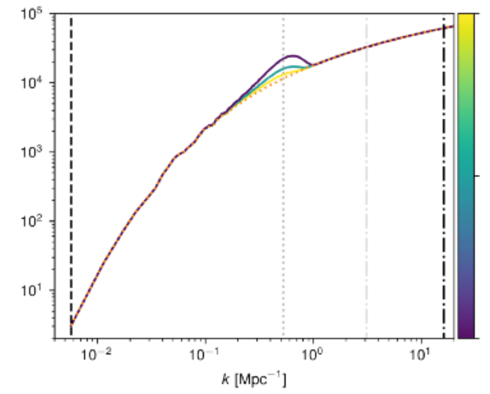

The search for new physics such as PINGs can be constrained using *WebSky2.0* mock maps.

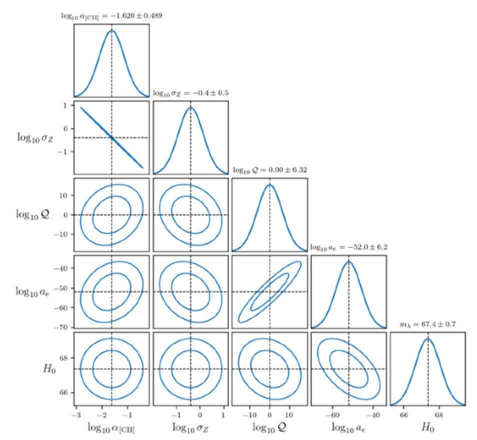

WebSky2.0 forecasts show LIM parameters can be differentiated from ΛCDM and early universe model parameters.

PINGs represent a novel science case for LIM surveys.

Extra Slides

To translate from DM halos to LIM mocks, we must formulate a line emission model

The [CII] model from Horlaville *et* al., [2309.15733]:

$$\frac{L_{[\mathrm{CII}],c}(M_c, z_c)}{L_\odot} = \alpha_{[\mathrm{CII}]} \frac{M_{\mathrm{HI},c}(M_c)}{M_\odot} \frac{\zeta_Z Z_c(M_c, z_c)}{Z_\odot}$$

where $\alpha_{[\mathrm{CII}]} \sim 0.024$ and ζ_Z is drawn from a log-normal distribution with scatter $\sigma_Z \sim 0.4$. The HI mass is a power law fit to simulations with an exponential cutoff at low halo masses

$$M_{\mathrm{HI},c}(M_c) = M_{\mathrm{HI},0} \left(\frac{M_c/M_\odot}{M_{\mathrm{min}}} \right)^{\alpha_{\mathrm{HI}}} \exp \left[- \left(\frac{M_c/M_\odot}{M_{\mathrm{min}}} \right)^{-0.35} \right]$$

e.g. see Villaescusa-Navarro et al., [1804.09180].

Advantages of *Peak Patch*:

- Accurately reproduces results of larger *N*-body and hydrodynamical codes, at far less expense, and competitively compared to other fast methods

- Support for making **light cones**, so more distant regions appear younger just as they do in observations

- Run from any initial energy distribution, so we can **easily incorporate non-Gaussian** models

- Dynamics done using **low-order perturbation theory** so catalogues are not overly sensitive to highly nonlinear dynamics that might be more significantly affected by non-Gaussian models

- **Fast and efficient** so we can vary many parameters between runs and simulate very large regions of space (~0.5 core years for the initial *Peak Patch* public release)

- Interfaces with ***WebSky*** to make mock sky maps.

We are making updates to the *WebSky* mapmaking pipeline, working toward a public release of *WebSky2.0* mocks featuring unprecedented resolution full-sky maps needed for upcoming surveys for cosmologies with a suite of Gaussian and non-Gaussian initial conditions.

- Relativistic corrections to tSZ (Zack Li)
- Overhaul of CIB spectral energy distributions (Dongwoo Chung)
- Post-Born approximation to lensing (Nate Carlson)
- Optimizing for computer architecture to make the largest possible halo catalogues (Nate Carlson)
- Peak patch updates

These mocks are necessary for next-gen surveys like SO and CCAT, which have much greater angular resolution and will require halo masses below $M200m \sim 10^{12} M_\odot$, the resolution which existing ***WebSky*** catalogues targeted.

Primordial intermittent NG (PING) with $\Delta\zeta(\mathbf{x}) = F_{\rm NL}[\chi(\mathbf{x})]$ arises during multi-field inflation if there is a potential feature with $m_\chi^2 < 0$.

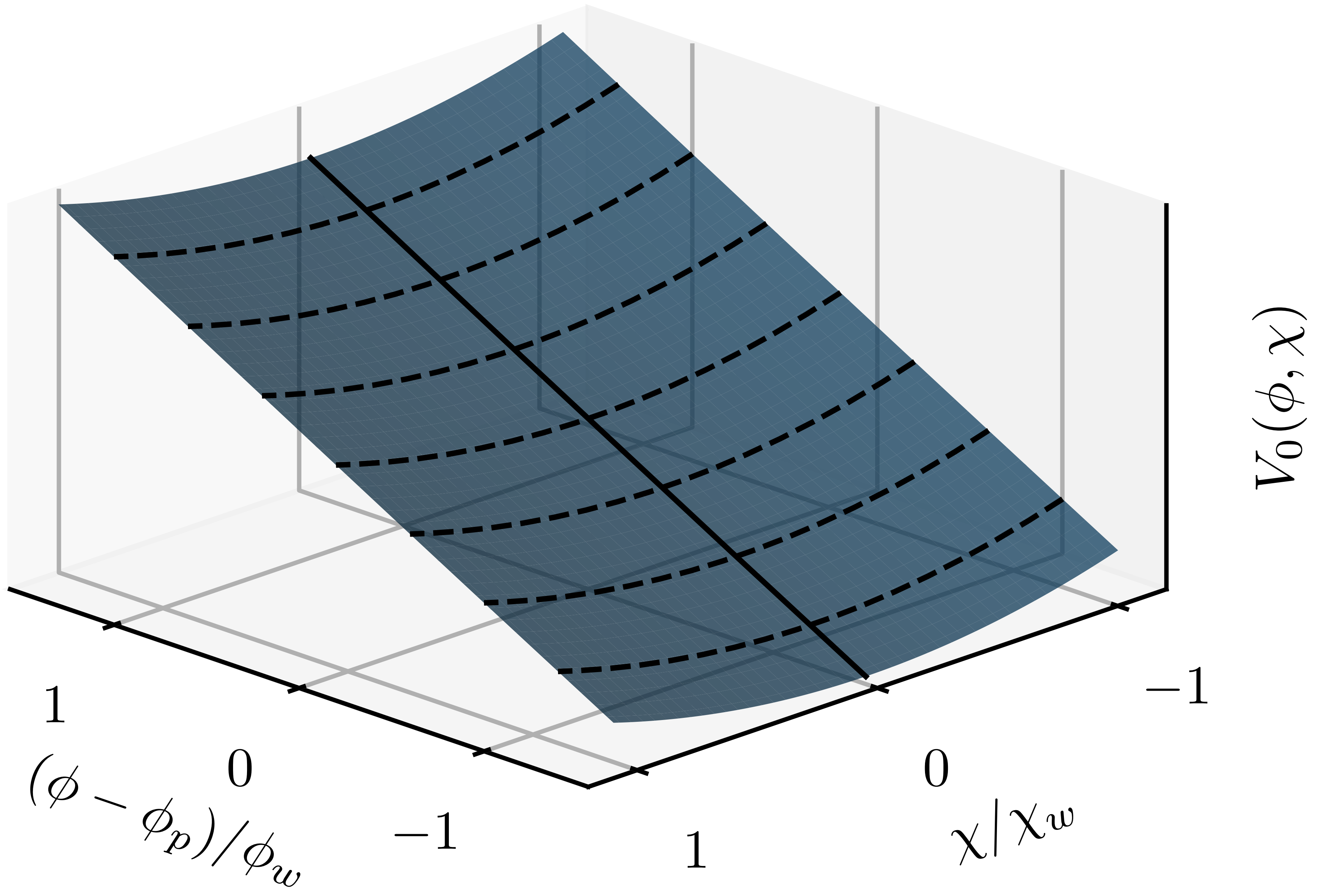

No instability

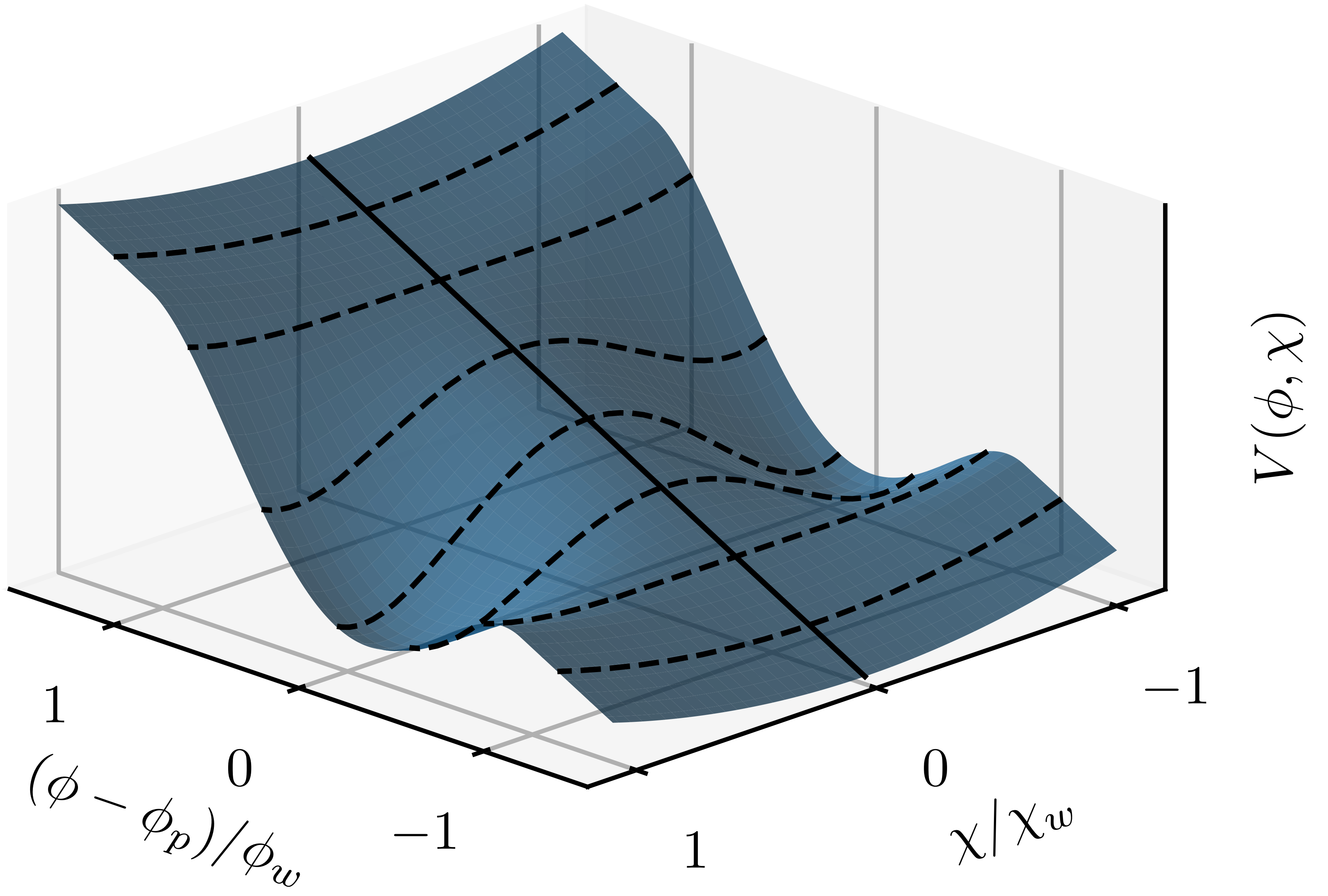

Instability

Figures from Morrison *et al*. in prep.

Primordial intermittent NG (PING) with $\Delta\zeta(\mathbf{x}) = F_{\rm NL}[\chi(\mathbf{x})]$ arises during multi-field inflation if there is a potential feature with $m_\chi^2 < 0$.

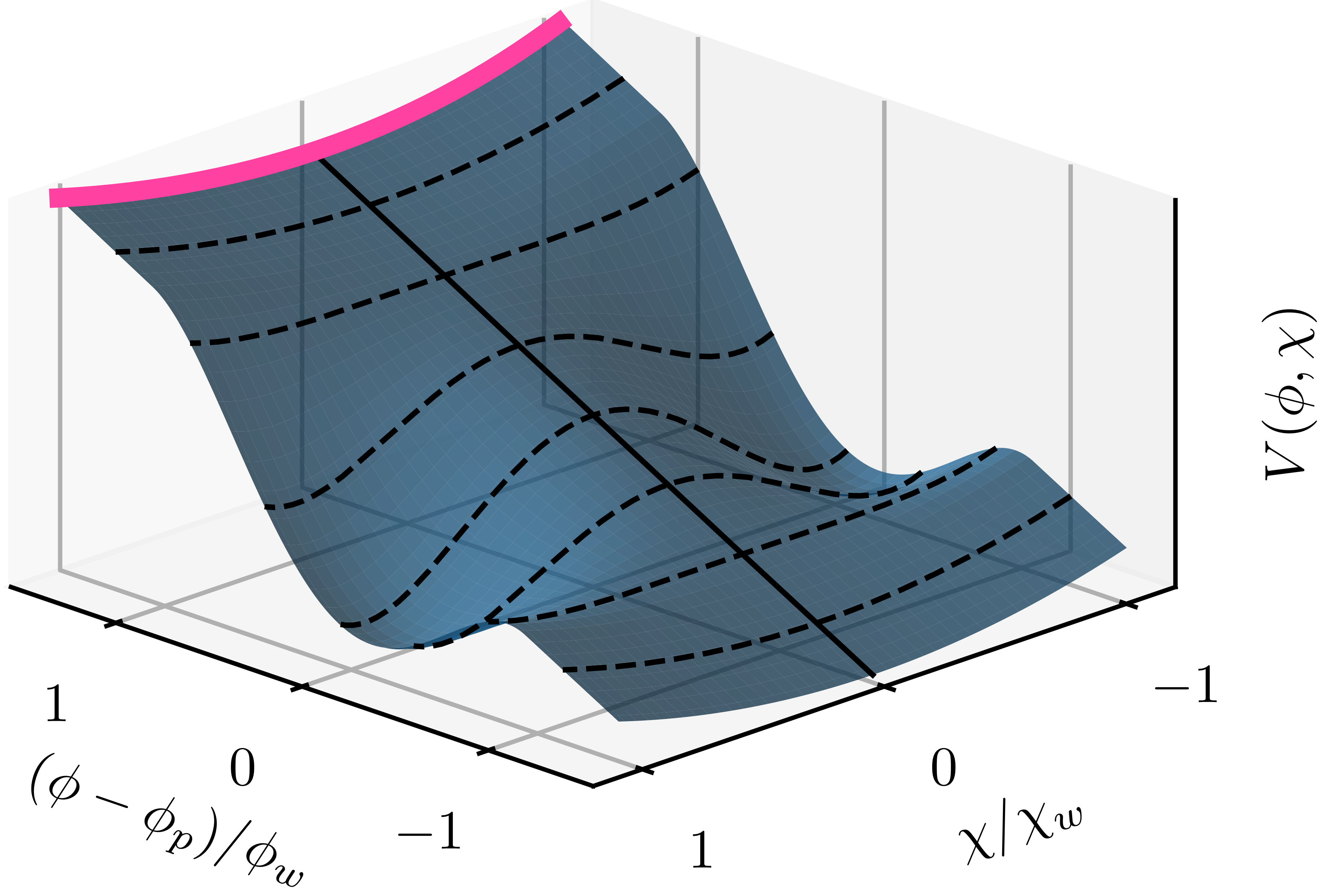

$\langle\phi\rangle = \phi_i$
instability turns on

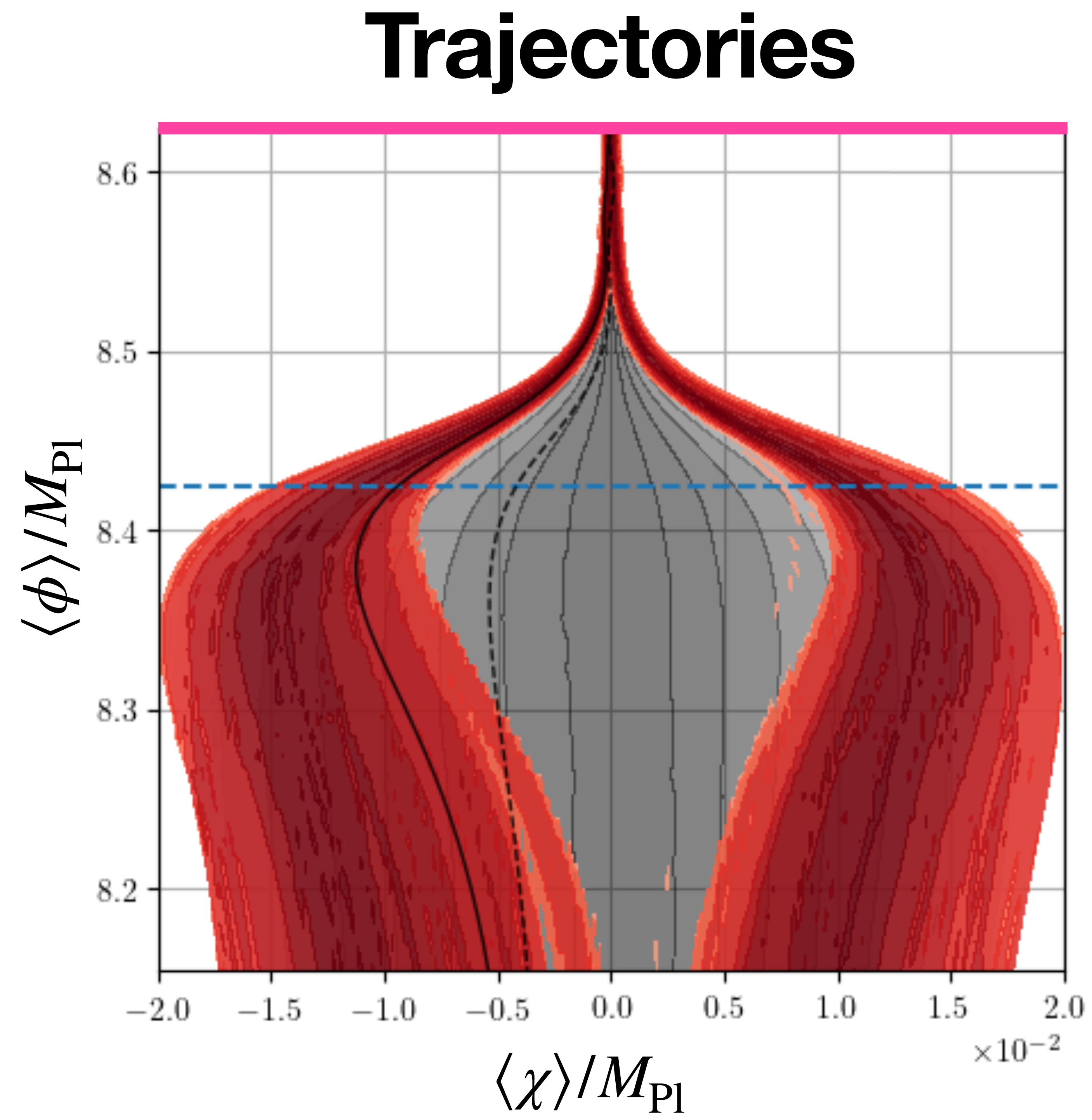

Figures from Morrison *et al*. in prep.

Primordial intermittent NG (PING) with $\Delta\zeta(\mathbf{x}) = F_{\rm NL}[\chi(\mathbf{x})]$ arises during multi-field inflation if there is a potential feature with $m_\chi^2 < 0$.

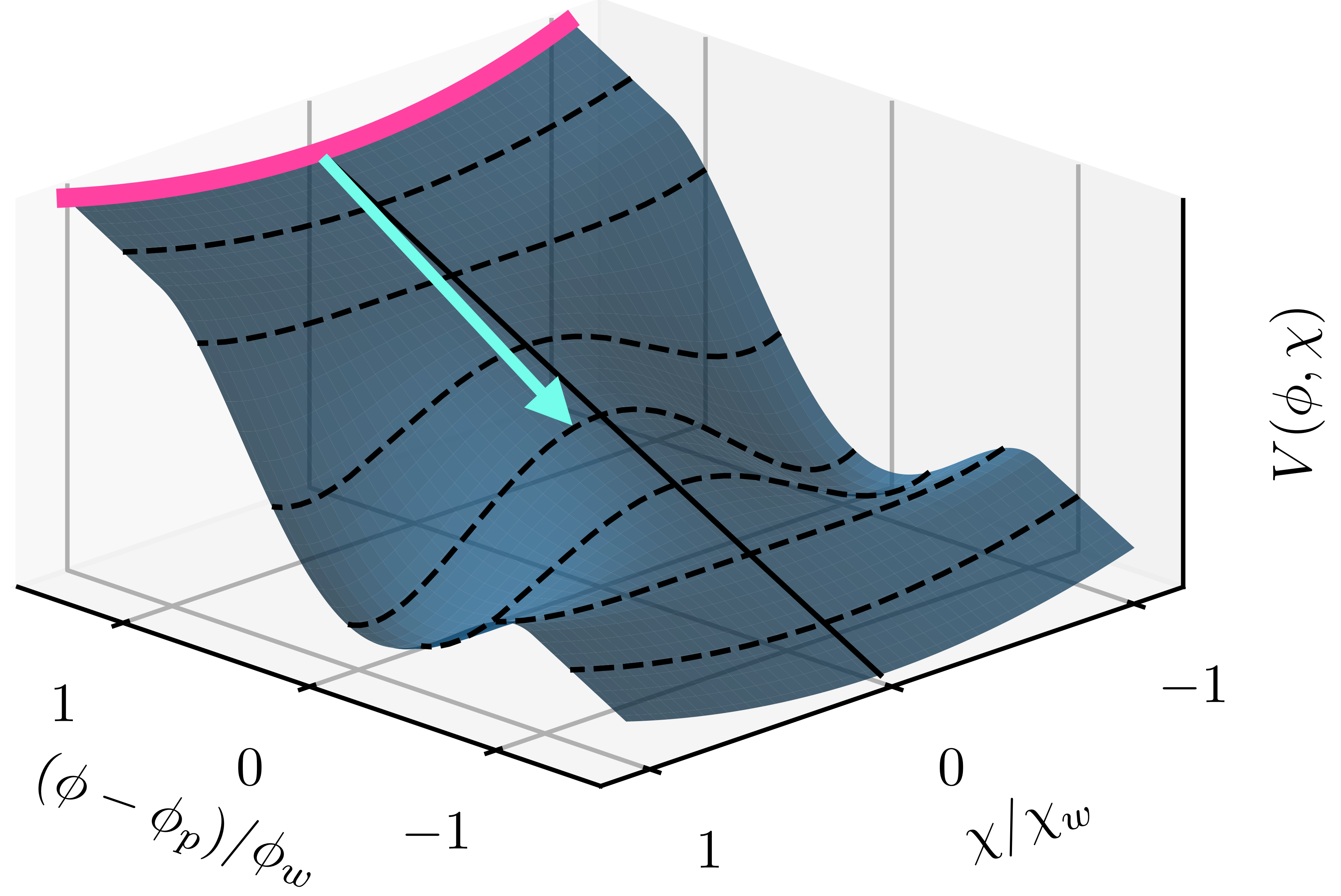

$\langle\phi\rangle = \phi_i$
instability turns on

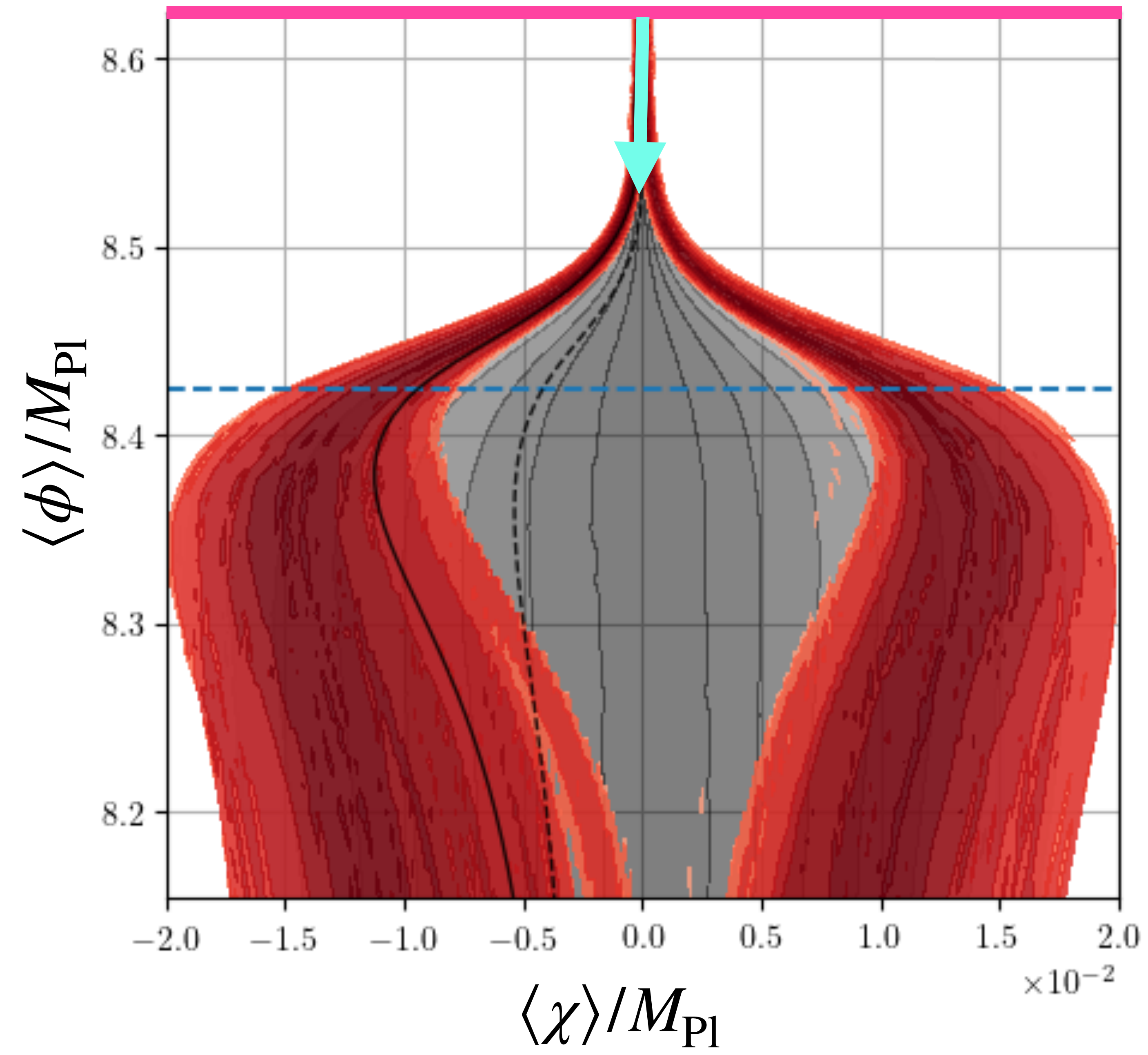

Figures from Morrison *et al*. in prep.

Primordial intermittent NG (PING) with $\Delta\zeta(\mathbf{x}) = F_{\rm NL}[\chi(\mathbf{x})]$ arises during multi-field inflation if there is a potential feature with $m_\chi^2 < 0$.

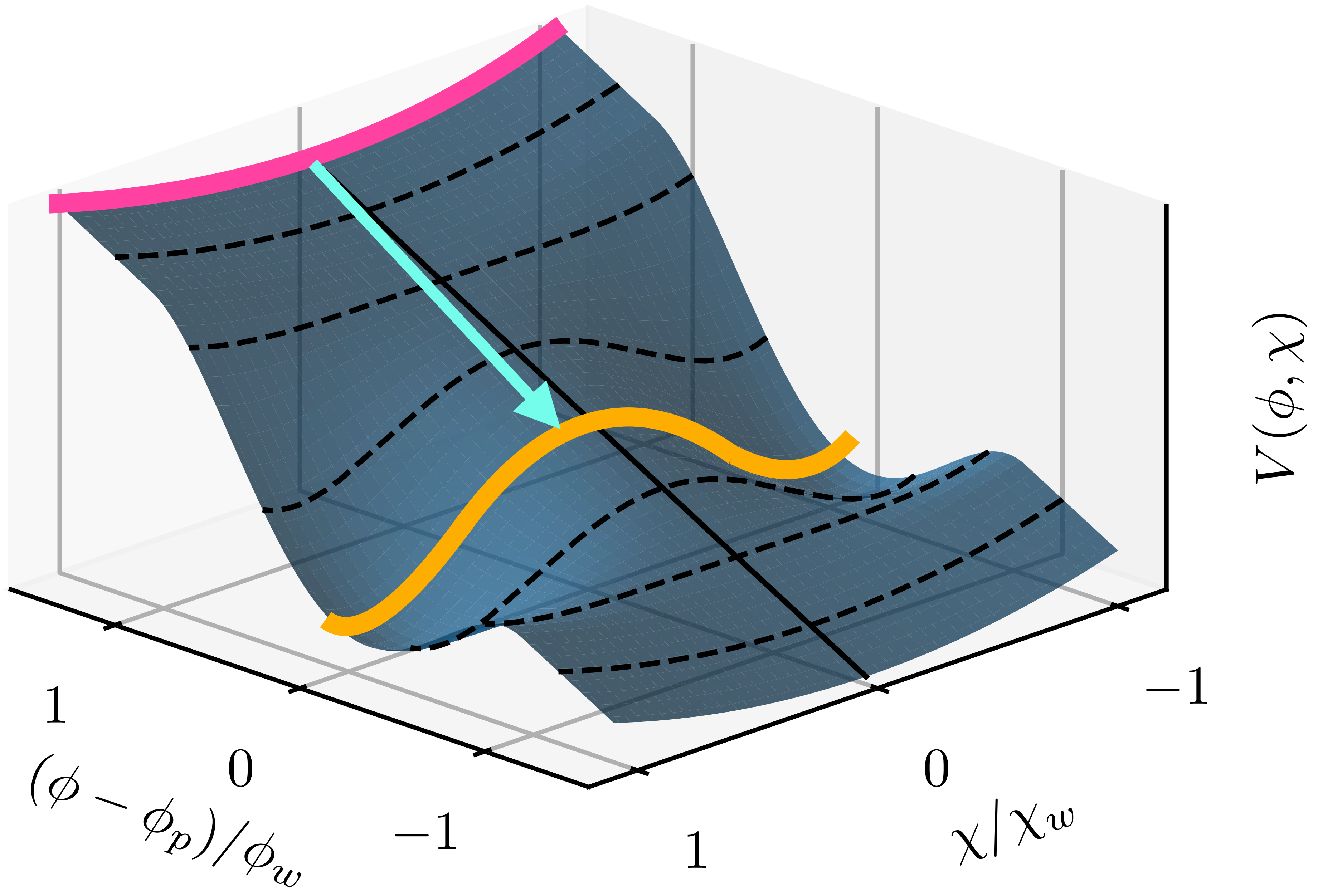

$\langle\phi\rangle = \phi_i$
instability turns on

$\langle\phi\rangle = \phi_p$
instability peaks

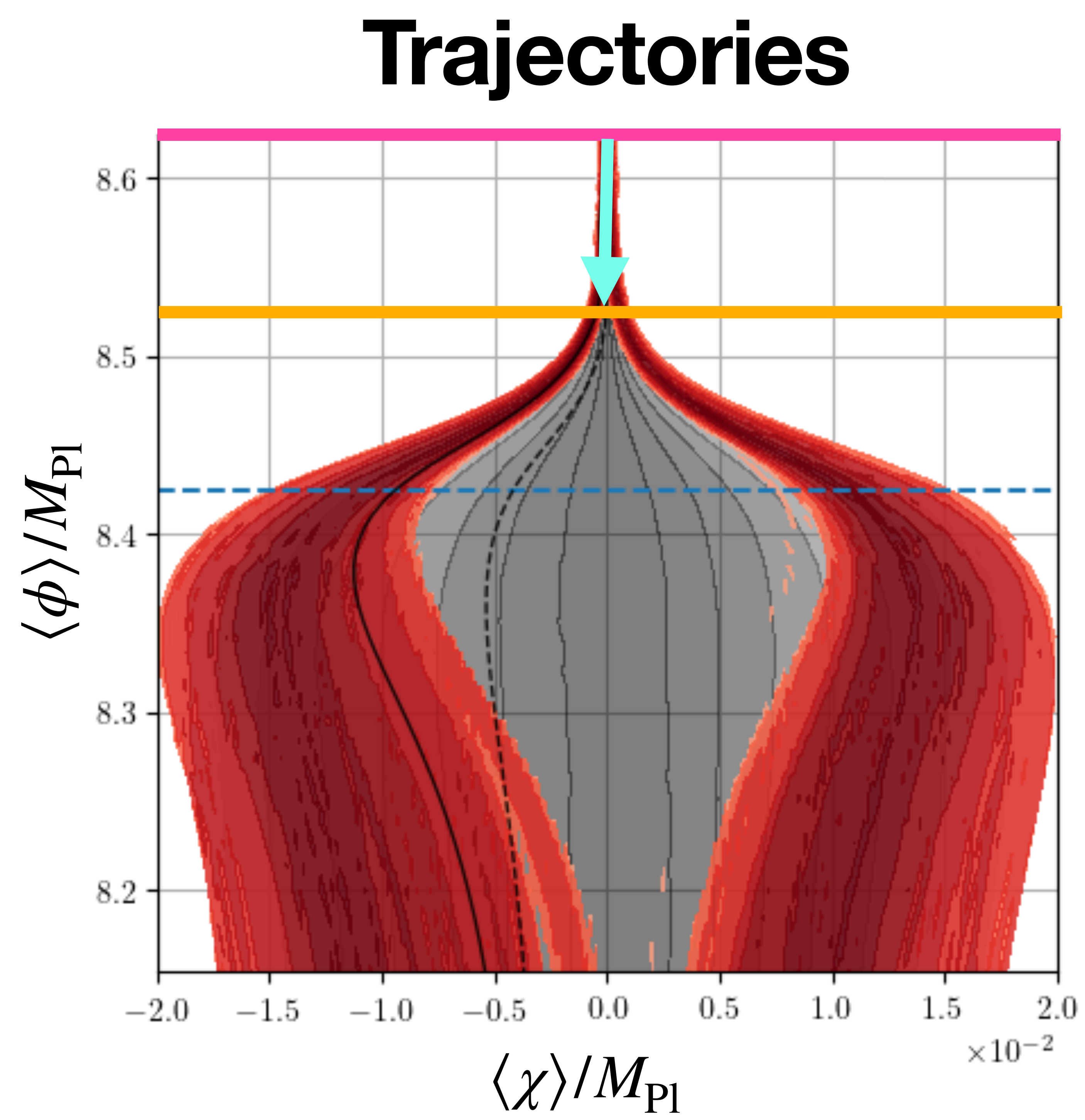

Figures from Morrison *et al*. in prep.

Primordial intermittent NG (PING) with $\Delta\zeta(\mathbf{x}) = F_{\rm NL}[\chi(\mathbf{x})]$ arises during multi-field inflation if there is a potential feature with $m_\chi^2 < 0$.

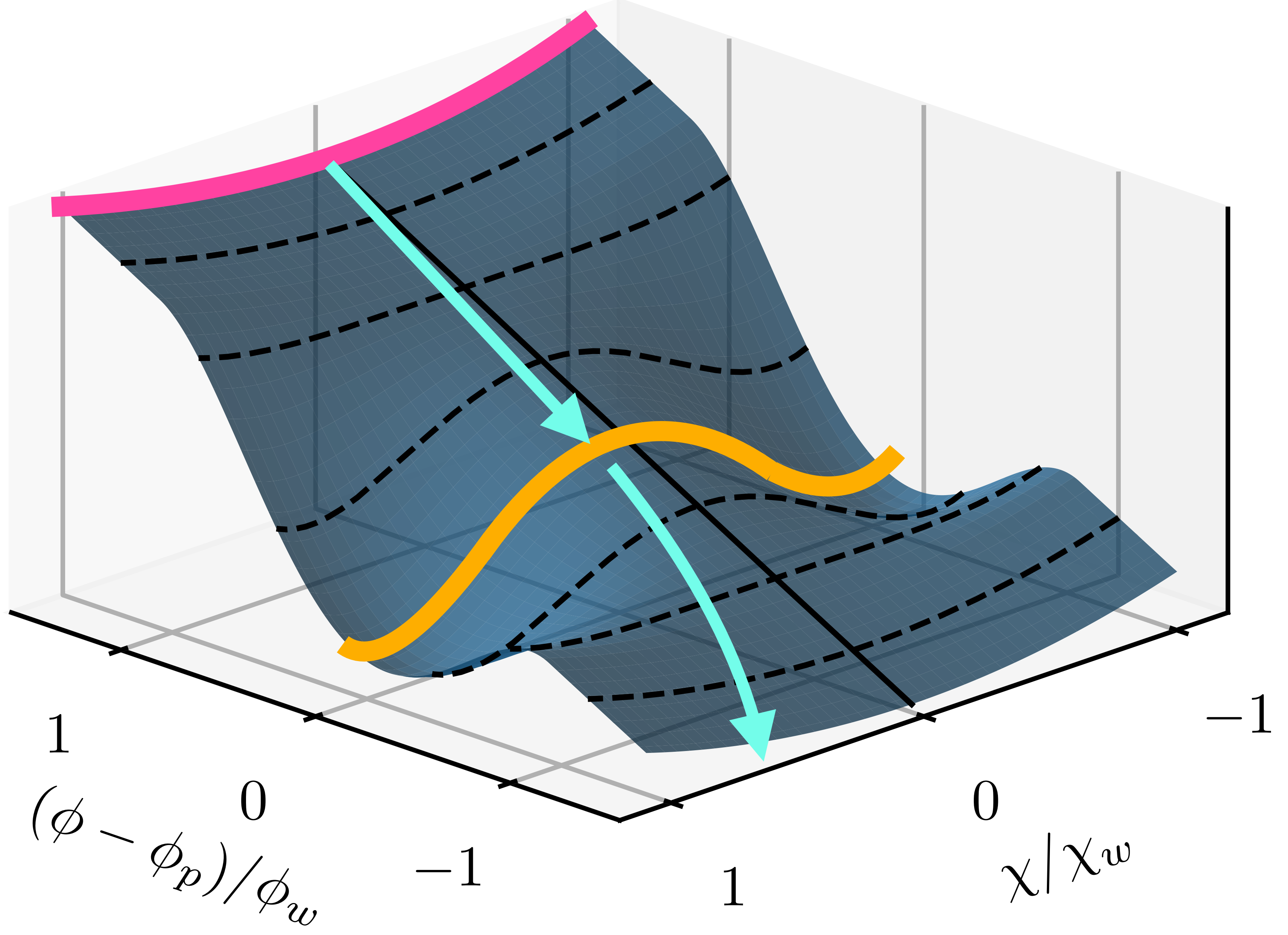

$\langle\phi\rangle = \phi_i$
instability turns on

$\langle\phi\rangle = \phi_p$
instability peaks

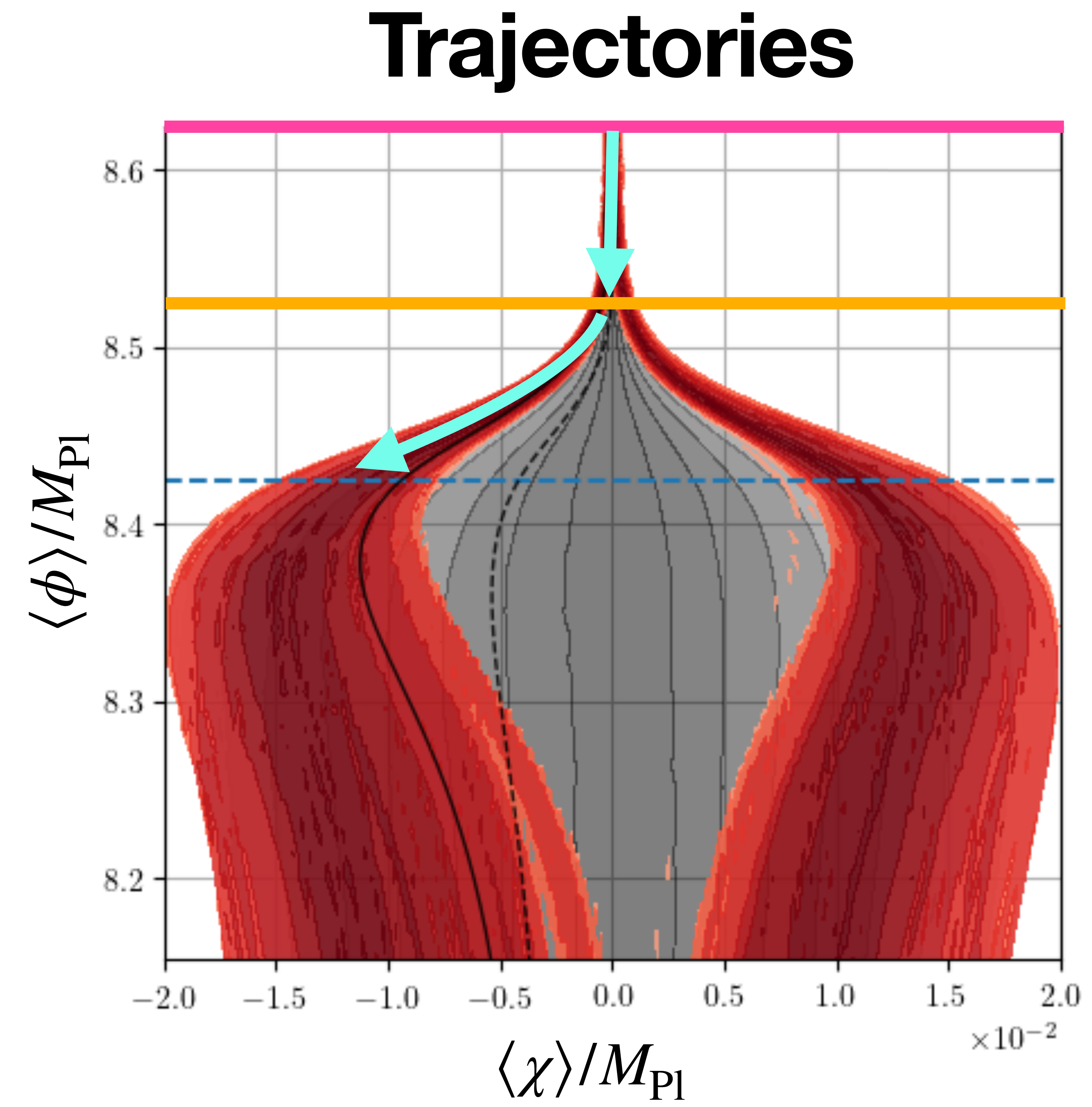

Figures from Morrison *et al*. in prep.

Primordial intermittent NG (PING) with $\Delta\zeta(\mathbf{x}) = F_{\rm NL}[\chi(\mathbf{x})]$ arises during multi-field inflation if there is a potential feature with $m_\chi^2 < 0$.

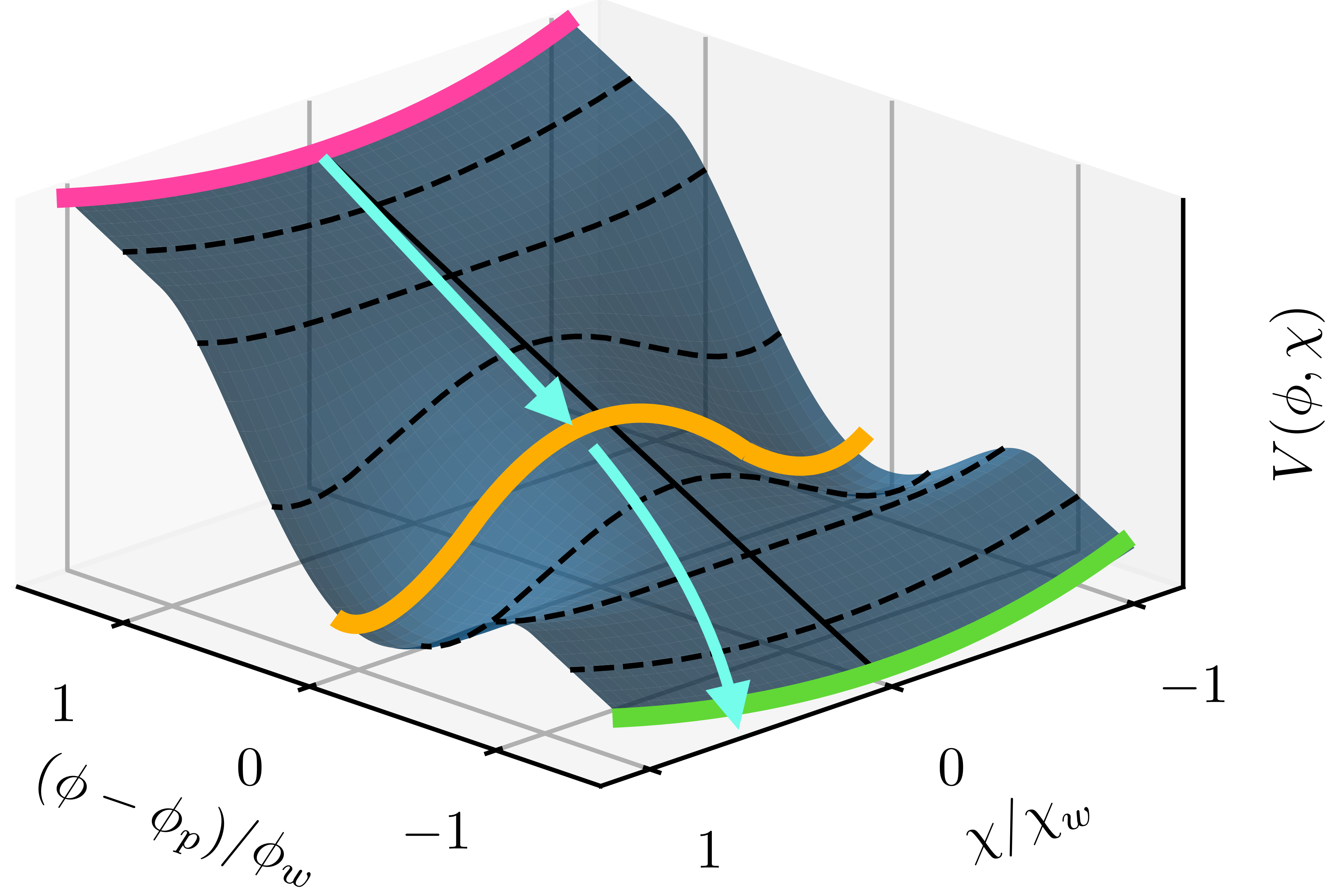

$\langle\phi\rangle = \phi_i$
instability turns on

$\langle\phi\rangle = \phi_p$
instability peaks

$\langle\phi\rangle = \phi_e$
instability turns off

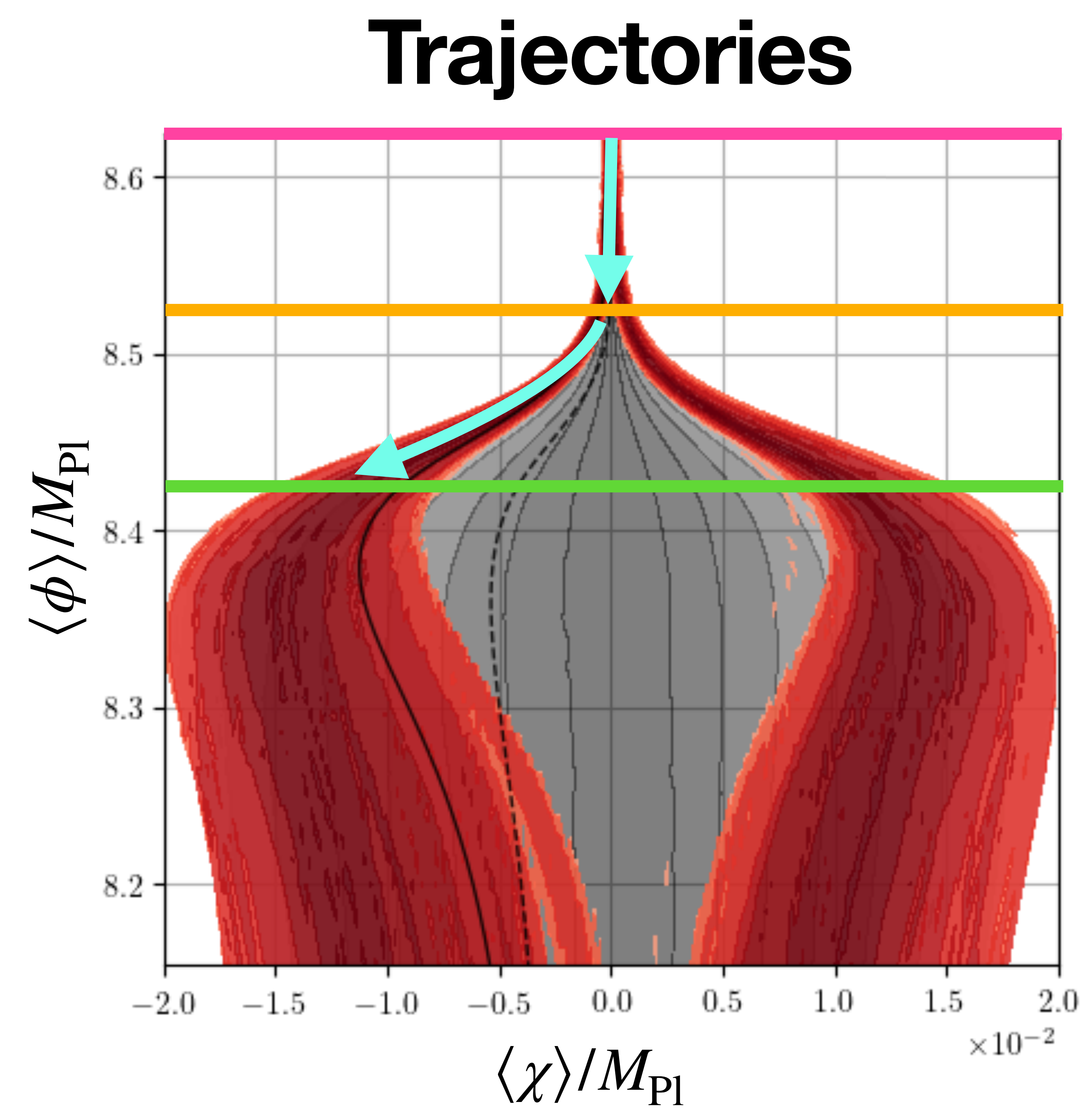

Figures from Morrison *et al*. in prep.

Primordial intermittent NG (PING) with $\Delta\zeta(\mathbf{x}) = F_{\mathrm{NL}}[\chi(\mathbf{x})]$ arises during multi-field inflation if there is a potential feature with $m_\chi^2 < 0$.

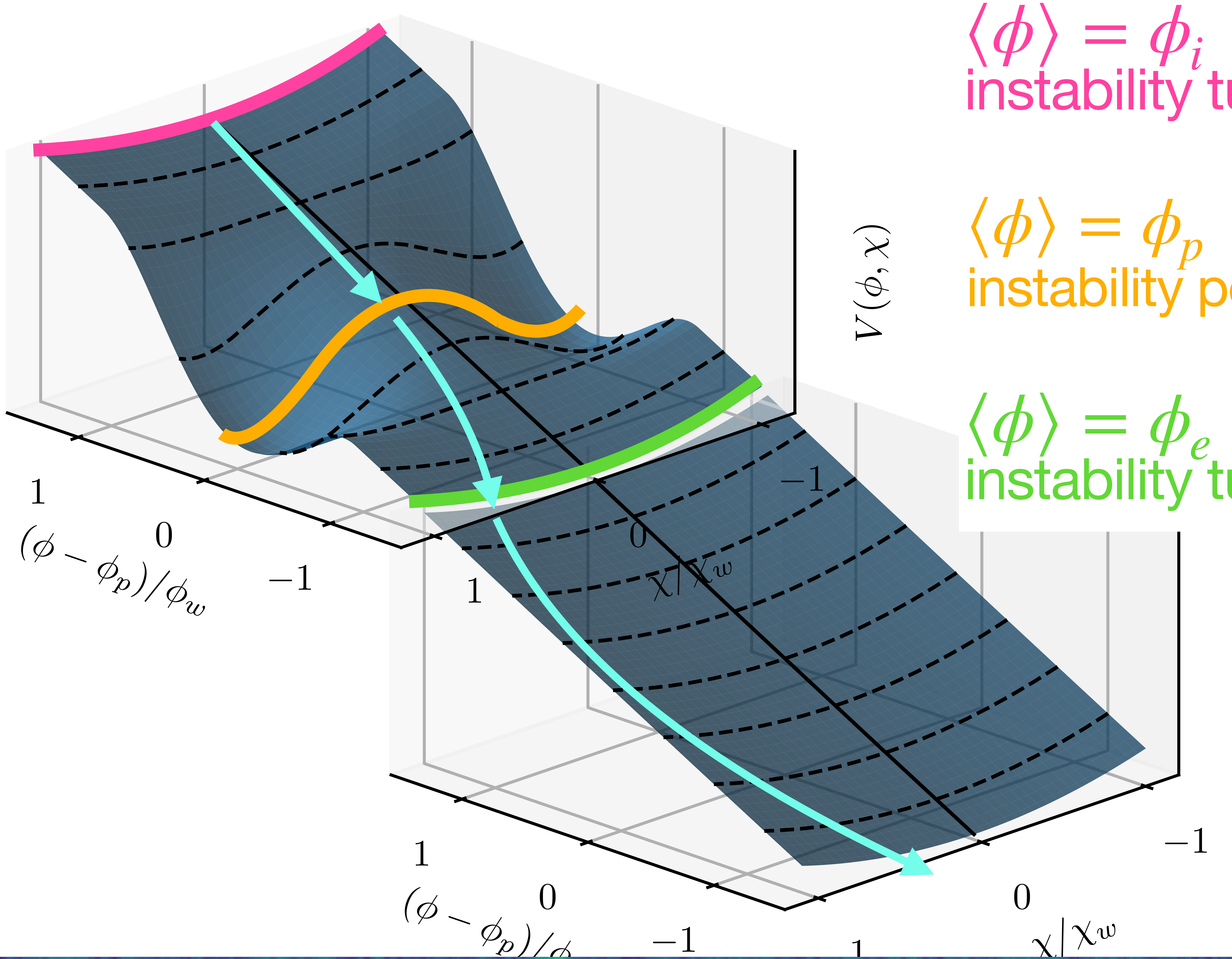

$\langle\phi\rangle = \phi_i$
instability turns on

$\langle\phi\rangle = \phi_p$
instability peaks

$\langle\phi\rangle = \phi_e$
instability turns off

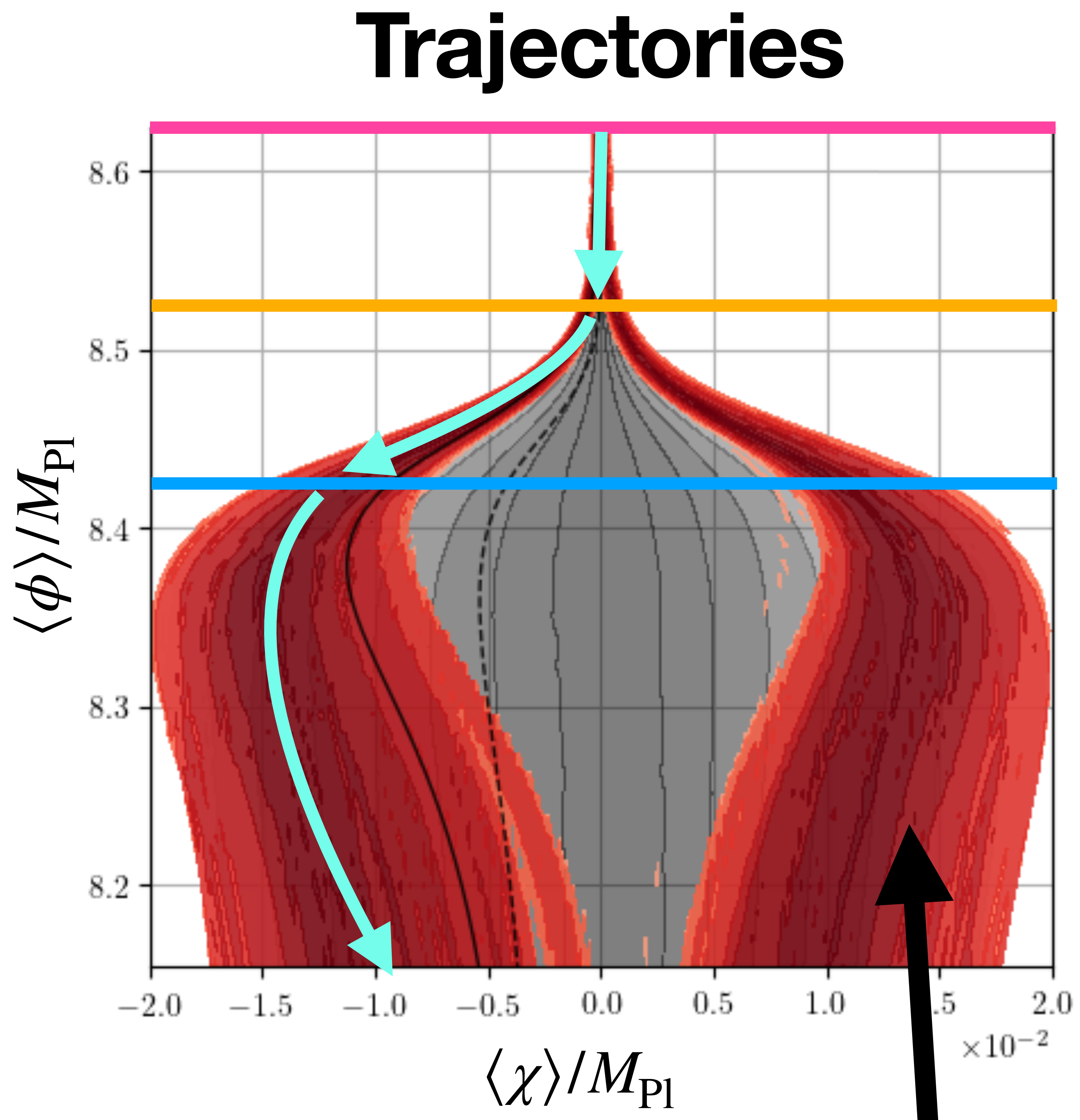

Most extreme trajectories ($\Delta\zeta > 5\sigma$)

Figures from Morrison *et al*. in prep.

Primordial intermittent NG (PING) with $\Delta\zeta(\mathbf{x}) = F_{\rm NL}[\chi(\mathbf{x})]$ arises during multi-field inflation if there is a potential feature with $m_\chi^2 < 0$.

The deflection of χ trajectories result in a perturbation to the inflaton $\Delta\phi$

$$\Delta\phi(\mathbf{x}) = \tilde{T}_{\chi^2\to\Delta\phi}(r) * \left[\chi(\mathbf{x}) * W(r)\right]^2$$

Trajectories

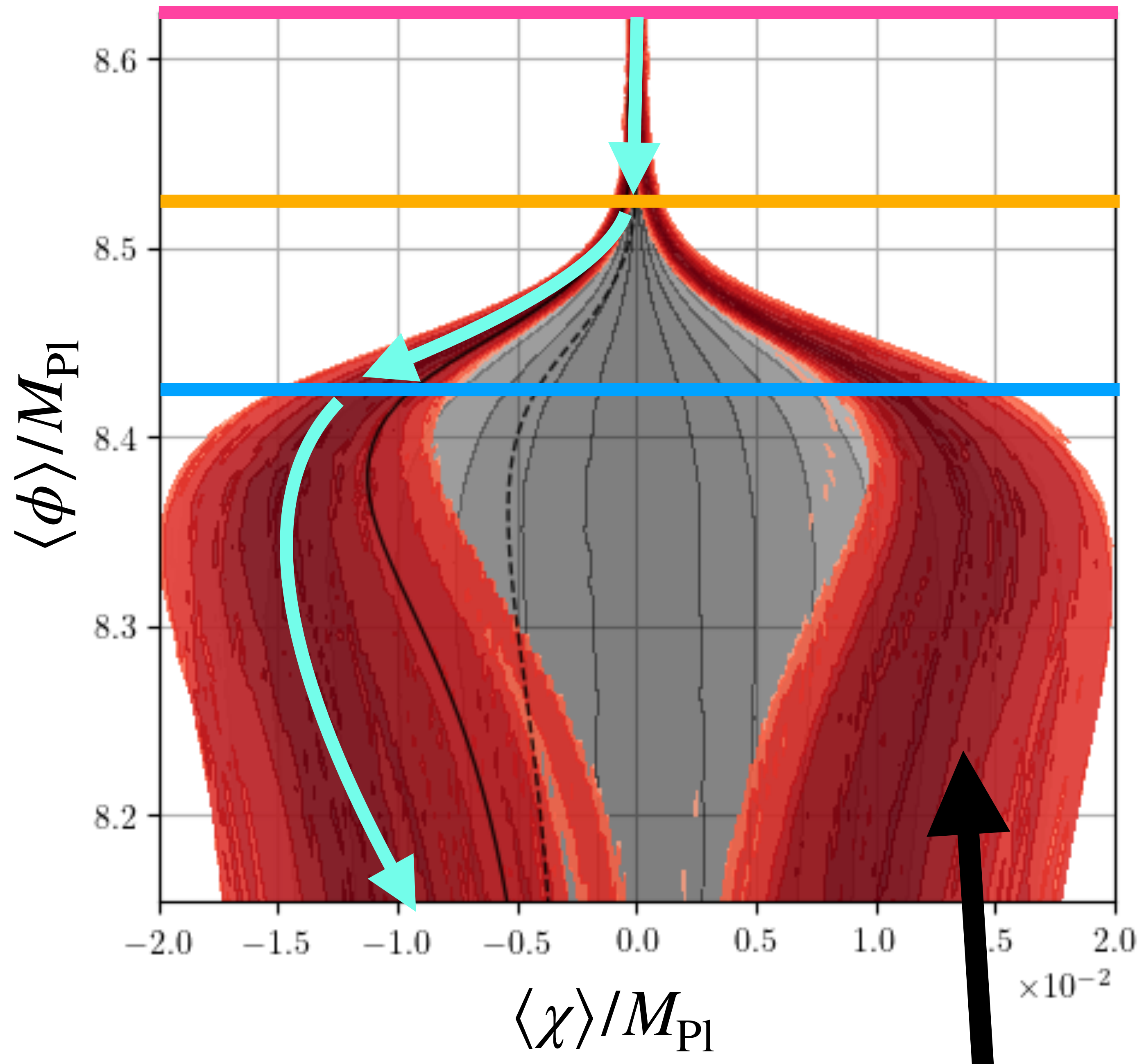

Most extreme trajectories
($\Delta\zeta > 5\sigma$)

Figures from Morrison *et al*. in prep.

Primordial intermittent NG (PING) with $\Delta\zeta(\mathbf{x}) = F_{\rm NL}[\chi(\mathbf{x})]$ arises during multi-field inflation if there is a potential feature with $m_\chi^2 < 0$.

The deflection of χ trajectories result in a perturbation to the inflaton $\Delta\phi$

$$\Delta\phi(\mathbf{x}) = \tilde{T}_{\chi^2\to\Delta\phi}(r) * \left[\chi(\mathbf{x}) * W(r)\right]^2$$

This gives a perturbation to ζ

$$\Delta\zeta(\mathbf{x}) = \tilde{T}_{\Delta\phi\to\Delta\zeta}(r) * \Delta\phi(\mathbf{x})$$

Trajectories

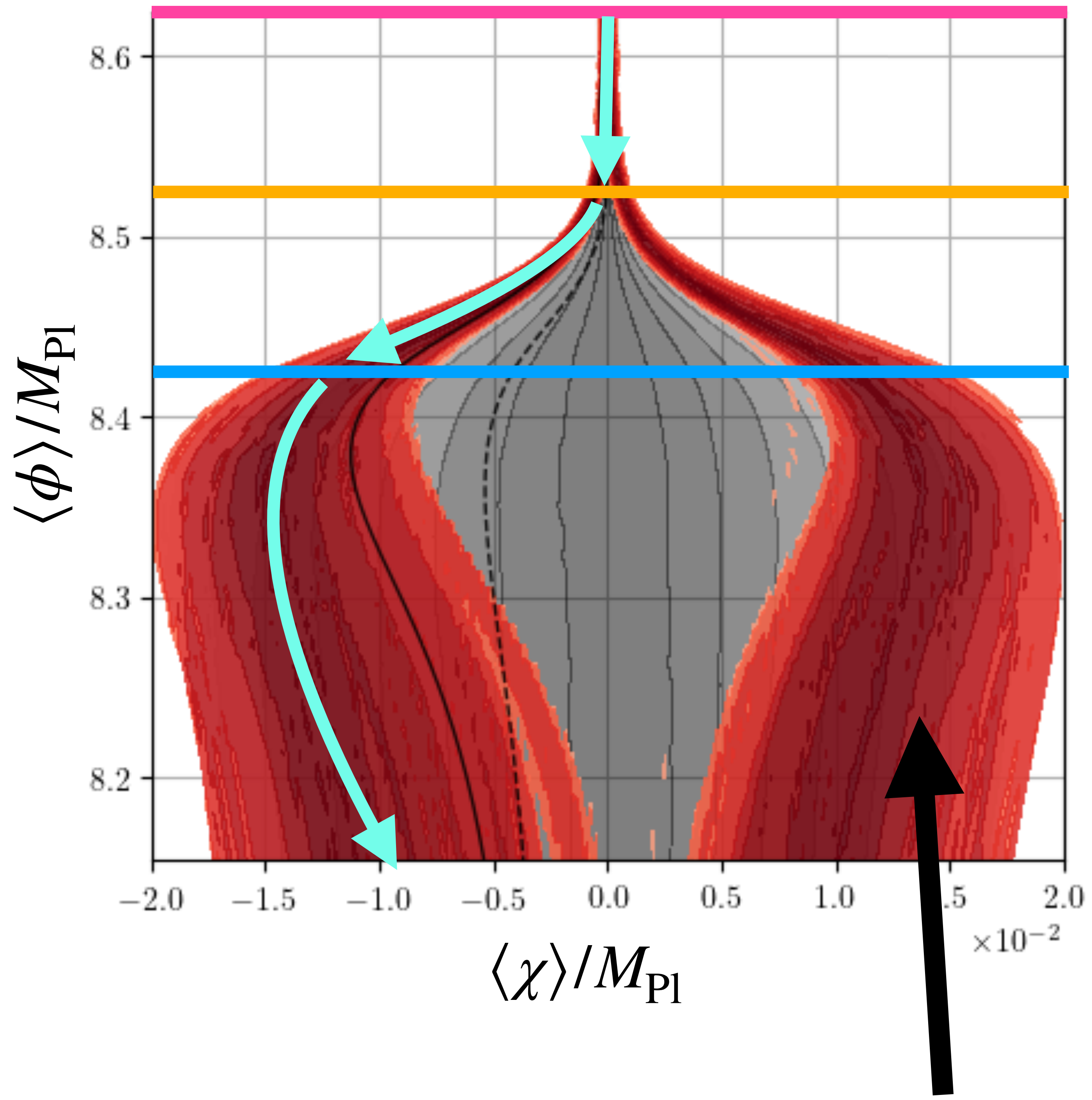

Most extreme trajectories ($\Delta\zeta > 5\sigma$)

Figures from Morrison *et al*. in prep.

Primordial intermittent NG (PING) with $\Delta\zeta(\mathbf{x}) = F_{\rm NL}[\chi(\mathbf{x})]$ arises during multi-field inflation if there is a potential feature with $m_\chi^2 < 0$.

The deflection of χ trajectories result in a perturbation to the inflaton $\Delta\phi$

$$\Delta\phi(\mathbf{x}) = \tilde{T}_{\chi^2\to\Delta\phi}(r) * \left[\chi(\mathbf{x}) * W(r)\right]^2$$

This gives a perturbation to ζ

$$\Delta\zeta(\mathbf{x}) = \tilde{T}_{\Delta\phi\to\Delta\zeta}(r) * \Delta\phi(\mathbf{x})$$

The result: a very complicated and not bispectrum friendly NG term.

Trajectories

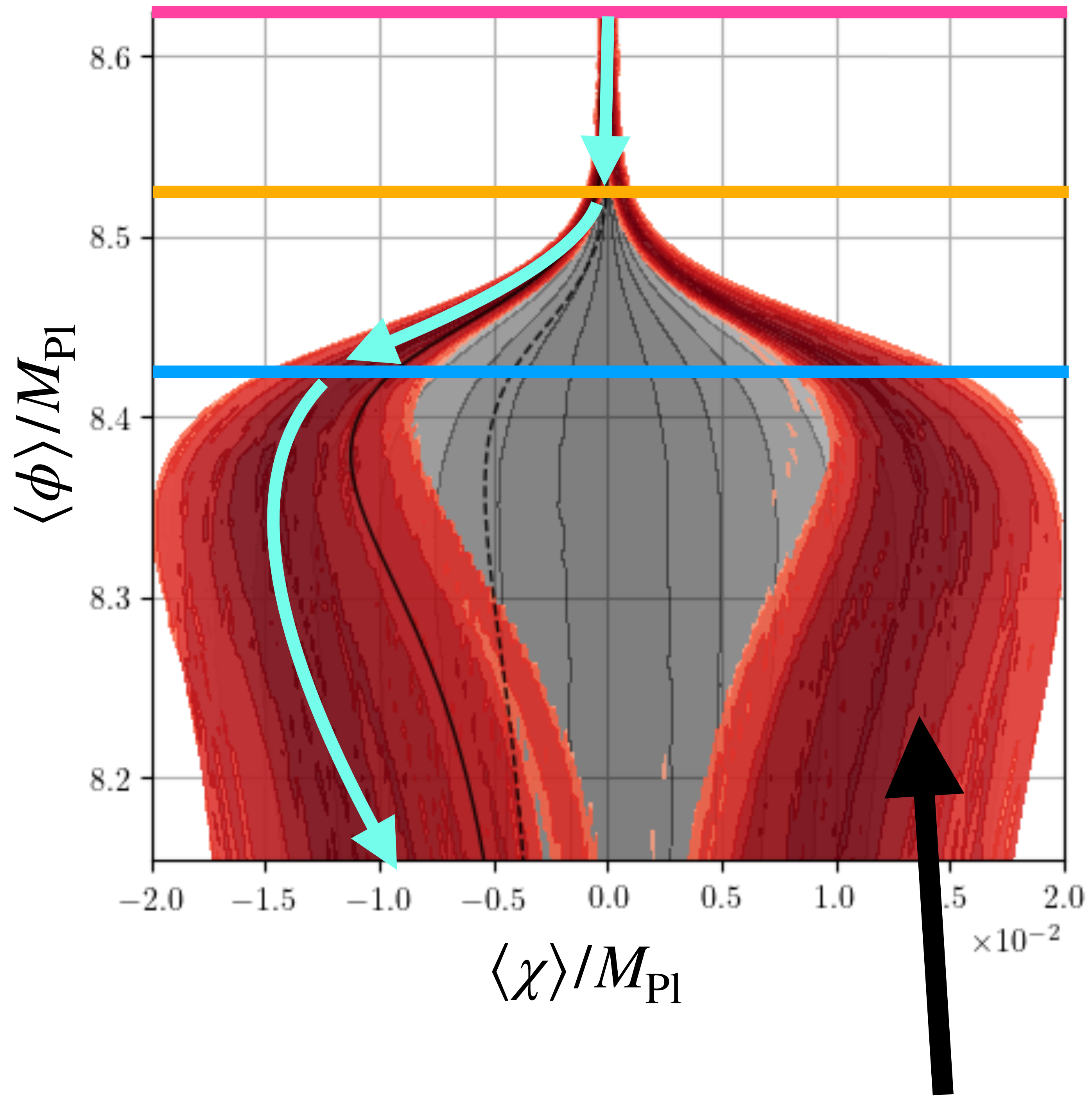

Most extreme trajectories ($\Delta\zeta > 5\sigma$)

Figures from Morrison *et al*. in prep.

When the PNG term $\delta_{nG}(\mathbf{x})$ is correlated with the Gaussian term $\delta_G(\mathrm{G})$, the two constructively interfere, amplifying the PNG. This need not be the case for uncorrelated PNG.

Gaussian overdensity $\delta_G(\mathbf{x})$

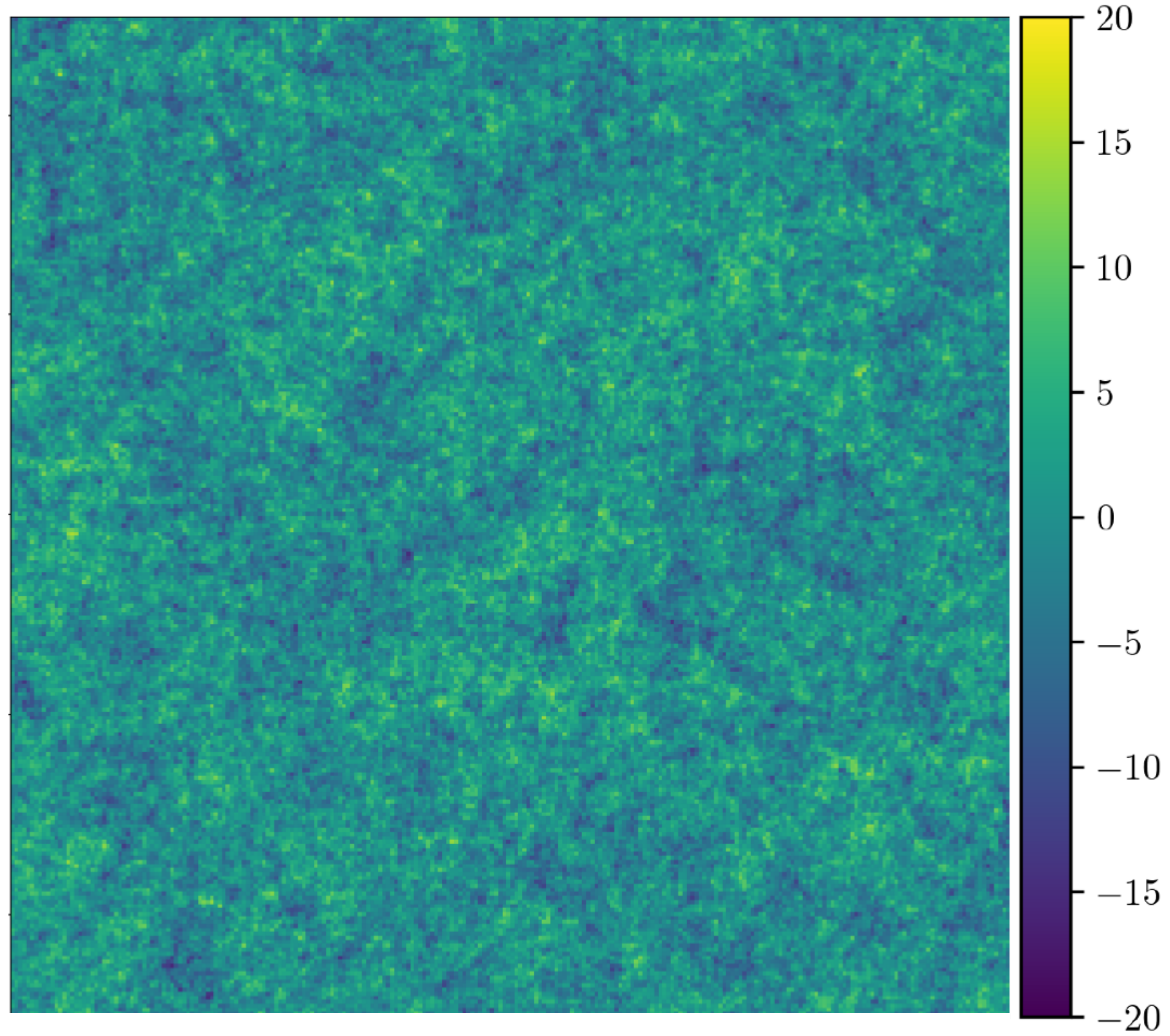

Overdensity sourced only by $\zeta_G(\mathbf{x})$

PNG $\delta_{nG}(\mathbf{x})$ ***correlated*** with $\delta_G(\mathbf{x})$

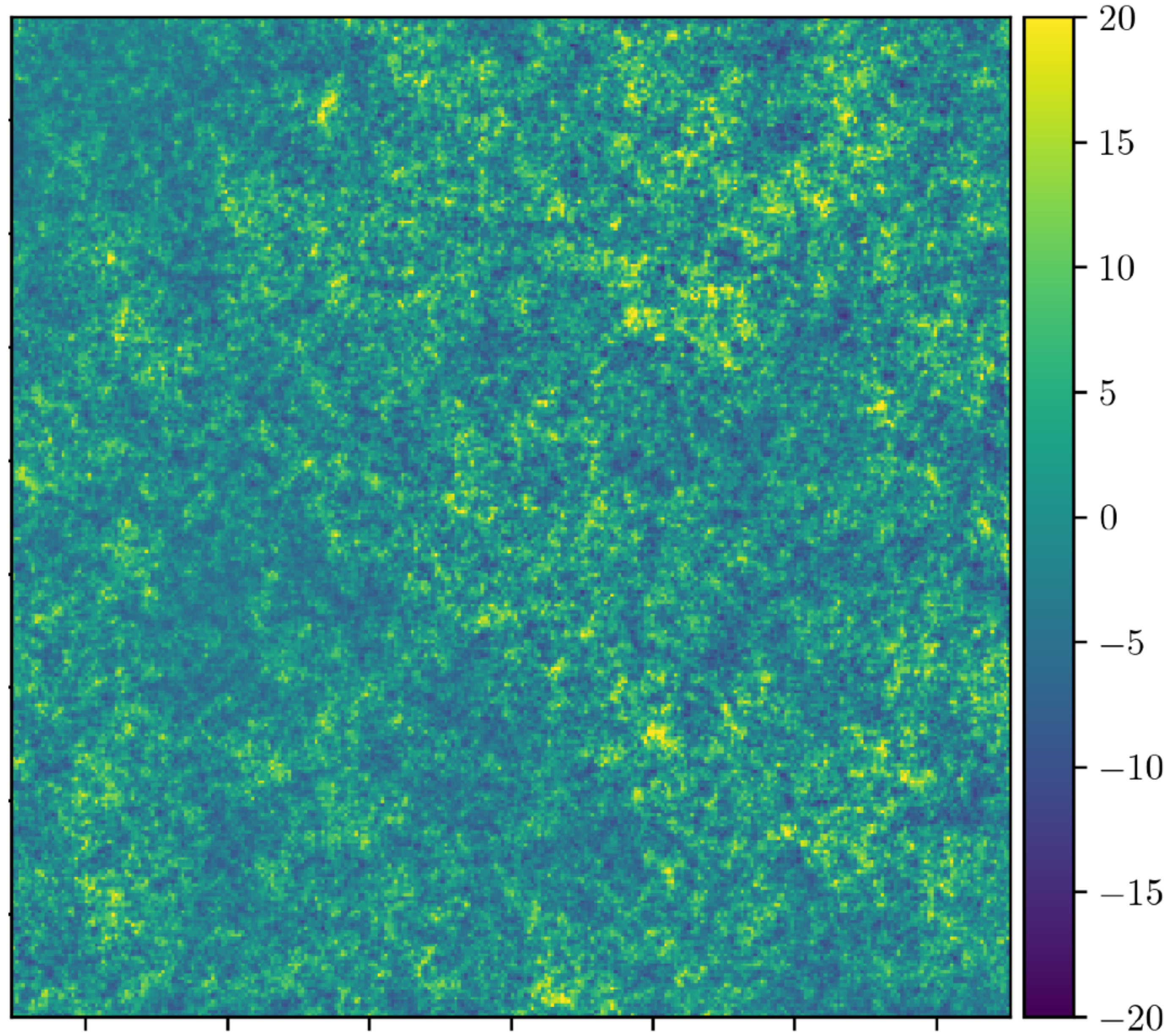

PNG with $f_{\mathrm{NL}} = 10^5$ sourced by $\zeta(\mathbf{x}) = \zeta_G(\mathbf{x}) + f_{\mathrm{NL}}\left(\zeta_G^2(\mathbf{x}) - \langle \zeta_G^2(\mathbf{x})\rangle\right)$

PNG $\delta_{nG}(\mathbf{x})$ ***uncorrelated*** with $\delta_G(\mathbf{x})$

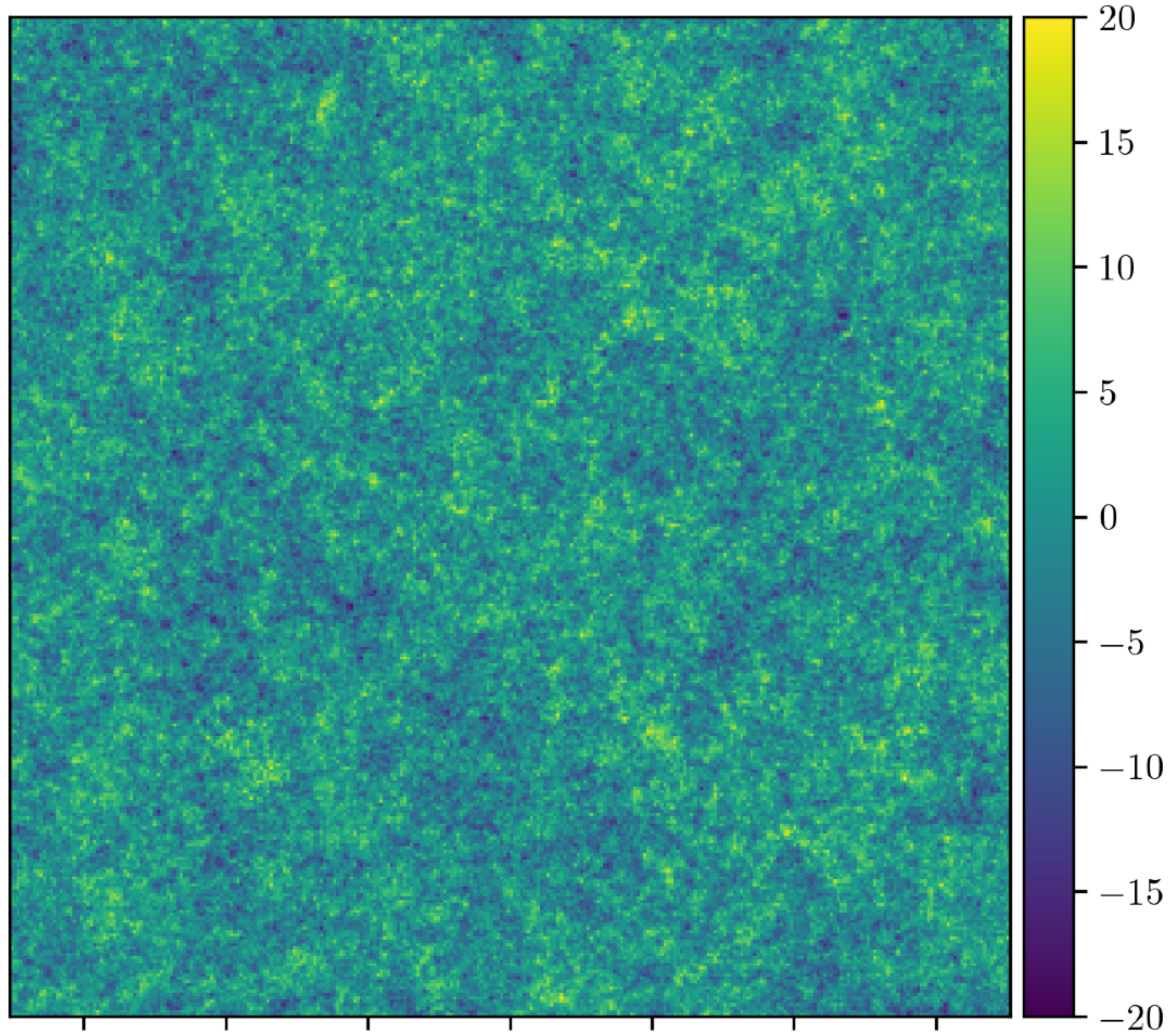

PNG from additional field $\chi(\mathbf{x}) \sim \delta_G(\mathbf{x})$ with $\tilde{f}_{\mathrm{NL}} = 10^5$ sourced by $\zeta(\mathbf{x}) = \zeta_G(\mathbf{x}) + \tilde{f}_{\mathrm{NL}}\left(\chi^2(\mathbf{x}) - \langle \chi^2(\mathbf{x})\rangle\right)$

In the third case, the field $\chi(\mathbf{x})$ has the same power spectrum as $\zeta_G(\mathbf{x})$ but used a different seed for the random number generator, so the only difference is that it is uncorrelated, and the field looks much more like the Gaussian field than the correlated PNG case.

From the power spectrum, we can generate mock early-universe fields like $\zeta(\mathbf{x})$ and the energy overdensity $\delta(\mathbf{x})$. These can be fed into *Peak Patch* to make mocks of the 3D dark matter distribution.

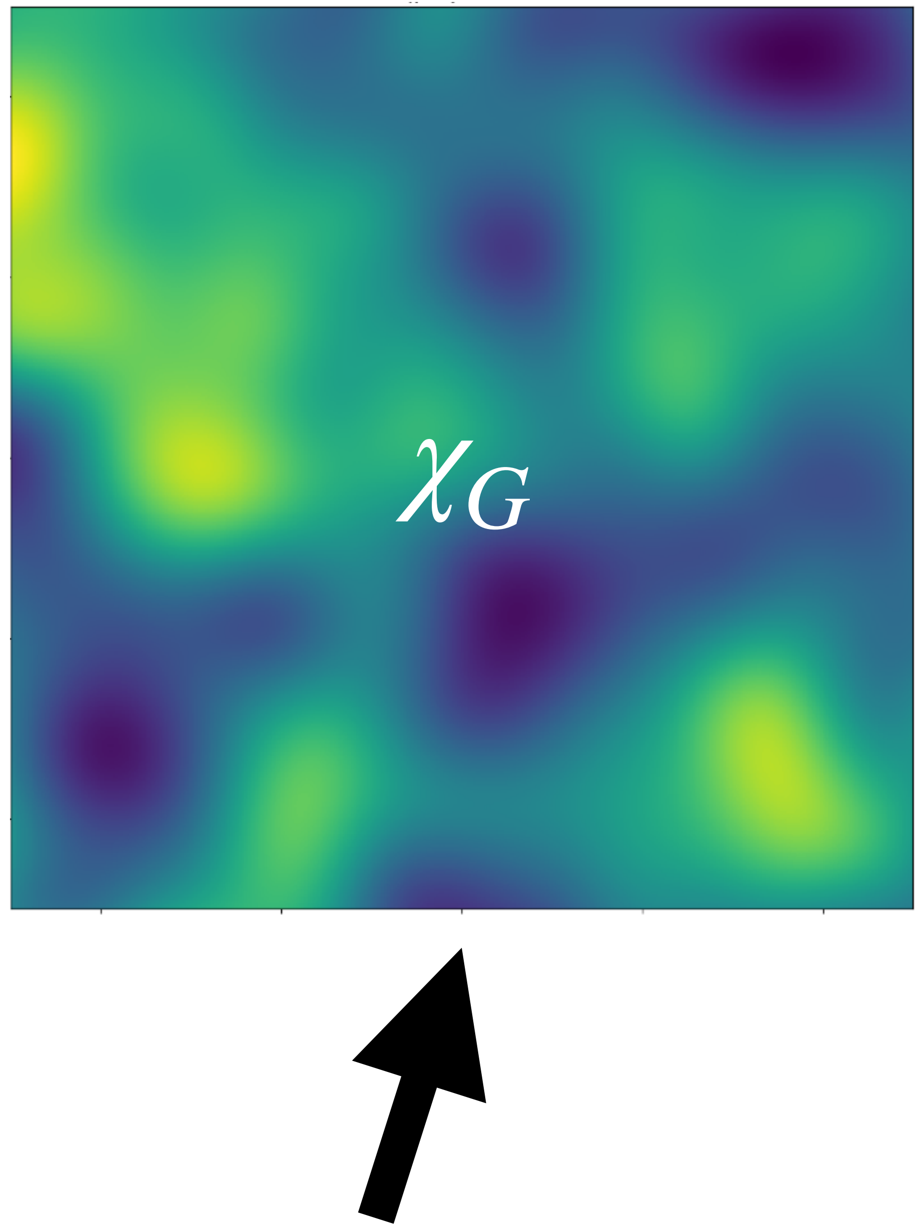

PING Gaussian field χ_G where $\Delta\zeta = F_{\mathrm{NL}}\left[\chi_G\right]$

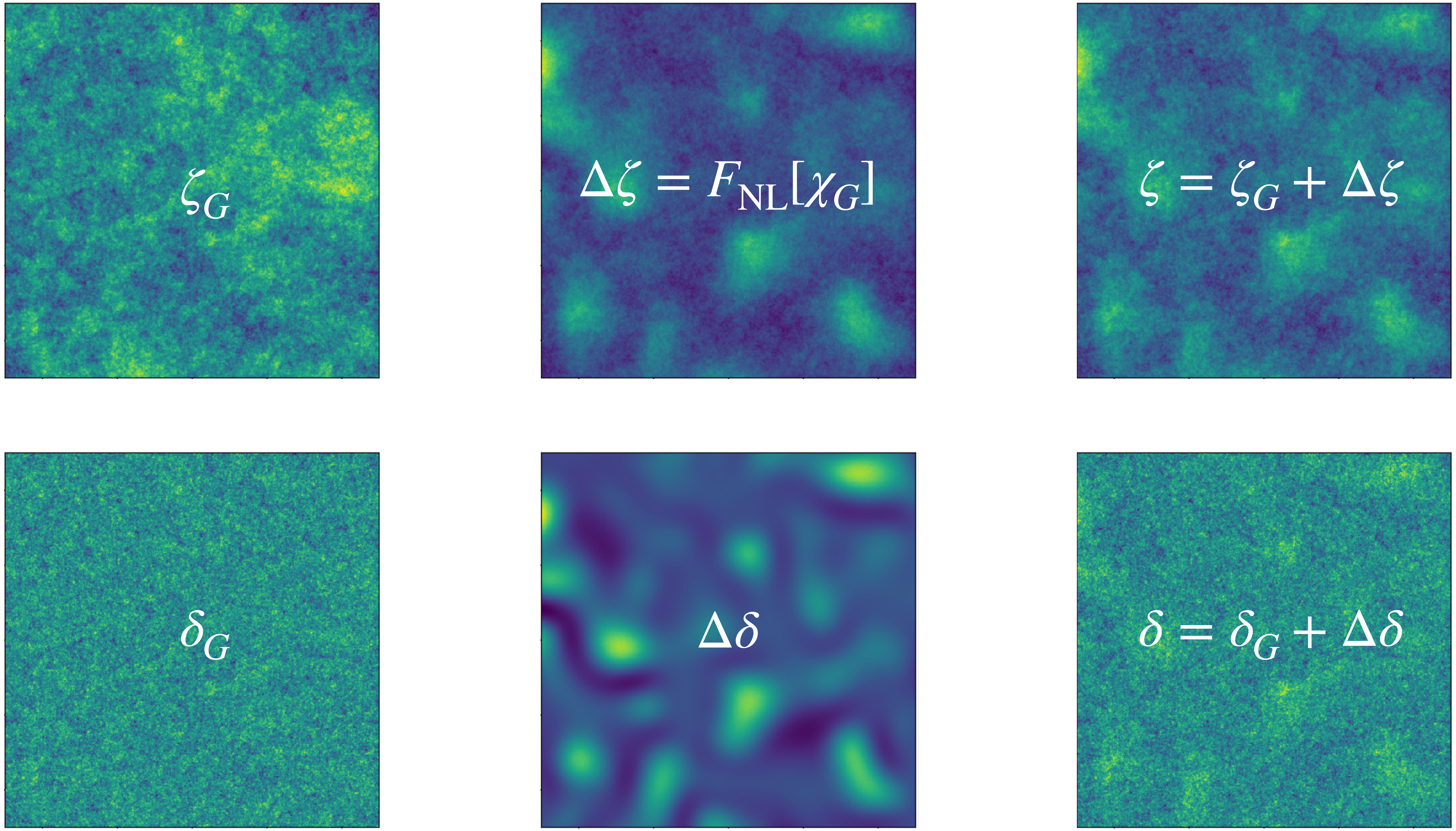

With PING spikes less than 1 Mpc, we observe an overabundance of small halos.

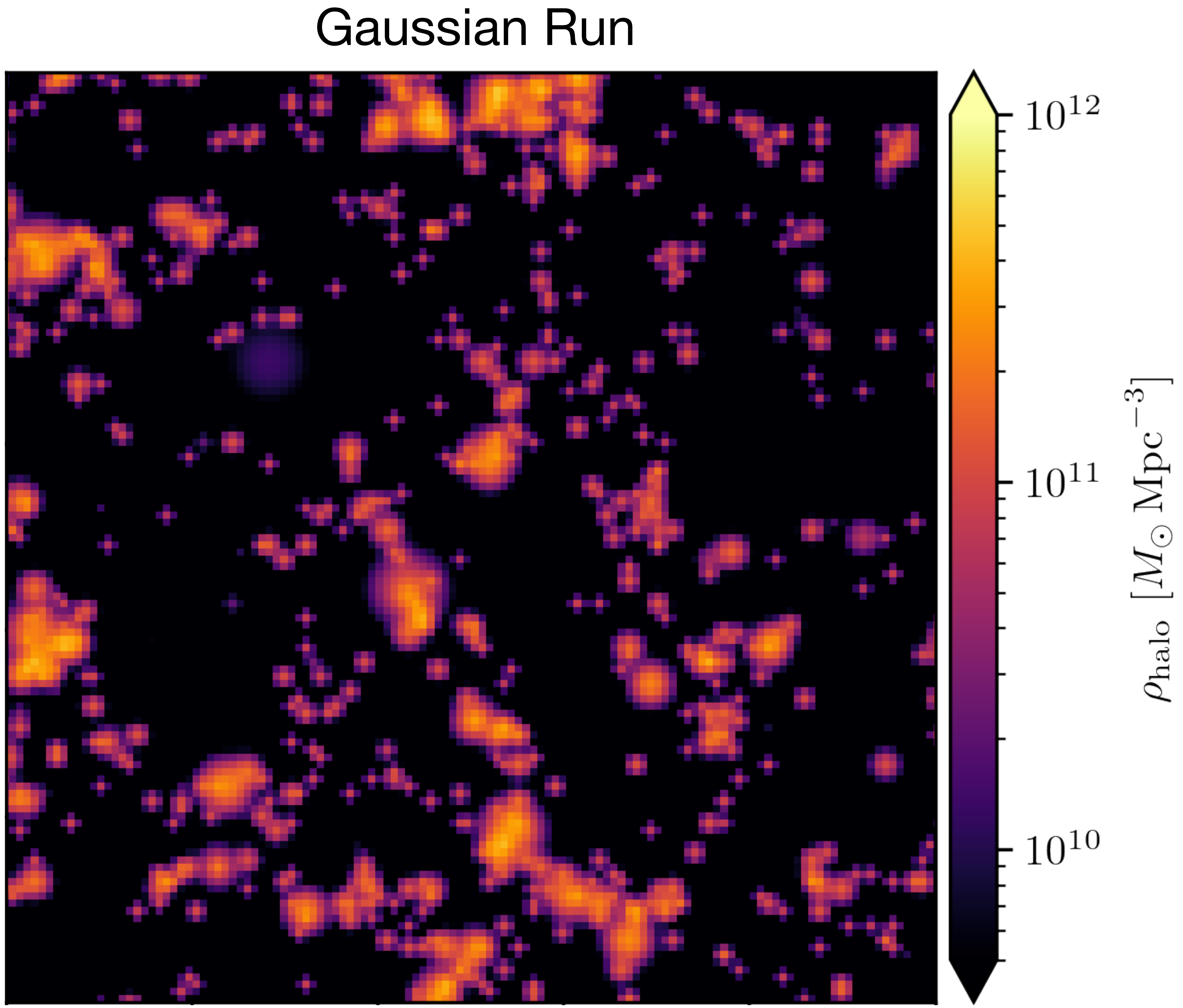

25 Mpc x 25 Mpc slice of the *Peak Patch* halo field.

With PING spikes less than 1 Mpc, we observe an overabundance of small halos.

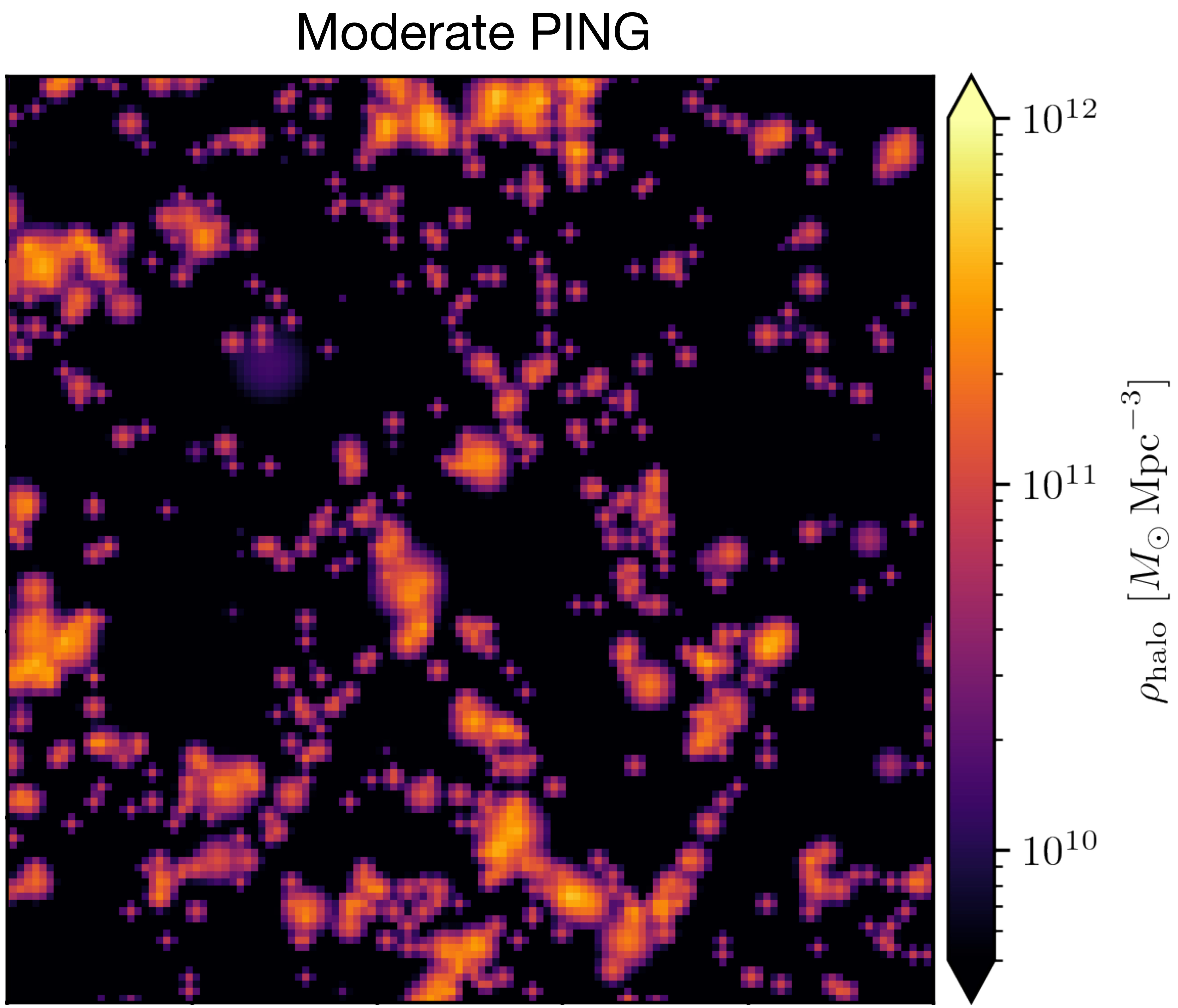

25 Mpc x 25 Mpc slice of the *Peak Patch* halo field.

With PING spikes less than 1 Mpc, we observe an overabundance of small halos.

Strong PING

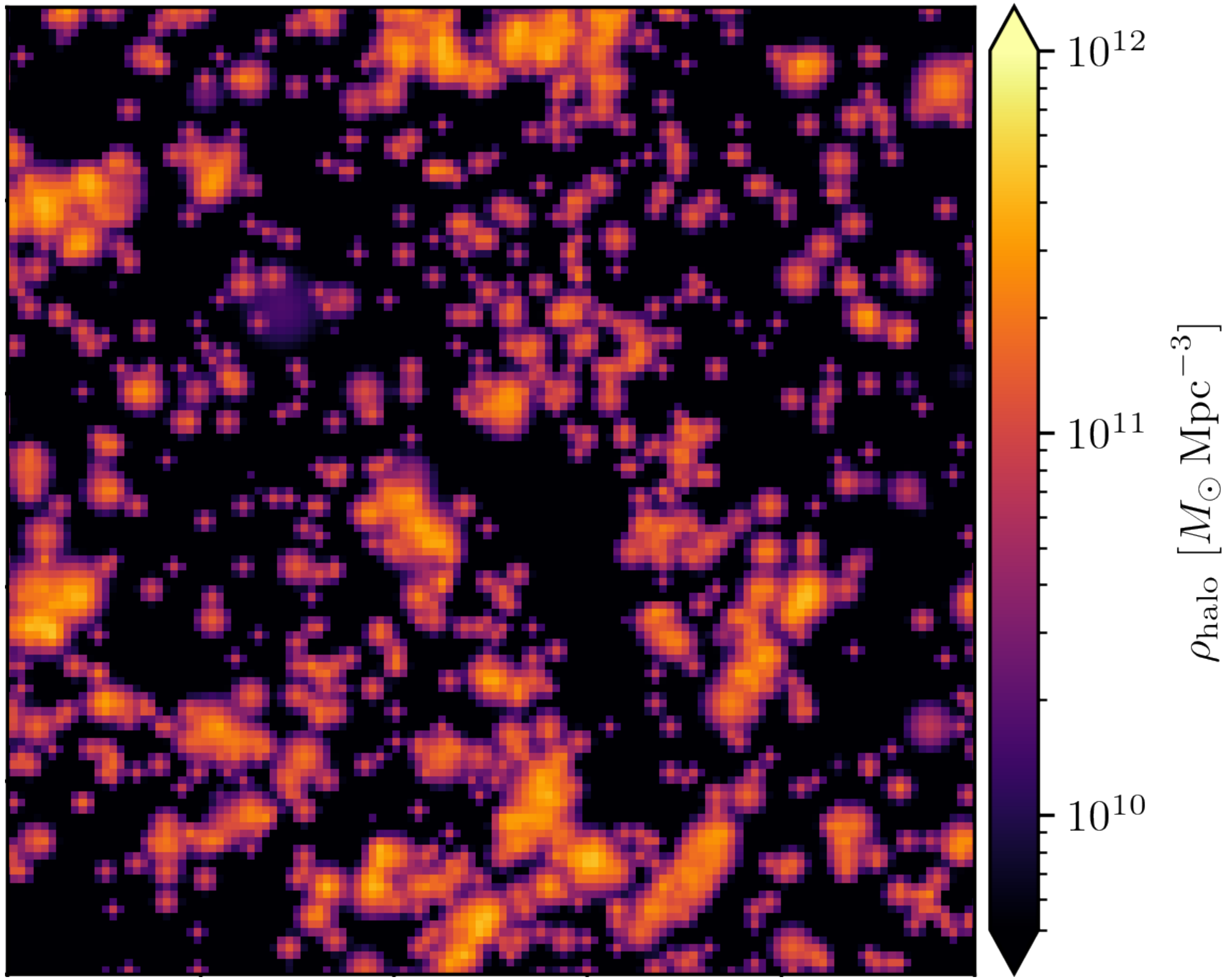

25 Mpc x 25 Mpc slice of the *Peak Patch* halo field.

Each *WebSky* response function has some combination of three components:

$$|\text{Web}\rangle \otimes \frac{|\text{Ski}\rangle + |\text{Sky}\rangle}{\sqrt{2}}$$

A **field component** comprises responses due to the material exterior to the halo's virial radius.

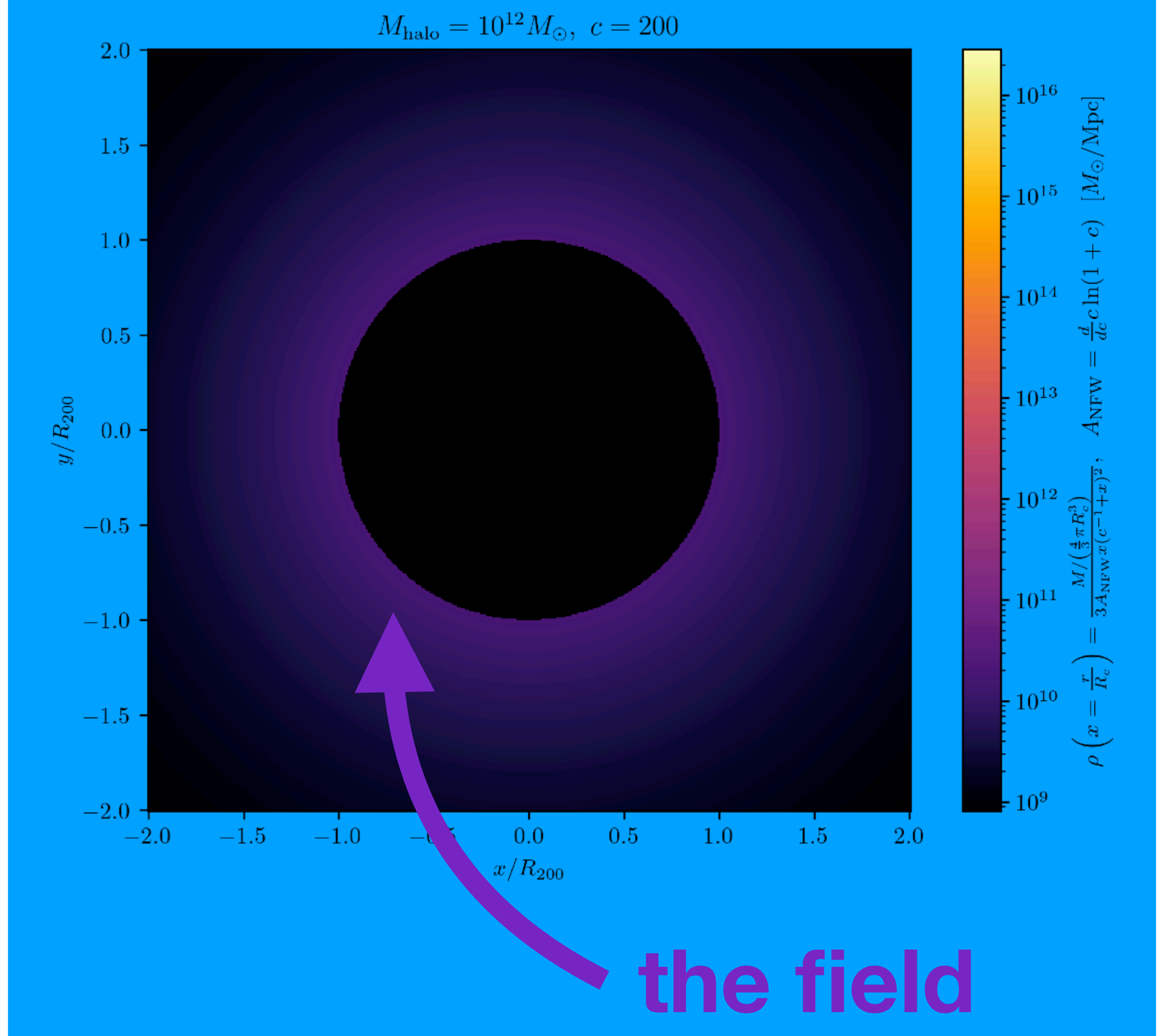

A **halo component** comprises responses due to bulk properties of the halos.

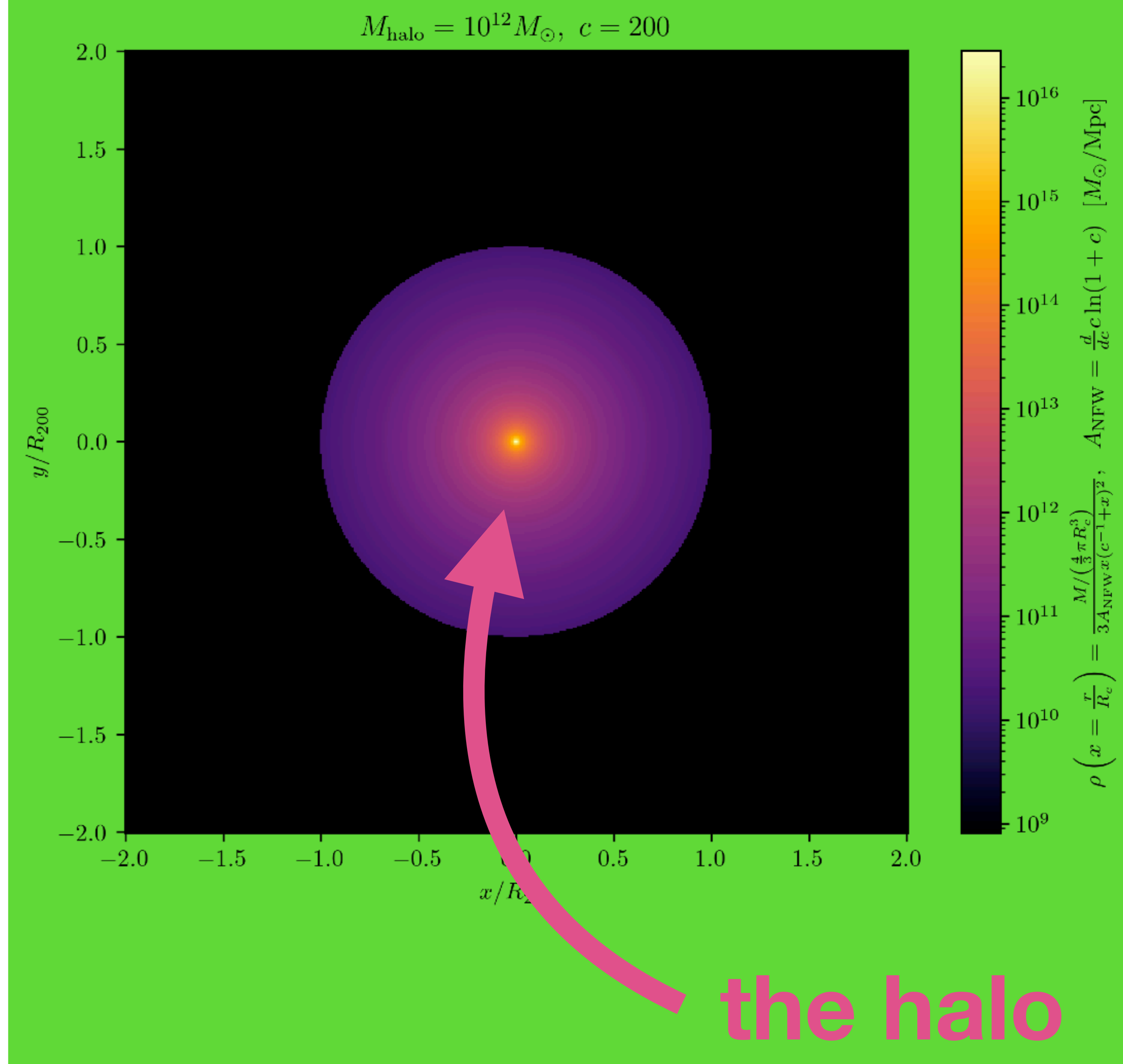

A **sub-halo component** comprises responses due to point-like sources within the halo.

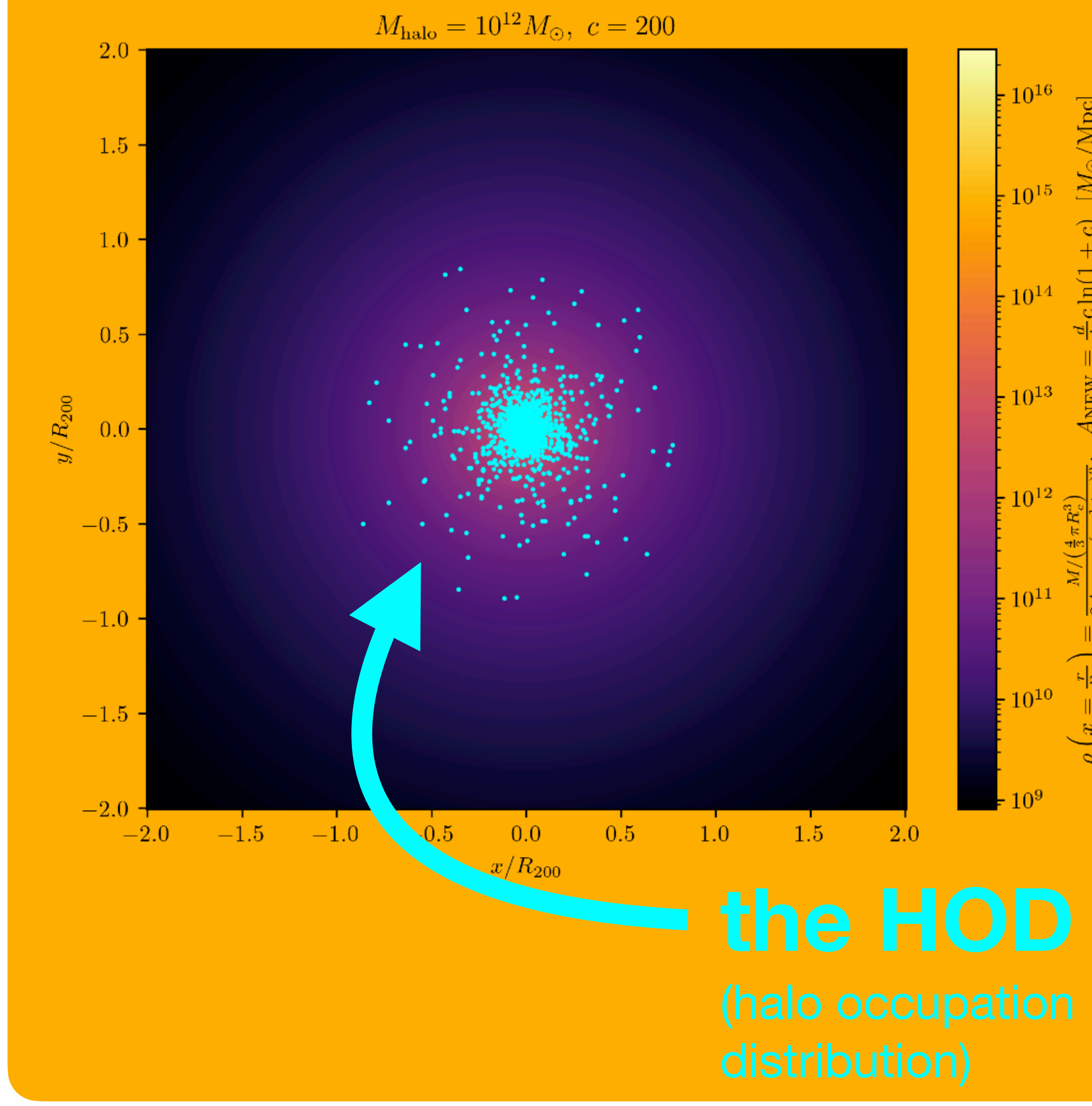

With *WebSky*, we trace out 3D $T_{\rm CO}$ emission that COMAP is sensitive to. We show the redshift evolution of $T_{\rm CO}$ with and without noise.

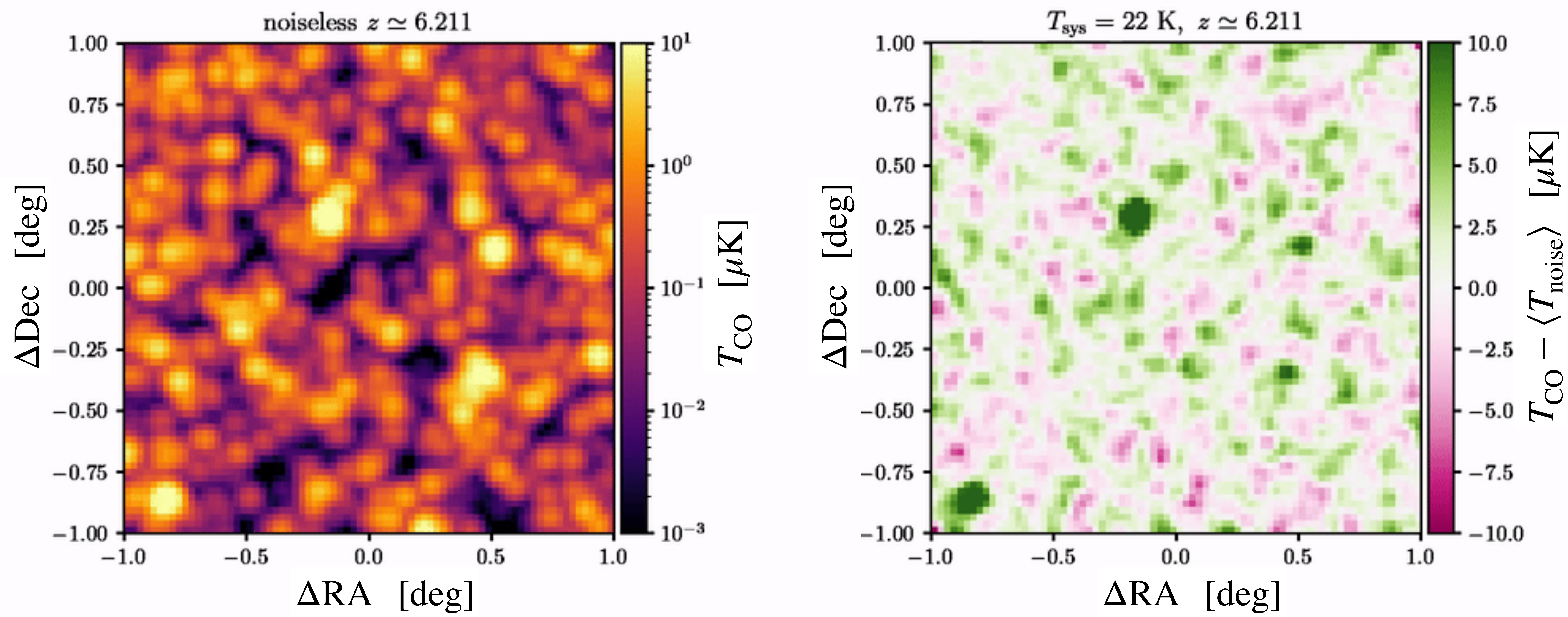

These maps show the theoretical CO emission in the COMAP Ku band from $z \simeq 6.2$ to $z \simeq 7.2$ from halos with $M_{\rm halo} \gtrsim 5 \cdot 10^{10} M_{\odot}$. This is higher resolution than we would see with COMAP.

With *WebSky,* we trace out 3D $T_{\rm CO}$ emission that COMAP is sensitive to. We show the redshift evolution of $T_{\rm CO}$ with and without noise.

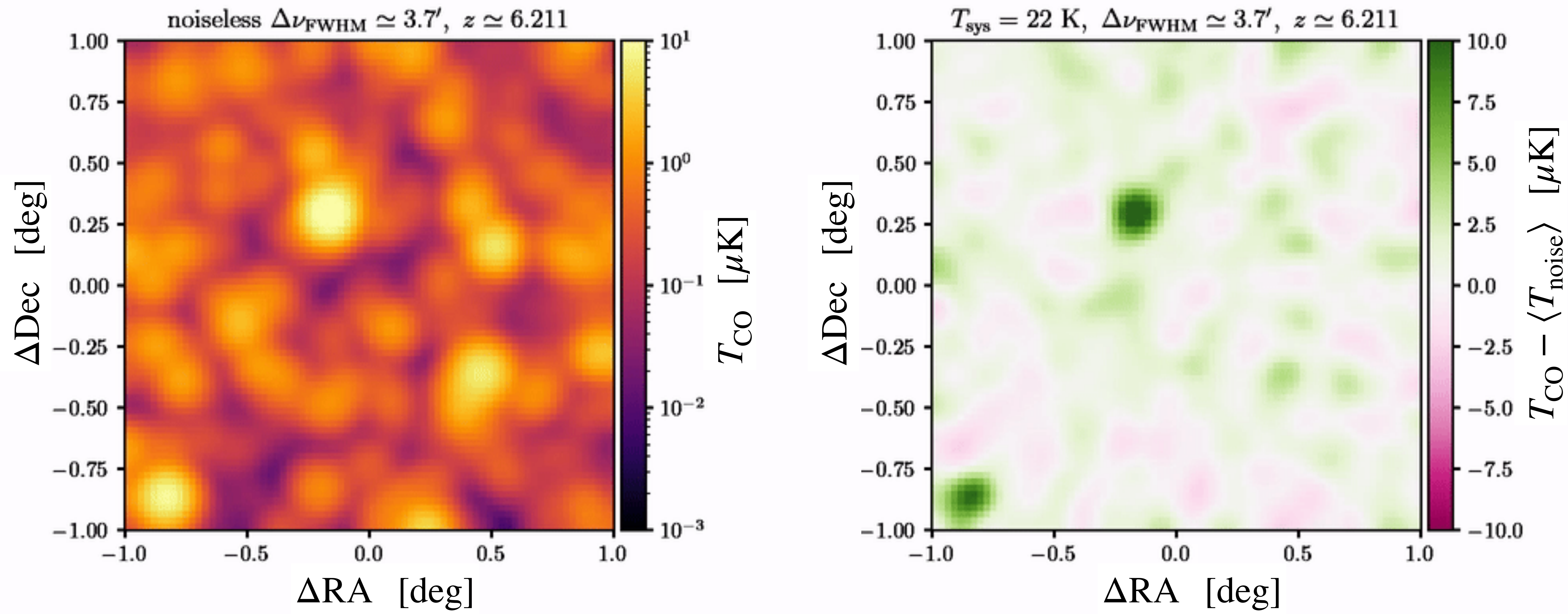

Applying a beam of $\Delta\nu_{\rm FWHM} \simeq 3.7$ arcmin yields maps comparable to those predicted for COMAP. This allows us to test cosmological models directly against data.

Voxel intensity distributions (VIDs) provide us a better metric for measuring the degree to which the distribution is non-Gaussian.

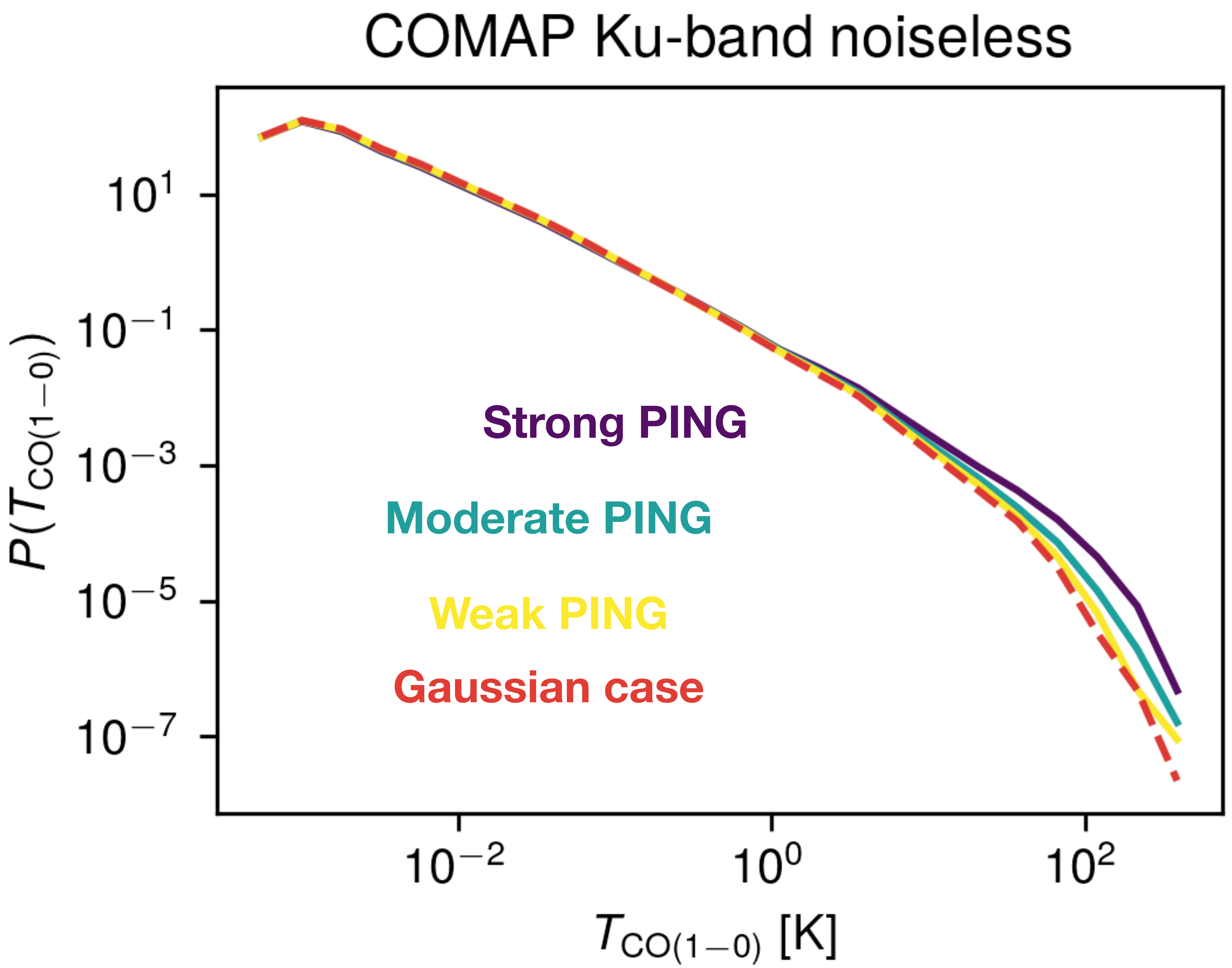

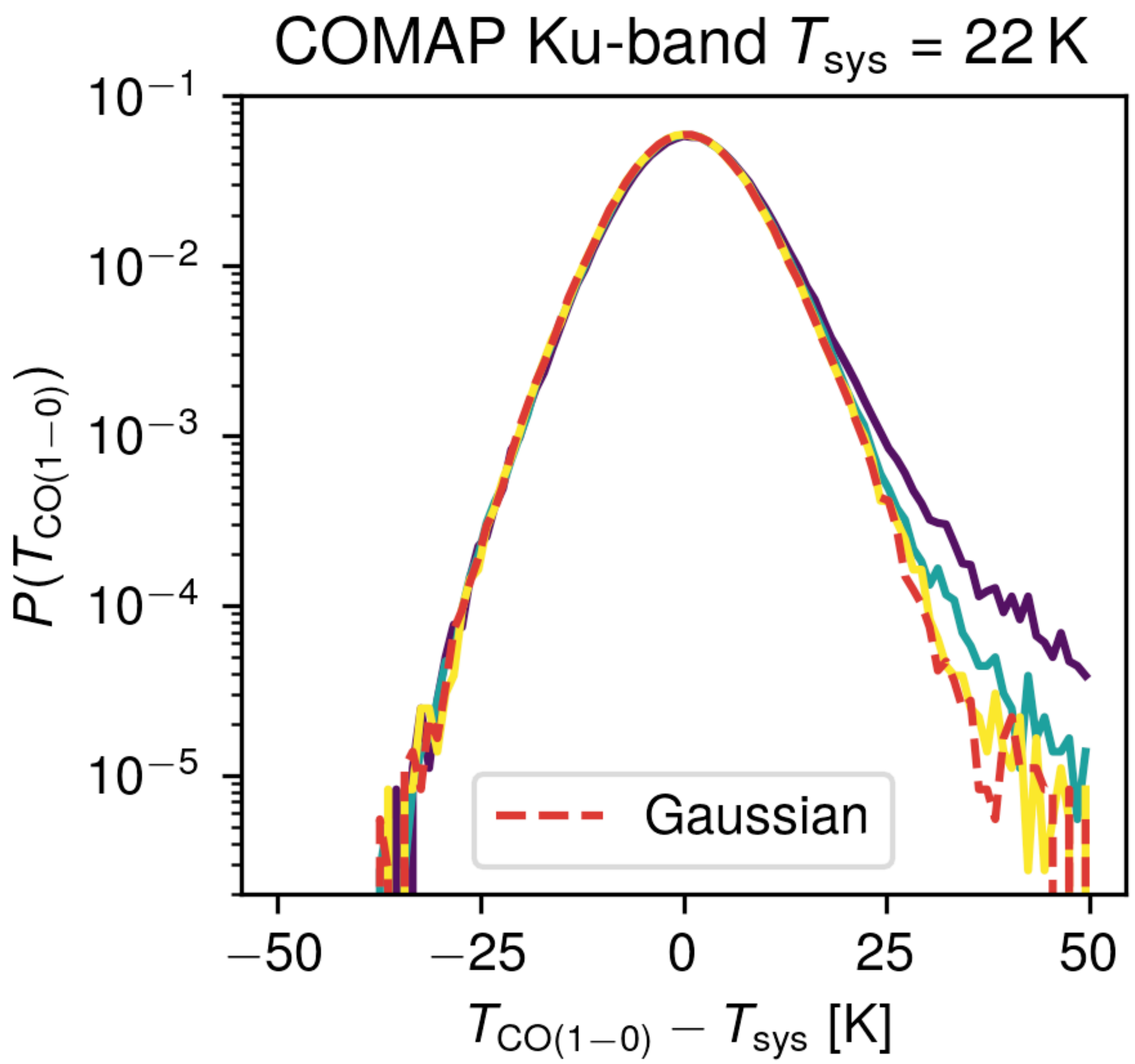

This does better than P(k) as we don't need the additional normalisation.

Voxel intensity distributions (VIDs) provide us a better metric for measuring the degree to which the distribution is non-Gaussian.

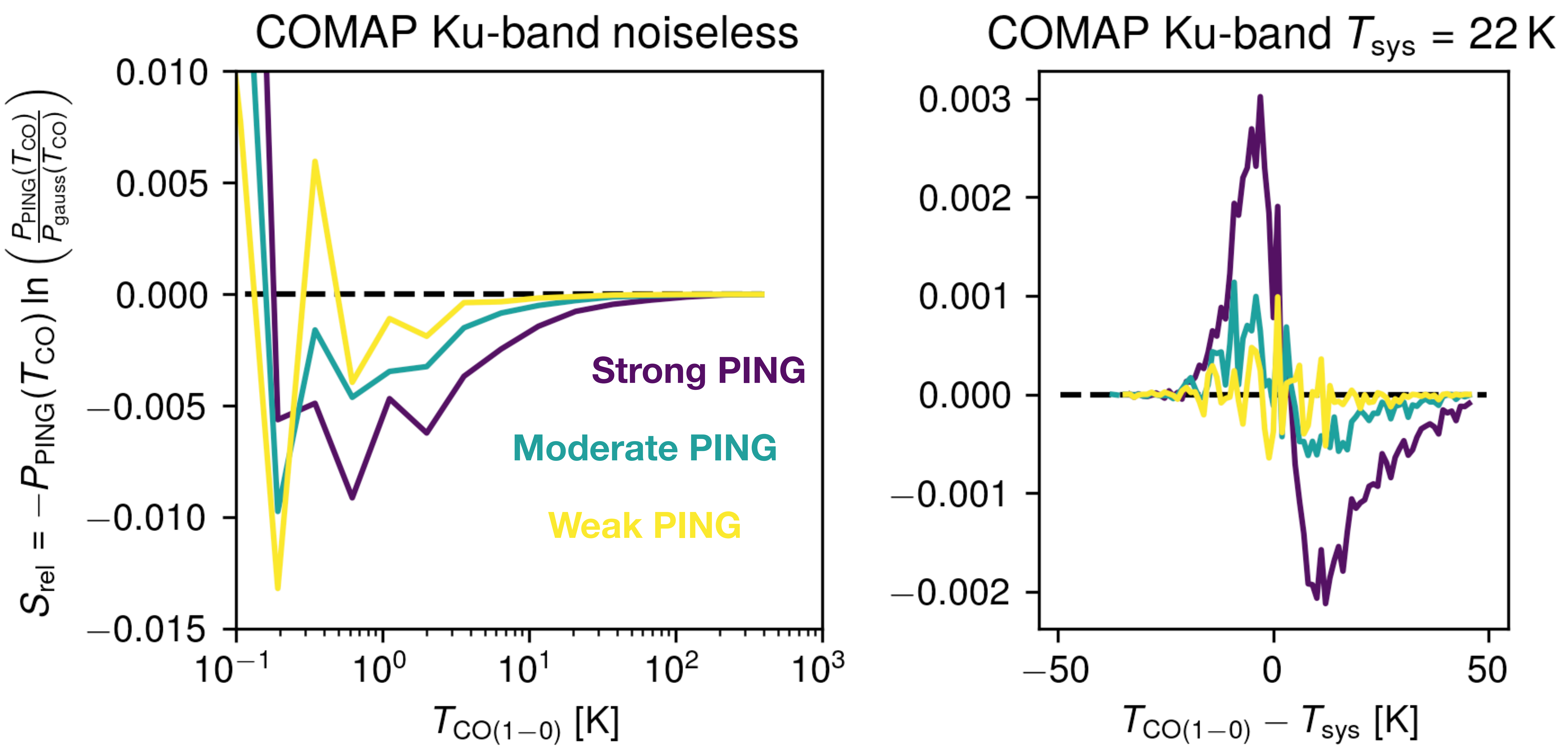

We see that the relative entropy has a similar form to that we saw for the binned halo mass functions.

Niagara

- 2,016 nodes w/ 40-core Intel Skylake at 2.4GHz or Cascade Lake cores at 2.5GHz
- Total 80 640 cores
- 188 GiB of RAM/node
- 6PB of scratch, 3PB of project space
- 256 TB burst buffer (Excelero + IBM Spectrum Scale).

Trillium

- 1,224 nodes, w/ 2x 96-core AMD EPYC "Zen5" CPUs.
- Total 235,008 CPU (3x Niagara)
- **768 GiB of RAM/node** (4x Niagara)

- 29 PB of all-flash storage

- 60 GPU compute nodes, each with 4 Nvidia H100 SXM 80GB GPUs and one 96-core AMD EPYC "Zen4" CPU
- The network will be fully non-blocking, meaning every node can talk to every other node at full bandwidth simultaneously.

Hardware delivery started 2024, and the new cluster will be available for users in the **spring of 2025**.

Forecasts

	$\alpha_{[CII]}$	σ_Z	$\log_{10} Q$	$\log_{10} a_e$	m_λ	m_χ	f_b	Ω_m	H_0	σ_8
$\alpha_{[CII]}$	1.00e+00	7.07e-01	-3.04e-01	-3.48e-02	-2.17e-01	-9.91e-02	5.38e-02	-1.07e-01	2.14e-01	-8.50e-01
σ_Z	7.07e-01	1.00e+00	-6.74e-02	-1.19e-01	-3.77e-01	-2.00e-01	2.92e-01	3.49e-01	-9.58e-02	-7.09e-01
$\log_{10} Q$	-3.04e-01	-6.74e-02	1.00e+00	7.90e-01	3.15e-02	4.64e-02	-2.35e-02	7.02e-02	-1.05e-01	1.75e-01
$\log_{10} a_e$	-3.48e-02	-1.19e-01	7.90e-01	1.00e+00	-4.16e-02	4.69e-02	-4.65e-01	3.91e-02	-3.54e-02	-1.35e-01
m_λ	-2.17e-01	-3.77e-01	3.15e-02	-4.16e-02	1.00e+00	9.23e-01	1.60e-01	-3.87e-01	2.03e-01	3.96e-01
m_χ	-9.91e-02	-2.00e-01	4.64e-02	4.69e-02	9.23e-01	1.00e+00	4.27e-02	-3.13e-01	2.74e-01	1.59e-01
f_b	5.38e-02	2.92e-01	-2.35e-02	-4.65e-01	1.60e-01	4.27e-02	1.00e+00	-2.43e-01	1.25e-01	2.84e-01
Ω_m	-1.07e-01	3.49e-01	7.02e-02	3.91e-02	-3.87e-01	-3.13e-01	-2.43e-01	1.00e+00	-8.87e-01	-2.58e-01
H_0	2.14e-01	-9.58e-02	-1.05e-01	-3.54e-02	2.03e-01	2.74e-01	1.25e-01	-8.87e-01	1.00e+00	4.57e-02
σ_8	-8.50e-01	-7.09e-01	1.75e-01	-1.35e-01	3.96e-01	1.59e-01	2.84e-01	-2.58e-01	4.57e-02	1.00e+00

Corr_{ij}: 1.00, 0.30, 0.10, 0.00, -0.10, -0.30, -1.00

	$\alpha_{[CII]}$	σ_Z	$\log_{10} Q$	$\log_{10} a_e$	m_λ	m_χ	f_b	Ω_m	H_0	σ_8
$\alpha_{[CII]}$	1.00e+00	-1.00e+00	4.69e-01	3.35e-01	-5.09e-02	-8.79e-03	4.11e-01	-7.36e-02	1.74e-01	2.64e-01
σ_Z	-1.00e+00	1.00e+00	-4.88e-01	-3.43e-01	6.46e-02	2.96e-03	-4.26e-01	8.06e-02	-1.84e-01	-2.68e-01
$\log_{10} Q$	4.69e-01	-4.88e-01	1.00e+00	7.18e-01	-3.81e-01	3.49e-02	4.12e-01	-1.88e-01	1.39e-01	1.51e-01
$\log_{10} a_e$	3.35e-01	-3.43e-01	7.18e-01	1.00e+00	-3.64e-02	-1.62e-01	6.69e-02	-2.11e-02	-2.97e-01	8.41e-02
m_λ	-5.09e-02	6.46e-02	-3.81e-01	-3.64e-02	1.00e+00	4.23e-01	7.29e-02	3.92e-01	-2.10e-01	4.92e-01
m_χ	-8.79e-03	2.96e-03	3.49e-02	-1.62e-01	4.23e-01	1.00e+00	1.73e-01	-1.87e-01	2.82e-01	2.59e-02
f_b	4.11e-01	-4.26e-01	4.12e-01	6.69e-02	7.29e-02	1.73e-01	1.00e+00	-1.15e-01	5.58e-01	7.23e-01
Ω_m	-7.36e-02	8.06e-02	-1.88e-01	-2.11e-02	3.92e-01	-1.87e-01	-1.15e-01	1.00e+00	-7.79e-01	3.17e-01
H_0	1.74e-01	-1.84e-01	1.39e-01	-2.97e-01	-2.10e-01	2.82e-01	5.58e-01	-7.79e-01	1.00e+00	1.92e-01
σ_8	2.64e-01	-2.68e-01	1.51e-01	8.41e-02	4.92e-01	2.59e-02	7.23e-01	3.17e-01	1.92e-01	1.00e+00

Corr_{ij}: 1.00, 0.30, 0.10, 0.00, -0.10, -0.30, -1.00

Forecasts

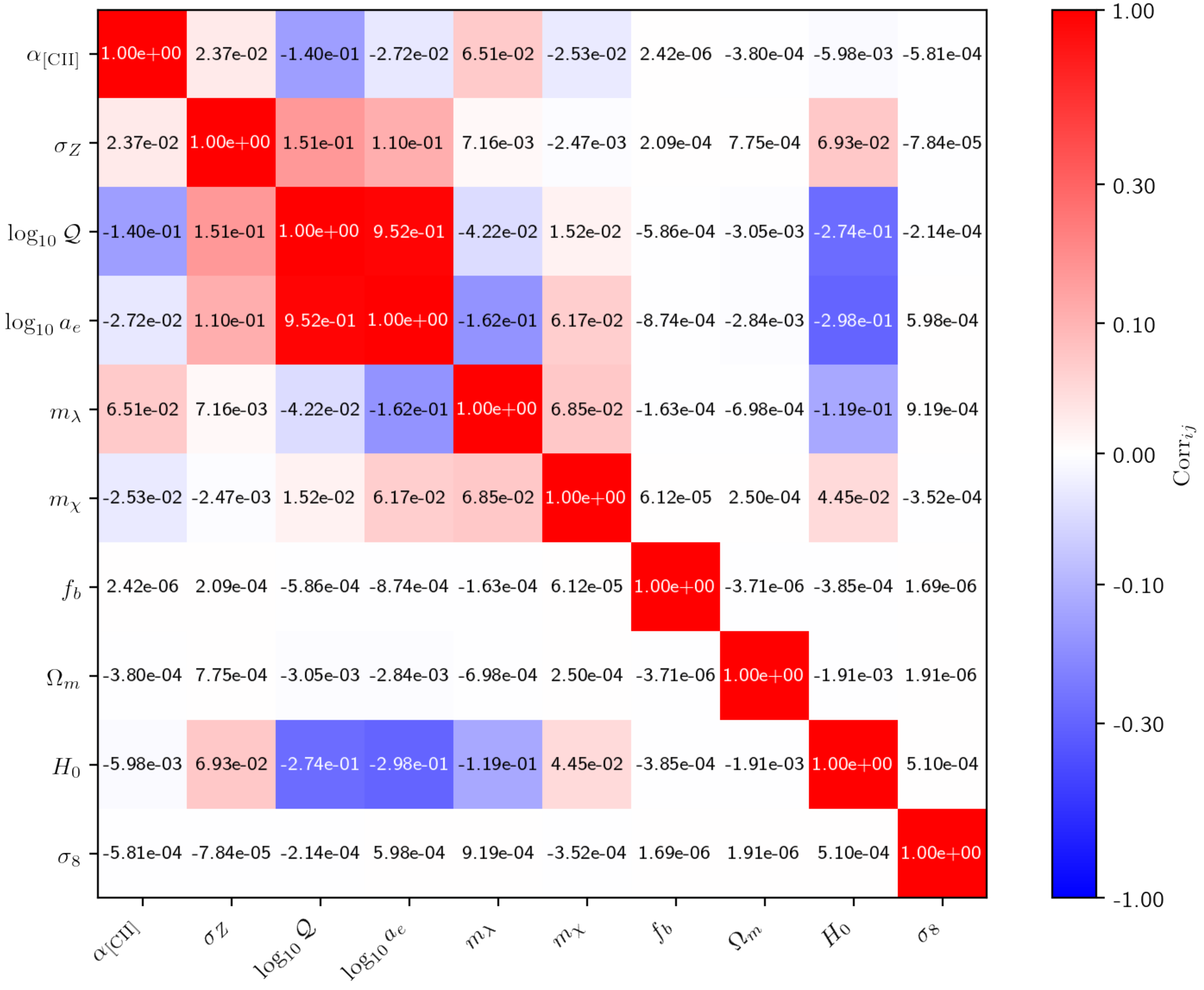

$\alpha_{[CII]}$ 1.00e+00 2.37e-02 -1.40e-01 -2.72e-02 6.51e-02 -2.53e-02 2.42e-06 -3.80e-04 -5.98e-03 -5.81e-04
σ_Z 2.37e-02 1.00e+00 1.51e-01 1.10e-01 7.16e-03 -2.47e-03 2.09e-04 7.75e-04 6.93e-02 -7.84e-05
$\log_{10} \mathcal{Q}$ -1.40e-01 1.51e-01 1.00e+00 9.52e-01 -4.22e-02 1.52e-02 -5.86e-04 -3.05e-03 -2.74e-01 -2.14e-04
$\log_{10} a_e$ -2.72e-02 1.10e-01 9.52e-01 1.00e+00 -1.62e-01 6.17e-02 -8.74e-04 -2.84e-03 -2.98e-01 5.98e-04
m_λ 6.51e-02 7.16e-03 -4.22e-02 -1.62e-01 1.00e+00 6.85e-02 -1.63e-04 -6.98e-04 -1.19e-01 9.19e-04
m_χ -2.53e-02 -2.47e-03 1.52e-02 6.17e-02 6.85e-02 1.00e+00 6.12e-05 2.50e-04 4.45e-02 -3.52e-04
f_b 2.42e-06 2.09e-04 -5.86e-04 -8.74e-04 -1.63e-04 6.12e-05 1.00e+00 -3.71e-06 -3.85e-04 1.69e-06
Ω_m -3.80e-04 7.75e-04 -3.05e-03 -2.84e-03 -6.98e-04 2.50e-04 -3.71e-06 1.00e+00 -1.91e-03 1.91e-06
H_0 -5.98e-03 6.93e-02 -2.74e-01 -2.98e-01 -1.19e-01 4.45e-02 -3.85e-04 -1.91e-03 1.00e+00 5.10e-04
σ_8 -5.81e-04 -7.84e-05 -2.14e-04 5.98e-04 9.19e-04 -3.52e-04 1.69e-06 1.91e-06 5.10e-04 1.00e+00
$\alpha_{[CII]}$ σ_Z $\log_{10} \mathcal{Q}$ $\log_{10} a_e$ m_λ m_χ f_b Ω_m H_0 σ_8
1.00 0.30 0.10 0.00 -0.10 -0.30 -1.00
Corr_{ij}

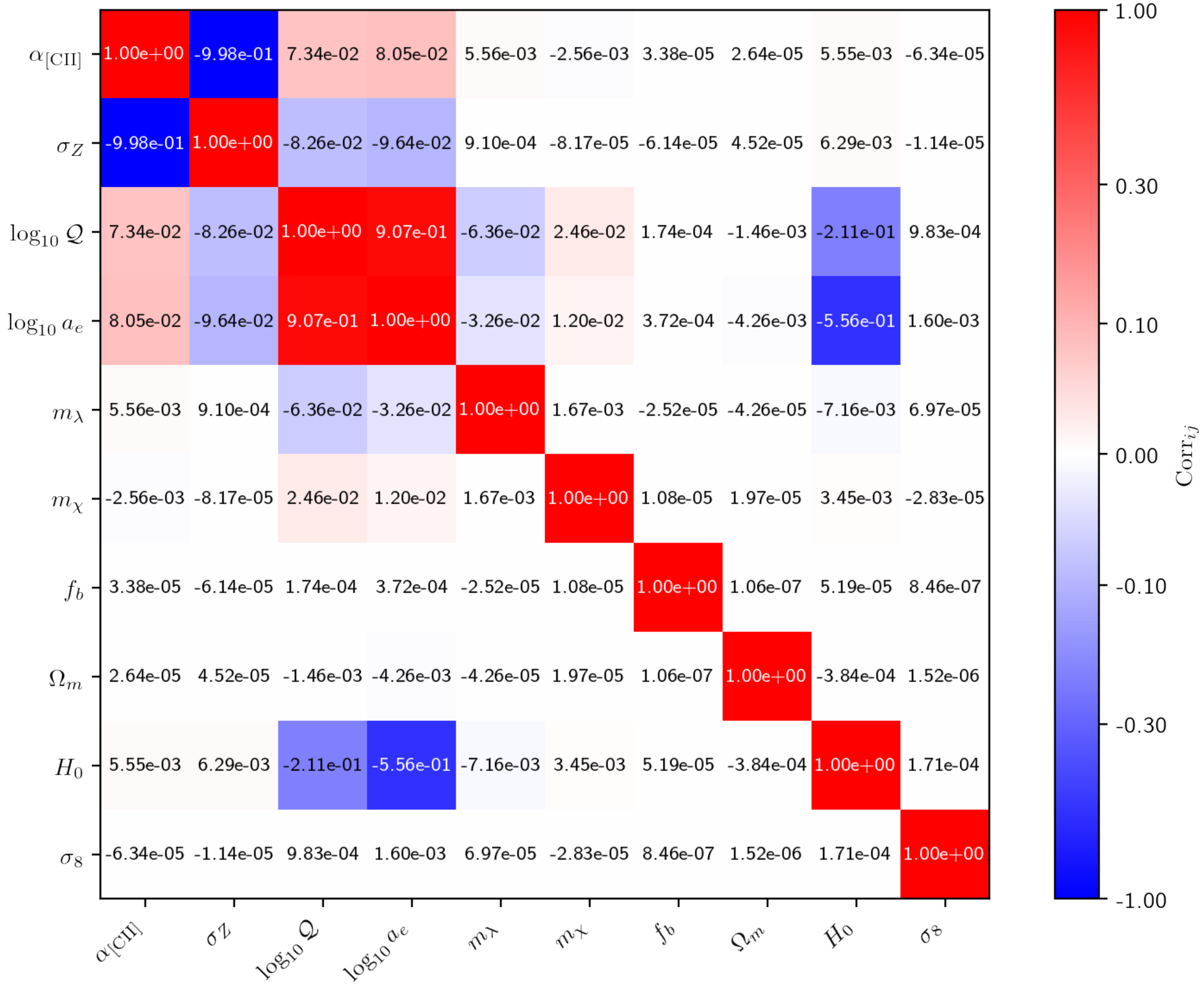

$\alpha_{[CII]}$ 1.00e+00 -9.98e-01 7.34e-02 8.05e-02 5.56e-03 -2.56e-03 3.38e-05 2.64e-05 5.55e-03 -6.34e-05
σ_Z -9.98e-01 1.00e+00 -8.26e-02 -9.64e-02 9.10e-04 -8.17e-05 -6.14e-05 4.52e-05 6.29e-03 -1.14e-05
$\log_{10} \mathcal{Q}$ 7.34e-02 -8.26e-02 1.00e+00 9.07e-01 -6.36e-02 2.46e-02 1.74e-04 -1.46e-03 -2.11e-01 9.83e-04
$\log_{10} a_e$ 8.05e-02 -9.64e-02 9.07e-01 1.00e+00 -3.26e-02 1.20e-02 3.72e-04 -4.26e-03 -5.56e-01 1.60e-03
m_λ 5.56e-03 9.10e-04 -6.36e-02 -3.26e-02 1.00e+00 1.67e-03 -2.52e-05 -4.26e-05 -7.16e-03 6.97e-05
m_χ -2.56e-03 -8.17e-05 2.46e-02 1.20e-02 1.67e-03 1.00e+00 1.08e-05 1.97e-05 3.45e-03 -2.83e-05
f_b 3.38e-05 -6.14e-05 1.74e-04 3.72e-04 -2.52e-05 1.08e-05 1.00e+00 1.06e-07 5.19e-05 8.46e-07
Ω_m 2.64e-05 4.52e-05 -1.46e-03 -4.26e-03 -4.26e-05 1.97e-05 1.06e-07 1.00e+00 -3.84e-04 1.52e-06
H_0 5.55e-03 6.29e-03 -2.11e-01 -5.56e-01 -7.16e-03 3.45e-03 5.19e-05 -3.84e-04 1.00e+00 1.71e-04
σ_8 -6.34e-05 -1.14e-05 9.83e-04 1.60e-03 6.97e-05 -2.83e-05 8.46e-07 1.52e-06 1.71e-04 1.00e+00
$\alpha_{[CII]}$ σ_Z $\log_{10} \mathcal{Q}$ $\log_{10} a_e$ m_λ m_χ f_b Ω_m H_0 σ_8
1.00 0.30 0.10 0.00 -0.10 -0.30 -1.00
Corr_{ij}

Forecasts

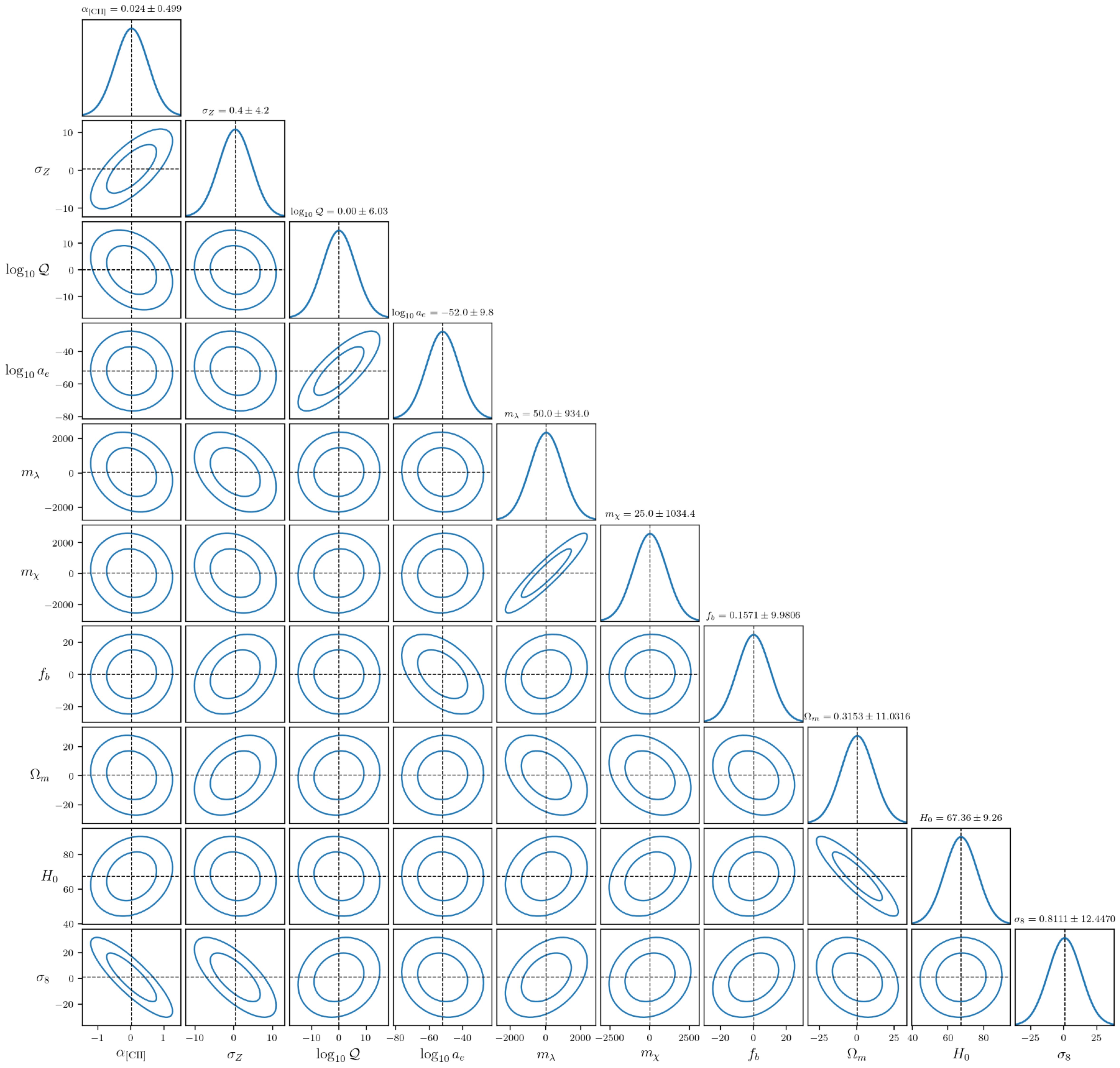

$\alpha_{[\mathrm{CII}]} = 0.024 \pm 0.499$
$\sigma_Z = 0.4 \pm 4.2$
$\log_{10} Q = 0.00 \pm 6.03$
$\log_{10} a_e = -52.0 \pm 9.8$
$m_\lambda = 50.0 \pm 934.0$
$m_\chi = 25.0 \pm 1034.4$
$f_b = 0.1571 \pm 9.9806$
$\Omega_m = 0.3153 \pm 11.0316$
$H_0 = 67.36 \pm 9.26$
$\sigma_8 = 0.8111 \pm 12.4470$
$\alpha_{[\mathrm{CII}]}$
σ_Z
$\log_{10} Q$
$\log_{10} a_e$
m_λ
m_χ
f_b
Ω_m
H_0
σ_8

Forecasts

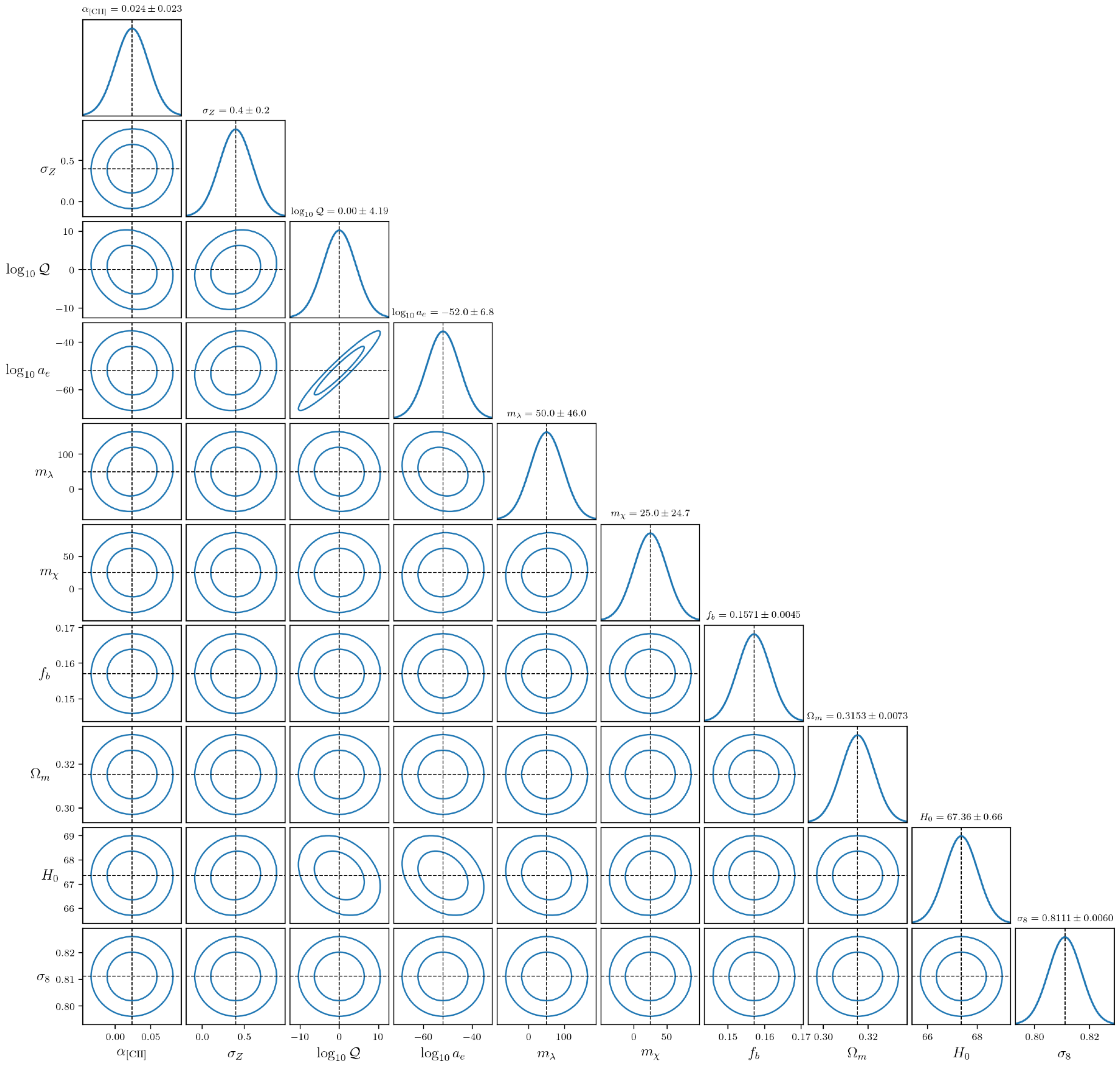

$\alpha_{[CII]} = 0.024 \pm 0.023$
$\sigma_Z = 0.4 \pm 0.2$
$\log_{10} Q = 0.00 \pm 4.19$
$\log_{10} a_e = -52.0 \pm 6.8$
$m_\lambda = 50.0 \pm 46.0$
$m_\chi = 25.0 \pm 24.7$
$f_b = 0.1571 \pm 0.0045$
$\Omega_m = 0.3153 \pm 0.0073$
$H_0 = 67.36 \pm 0.66$
$\sigma_8 = 0.8111 \pm 0.0060$
$\alpha_{[CII]}$
σ_Z
$\log_{10} Q$
$\log_{10} a_e$
m_λ
m_χ
f_b
Ω_m
H_0
σ_8

WebSky models response functions to various observables, giving us the galaxy-halo connection. For Gaussian initial conditions:

tSZ and kappa slices from z ~ 2.5 to z ~ 3.5

WebSky models response functions to various observables, giving us the galaxy-halo connection. For non-Gaussian initial conditions:

tSZ and kappa slices from z ~ 2.5 to z ~ 3.5

Non-Gaussianity on the sky with the *WebSky* simulations

CIB signal **without PING**

$8.182^\circ \times 8.182^\circ$ integrated CIB signal from $z \in [2.53,\ 3.56]$ with Gaussian initial conditions.

Non-Gaussianity on the sky with the *WebSky* simulations

CIB signal **with PING**

$8.182^\circ \times 8.182^\circ$ integrated CIB signal from $z \in [2.53,\ 3.56]$ with non-Gaussian initial conditions.